CYTOCHROME P450 DERIVED OXYLIPIDS INDUCE VASCULAR BARRIER DYSFUNCTION IN AN OXIDATIVE STRESS DEPENDENT MECHANISM

By

Vengai Mavangira

A DISSERTATION

Submitted to
Michigan State University
in partial fulfillment of the requirements
for the degree of

Comparative Medicine and Integrative Biology – Doctor of Philosophy

2016

ABSTRACT

CYTOCHROME P450 DERIVED OXYLIPIDS INDUCE VASCULAR BARRIER DYSFUNCTION IN AN OXIDATIVE STRESS DEPENDENT MECHANISM

By

Vengai Mavangira

Oxidative stress contributes to the pathology of several inflammatory-based diseases of humans and animals. In acute inflammation, the production of metabolites with prooxidant effects occurs rapidly, overwhelming the protective mechanism resulting in acute cellular damage. A major challenge has been identifying ways of effective controlling oxidative stress to improve responses to therapies for the conditions characterized by oxidative stress such as sepsis. Despite decades of research and the equivocal success associated with use of antioxidants, the control of oxidative stress continues to be problematic. Among many reasons, the inability to deliver antioxidants to specific subcellular sites where they may be most beneficial may explain some of the disappointing results of antioxidants during disease. As such, renewed interest focused at improving antioxidant delivery to sites of prooxidant metabolite formation is critical. Another alternative is to target the specific pathways involved in the formation of reactive metabolites such as those involved in lipid metabolism. To determine which lipid metabolizing pathways maybe most relevant, we utilized the severe coliform mastitis disease as a model for oxidative stress to evaluate the extent of lipid metabolism during severe inflammation. The hypothesis for Chapter 2 therefore, was that oxylipid biosynthesis in severe acute inflammation is influenced by substrate availability, metabolism pathway, and the activities of key metabolic enzymes. Results of that study showed an extensive profile of lipid oxygenation products (oxylipids) broader than previously reported. In addition, increased substrate availability as evidenced by greater polyunsaturated fatty acids (PUFA) concentrations, involvement of multiple biosynthetic

pathways, and various degrees of metabolism accounted for the variety in the oxylipid profiles detected. Follow up studies evaluated the concurrent oxidative stress during changes observed for the oxylipid profiles. The hypothesis for that work reported in Chapter 3 was that a specific oxylipid produced during bovine coliform mastitis would reliably detect the concurrent severe oxidative stress. This work showed that a specific biomarker of oxidative stress frequently used in human diseases, 15-F_{2t}-isoprostane correlated positively with several biomarkers of oxidative stress. The same oxidative stress biomarkers, including 15-F_{2t}-isoprostane, correlated with an oxylipid from the cytochrome P450 pathway known as 20-HETE. Human observational studies on diseases such as hypertension and laboratory disease models showed that 20-HETE was shown to potently induce inflammation and oxidative stress. Many of these conditions are associated with vascular dysfunction. Therefore, we hypothesized that 20-HETE contributes to the pathology that occurs during severe coliform mastitis of dairy cattle by inducing oxidative stress-dependent endothelial cell death thus disrupting vascular barrier integrity. Utilizing a primary bovine endothelial cell culture system, the effects of direct exposure to 20-HETE on the barrier integrity were evaluated through determining the development of oxidative stress and the functional consequence on barrier integrity. Results support a role of 20-HETE in mediating changes related to oxidative stress as inducing the disruption of barrier integrity, and supports the idea of targeting this pathway in modulating the oxidative stress responses during diseases in which there is enhanced 20-HETE biosynthesis. Further work should focus on characterizing the sources of 20-HETE biosynthesis and the mechanisms of its regulation to facilitate the development of targeted and specific therapies that modulate 20-HETE biosynthesis.

This thesis is dedicated to my family and others who supported me through this journey with special mention of Jeffery W. Tyler, the light to my professional career; thank you for everything.

ACKNOWLEDGEMENTS

I would like to acknowledge the support provided by the Comparative Medicine and Integrative Biology program and the Large Animal Clinical Sciences at Michigan State University (MSU). This work was made possible based on initial data generated from samples collected at the Training Center for Dairy Professionals at the Green Meadow Farms. I would also like to acknowledge my primary advisor, Dr. Lorraine Sordillo and the members of my graduate guidance committee consisting of Drs. A. Daniel Jones III, Tom Herdt, and Robert Roth, whose expert advice and encouragement were instrumental in keeping me focused. I would also like to acknowledge the support offered by the members of the MSU Mass Spectrometry Core Facility and the technical expertise provided by Jeff Gandy and Jennifer De Vries, and all past and present graduate and undergraduate members of the Meadow Brook Laboratory for technical assistance. I would also like to acknowledge the funding sources including the USDA National Institute for Food and Agriculture grant (2011-67015-30179), Michigan AgBioResearch project (MICL02143), the Matilda R. Wilson Fund (Detroit, MI), and the College of Veterinary Medicine Endowed Funds (Sterner Fund). Finally, I am indebted to the support of my family that has been patient, flexible, and accommodating to ensure success in my long, but full-filling training experiences.

TABLE OF CONTENTS

LIST OF TABLES

LIST OF FIGURES

CHAPTER 1

THE CONTRIBUTION OF LIPID MEDIATORS TO OXIDATIVE STRESS DURING INFLAMMATION – A LITERATURE REVIEW

Vengai Mavangira[1] and Lorraine M. Sordillo*[1]

[1]Department of Large Animal Clinical Sciences, College of Veterinary Medicine, Michigan State University, East Lansing 48824

***Corresponding author**

Dr. Lorraine M. Sordillo,

Department of Large Animal Clinical Sciences

College of Veterinary Medicine

Michigan State University

sordillo@msu.edu

Tel: (517) 432-8821

Fax: (517) 432-8822

Abstract

Oxidative stress is an integral part of several inflammatory-based diseases of both humans and animals that results in damage to cellular macromolecules. Cellular macromolecules targeted by oxidative damage include DNA, proteins, and lipids with consequent cellular death and organ dysfunction. Lipids, particularly polyunsaturated fatty acids (PUFA), are sensitive to modification during oxidative stress which occurs while they are esterified or when hydrolyzed from phospholipid membranes. Excess reactive oxygen species (ROS) are formed during inflammation-based conditions and can oxygenate PUFA to oxylipids capable of initiating oxidant damage. Alternatively, lipid metabolizing enzymes induced during inflammation catalyze the formation of produce oxylipids generating ROS as byproducts. Some of the oxylipids produced are potent ROS that mediate pathology during oxidative stress, whereas some are involved in the resolution of oxidative stress. In mediating their effects, oxylipids either directly or indirectly target sites of ROS production to increase or decrease excessive ROS formation. This review discusses the evidence supporting the roles of oxylipids in the development of oxidative stress either by stimulating the production of oxidants or due to the relative deficiencies of oxylipids with antioxidant effects. Further, the utility of some of the oxylipids as oxidative stress markers that can be exploited in developing and monitoring therapies for inflammatory-based diseases is discussed. Understanding of the link between some oxylipids and the development or resolution of oxidative stress could provide novel therapeutic targets to limit immunopathology, reduce antibiotic usage, and optimize the resolution of inflammatory-based diseases.

Key words: antioxidant, cyclooxygenase, cytochrome P450, eicosanoid, isoprostane, lipoxygenase, oxidant, oxidative stress, oxylipid, oxylipin, reactive metabolites, redox.

Defining Oxidative Stress

Oxidative stress refers to the damage occurring to cellular macromolecules as a consequence of an imbalance between oxidants and antioxidants (Halliwell, 2007). Macromolecules targeted for oxidative damage include lipids, proteins, and DNA (Dalle-Donne et al., 2005, Lee and Pervaiz, 2011, Davies and Guo, 2013). Oxidants comprise radical and non-radical molecules that mediate oxidation of the susceptible macromolecules. The bulk of the oxidants are reactive oxygen species (ROS); however, reactive nitrogen species (RNS) also contribute to the overall pool of oxidants. Free radical oxidants, for example, have the capacity to induce proton removal by the presence of unpaired electrons (Villamena, 2013). Alternatively, the presence of highly electronegative atoms, including oxygen in ROS such as hydrogen peroxide (H_2O_2) and nitrogen in RNS such as peroxynitrite, result in asymmetric electron arrangements that confer the ability to induce oxidation reactions (Villamena, 2013). Collectively, ROS and RNS are referred to as reactive metabolites (RM) whose production occurs both in physiological and pathological states.

Reactive metabolites are normal products of metabolism and are essential for signaling functions which are necessary for cellular processes including proliferation, differentiation, and metabolic adaptations (Valko et al., 2007). For example, the generation of ATP in the mitochondria through the Krebs' cycle and the electron transport chain generates O_2^- and H_2O_2 as byproducts (Cabreiro et al., 2011). Approximately 1-3 % of electrons during the mitochondrial oxidative phosphorylation reactions are transferred are to oxygen to form superoxide (O_2^-) (Holmstrom and Finkel, 2014). Superoxide dismutase (SOD) enzymes catalyze the direct conversion of O_2^- to H_2O_2. Both O_2^- and H_2O_2 participate in phosphorylation of various proteins that are part of signaling networks such as mitogen-activated protein kinase (MAPK) phosphatases, by oxidizing

thiol-containing cysteine residues (Glasauer and Chandel, 2013). The production of RM also increases during periods of increased metabolic demands such as exercise or changes in physiological states like pregnancy (Avila et al., 2015, Medeiros-Lima et al., 2016). Reactive metabolites also increase during regulated inflammatory processes to levels necessary for effective innate and adaptive immune functions. The ability of cellular protective responses to limit the RM produced are kept within physiological limits to prevent cellular damage.

In contrast to the physiological production of RM, uncontrolled inflammation is characterized by excessive levels of RM that contribute to the pathology of diseases. For example, O_2^- and H_2O_2 initiate oxidation of lipids in human low-density lipoproteins, contributing to the development of atherosclerosis (Darley-usmar et al., 1992). Whereas mitochondria are a major source of excessive RM production during inflammatory conditions (Huet et al., 2009), significant contributions also come from upregulated enzyme pathways. Inducible nitric oxide synthase (iNOS), xanthine oxidase (XO), and the nicotinamide adenine dinucleotide phosphate oxidase (NOX) enzymes are all upregulated by inflammatory stimuli. Inducible NOS (iNOS) is upregulated and generates excess nitric oxide which induces widespread vasodilation and generation of peroxynitrite in acute inflammation (Sorokin, 2016). Specifically, iNOS expression in murine macrophages and human kidney cells is induced by LPS (Chan and Riches, 2001, Quoilin et al., 2014). The XO enzymes are stimulated by LPS, hypoxia, and cytokines including interleukin-1β (Hassoun et al., 1998) all of which are present during acute inflammation (Huet et al., 2009).

Cells have an elaborate system of antioxidants that neutralize, metabolize and delay the production of oxidants. Antioxidants include endogenous enzymes such as superoxide dismutases (SOD), glutathione peroxidases (GPxs), thioredoxin reductases (Trx), peroxiredoxins,

catalases, and heme oxygenase (HO) (Bhattacharyya et al., 2014). Dietary sources also contribute to the non-enzymatic pool of antioxidants which include trace minerals (selenium, copper, zinc), polyphenols, vitamins (A, C, D, and E), and the vitamin A precursor, beta-carotene (Al-Gubory et al., 2010). Enzymatic and non-enzymatic antioxidants work in concert to protect against ROS-induced cellular damage. For example, SOD enzymes are dependent on trace minerals, copper (Cu) and manganese (Mn), in the dismutation of O_2^- to H_2O_2 (McCord and Fridovich, 1969). Subsequently, the reduction of H_2O_2 to water and oxygen is mediated by catalases or the selenium (Se)-dependent GPx and Trx reductase enzymes (Cohen and Hochstein, 1963). The reduction of H_2O_2 and other hydroperoxides is coupled to the oxidation of the tripeptide cofactor, reduced glutathione (GSH) to the oxidized state (GSSG) (Cohen and Hochstein, 1963). The GSSG is converted by the glutathione reductase system to GSH which becomes available for further GPx- or Trx-mediated metabolism (Cohen and Hochstein, 1963). Indeed, the balance between GSH and GSSG is crucial as its perturbations can alter cellular redox tone and affect signaling pathways and the development of oxidative stress. For example, exposure of human umbilical endothelial cells (HUVECs) to plasma from septic patients increased RM production and cellular apoptosis that were ameliorated by exposure to the GSH precursor, N-acetyl cysteine (Huet et al., 2008). Reduced GSH can scavenge pre-formed RMs and also participate in regenerating and maintaining the functional forms of other antioxidant enzymes such as vitamins (Ho and Chan, 1992). For example, vitamin E radical formed during the neutralization of free radicals in the cell membranes is recycled back to reduced vitamin E (tocopherol) by GSH and peroxidase enzymes (Yamauchi, 1997).

The activation of antioxidant response genes is another important mechanism essential for limiting the excessive RM accumulation. For example, the nuclear factor related erythroid factor

2 (NrF2) transcription factor is activated during oxidative stress and acts as a master regulator of several antioxidant response genes including those involved in the synthesis of HO-1, GSH, GPx and Trx enzymes (Ruiz et al., 2013). When unstimulated in the cytoplasm, NrF2 is bound to Kelch-Like-ECH Associated Protein 1 (KEAP-1) protein by interacting with cysteine residue which targets it for proteasomal degradation (Ruiz et al., 2013). During oxidative stress or in the presence of NrF2 agonist, oxidation of the cysteine residues dissociates NrF2 from KEAP-1 and translocates to the nucleus. After forming dimers with other transcription factors, NrF2 activates antioxidant response elements in the promoter regions of antioxidant genes (Ruiz et al., 2013). Enzymatic and non-enzymatic components collectively contribute to the overall cellular anti-oxidant potential, which is crucial for defense against oxidative cellular damage during inflammatory-based diseases.

The imbalance between oxidants and antioxidants develops as a consequence of one or a combination of several factors including overproduction of oxidants, depletion of antioxidant potential, and deficiencies in antioxidant components (Valko et al., 2007). Consequently, direct structural damage or chemical modifications occur to lipids and proteins, negatively impacting the normal functions plasma membranes (Valko et al., 2007). Lipids are the major macromolecules present in plasma membranes of cells and their internal organelles, and their oxidation can impact the function and viability of cells in several ways. For example, lipid peroxidation resulted in increased membrane fluidity in ethanol-induced oxidative stress in hepatocytes (Sergent et al., 2005) by affecting the lipid structure and packing in lipid raft domains (Aliche-Djoudi et al., 2013). Lipid peroxidation products and secondary by-products also may induce toxic modification of proteins and DNA resulting in cell death (Sordillo et al., 2005, Dalle-Donne et al., 2006). Protein oxidation resulting from oxidative stress also can affect

cellular function because of altered protein structure. Altered protein structure occurs when thiol groups in amino acid residues such as cysteine and lysine are covalently modified resulting in loss of function (Dalle-Donne et al., 2005). The damage to DNA may be a direct oxidation of bases (Kehrer, 2000) or adduct formation with either lipid or protein oxidation products affecting cellular structure, function, or viability (Lonkar and Dedon, 2011). Understanding the formation of oxidant-induced damage to macromolecules is not only critical to identifying targets for anti-oxidant intervention during disease, but also as potential markers of oxidative stress.

Lipid metabolism is involved in the development of oxidative stress because of its link to inflammation. Evidence shows that lipid metabolizing enzymes are also regulated during inflammation including increased cyclooxygenase (COX) 2, lipoxygenase (LOX), and some cytochrome P450 (CYP) isoforms based on the enhanced production of lipid metabolites from these pathways (Schmelzer et al., 2005, Zarbock et al., 2009, Anwar-mohamed et al., 2010, Willenberg et al., 2015). In some studies, however, several CYP isoforms were suppressed during acute inflammation (Theken et al., 2011). Interestingly, several of the sources of excessive ROS formation are targets of some oxylipid metabolites. For example, 20-hydroxyecosatetraenoic acid (20-HETE) is a CYP-derived oxylipid metabolite that enhances RM production by increasing mitochondrial production and activating NOX enzymes (Bao et al., 2011b, Han et al., 2013). Conversely, the expression of NOX enzymes was decreased by Lipoxin A4 derived from the LOX pathway (Wu et al., 2015). Therefore, understanding the contribution of lipid metabolism is critical for enhancing the resolution of oxidative stress by decreasing pro-oxidant lipids and increase those with antioxidant effects.

In many diseases, oxylipids were shown to regulate several parts of the initiation, progression, and resolution of inflammation. One way of oxylipid-dependent regulation of inflammation is by

influencing the development of oxidative stress (Figure 1). First, some lipid metabolizing enzyme pathways produce RM, particularly O_2^-, as a by-product. Second, some primary oxylipid metabolites such as hydroperoxides from the LOX pathway are potent RM that directly induce cellular oxidative stress and apoptosis (Sordillo et al. 2005). Third, other oxylipid metabolites such as 20-HETE, exert their pro-oxidant effects indirectly by stimulating RM production from sources such as the mitochondria and the NOX enzyme pathway (Lakhkar et al. 2016, Han et al. 2013). Fourth, some oxylipids exert antioxidant effects by directly or indirectly targeting and decreasing production RM from sources such as mitochondria. The link between oxylipids and oxidative stress, therefore, offers opportunities for modulating inflammatory processes by directly targeting the metabolic pathways of these metabolites. The following sections focus on the demonstrated links between some oxylipids and oxidative stress during diseases and the opportunities that exist for controlling oxidative stress by targeting oxylipid biosynthesis.

Role of Oxylipids in Oxidative Stress

Overview of oxylipid biosynthesis

Polyunsaturated fatty acids (PUFA) such as the omega 6 (n-6) fatty acids (arachidonic acid (AA), linoleic acid (LA) and omega 3 (n-3) fatty acids including α-linolenic (ALA), eicosapentaenoic acid (EPA) and docosahexaenoic acid (DHA) are the common substrates for oxylipid synthesis (O'Donnell et al., 2009). The metabolism of PUFA substrates occurs after their hydrolysis from cell membrane phospholipids catalyzed by members of the phospholipase (PL) enzymes, predominantly by PLA2. (Buczynski et al., 2009) Alternatively, PUFA are metabolized while still esterified in cell membranes, (Milne et al., 2011) which may explain their ability to modify cell function by altering the properties of the cell membrane lipid bilayer. The enzymatic pathways of COX, LOX, and CYP are involved in metabolizing PUFA with evidence

of substrate preferences. For example, CYP enzymes will readily oxygenate EPA and DHA over LA and AA when incubated with equimolar concentrations of these PUFA (Arnold et al., 2010b). Non-enzymatic pathways are also involved in the oxygenation of PUFA mediated by free radicals such as O_2^-. Together, the biosynthetic pathways generate several oxylipids with at least 158 metabolites identified to date from human plasma (Wang et al., 2014b).

The general mechanism of oxylipid biosynthesis follows the removal of susceptible hydrogen atoms from PUFA structure and the concurrent or subsequent insertion of one or more oxygen molecules (O'Donnell et al., 2009). In the enzyme-mediated oxygenation of PUFA, the initial formation of radicals at the active site is required for hydrogen abstraction. The free radical for COX enzymes is formed on active site tyrosyl residues, whereas, a heme and non-heme iron radicals are present in CYP and LOX enzymes, respectively (Kulmacz et al., 2003, Schneider et al., 2007, Ortiz de Montellano, 2010). Non-enzymatic metabolism also follows the same general mechanism but the free radical-mediated proton removal lacks the stereospecificity demonstrated by enzymatic pathways leading to the formation of an assortment of oxylipids (Milne et al., 2011).

Role of oxylipid biosynthesis in ROS formation

The oxygenation of PUFA generates lipid hydroperoxides that add to the pool of ROS during oxidative stress (Bhattacharyya et al., 2014). The LOX enzymes exist as several isoforms including 5-, 8-, 12-, and 15-LOX based on the site of oxygen insertion in the PUFA substrate (Kuhn et al., 2015). The active site Fe^{2+} is oxidized to the ferric hydroxide in the process of dioxygen insertion into the PUFA substrate and subsequently reduced to the Fe^{2+} form after reduction of the hydroperoxide ion (Ivanov et al., 2010). The hydroperoxides are potent ROS metabolites that were shown to participate in the development of pathological conditions. For

example, the linoleic acid derived-13-hydroxyoctadecadienoic acid (13-HODE), was predominantly formed from the enzymatic pathway at the onset of atherosclerosis [50], suggesting an increased production of the upstream hydroperoxide, 13-hydroperoxyoctadecadienoic acid (13-HpODE) (Kuhn et al., 1997). The specific cellular effects of 13-HpODE and the AA-derived 15-hydroxyperoxyeicosatetraenoic acid (15-HpETE) relevant to the pathogenesis of atherosclerosis may include oxidative stress-dependent endothelial cell apoptosis (Sordillo et al., 2005, Ryman et al., 2016). Specifically, 15-HpETE enhanced apoptosis by inhibiting protein kinase B (also known as Akt) signaling, downregulating the anti-apoptotic factor Bcl2 and upregulating pro-apoptotic Bax and the executioner caspase 3 (Sordillo et al., 2005, Soumya et al., 2014). The effects of 15-HpETE are similar to the direct effects of H_2O_2 demonstrated on human gingival fibroblasts (Gutiérrez-Venegas et al., 2015) showing that the primary oxygenation metabolites serve as inherent reactive electrophiles.

The catalytic mechanism during PUFA oxygenation can produce O_2^- as a byproduct particularly when the reduction of oxygen is uncoupled from its insertion in a PUFA substrate. Studies have suggested that both COX and LOX enzymes are inefficient sources of O_2^- due to their utilization of dioxygen in PUFA oxygenation (Noguchi et al., 2002). However, significant production of $^-$ reactive metabolites was shown for hepatic CYP enzymes incubated with inhibitors of both SOD and catalase enzymes involved in the metabolism of O_2^- and H_2O_2, respectively (Bondy and Naderi, 1994). Co-incubation of hepatic microsomes with ethanol, toluene, and phenobarbital did not enhance the production of ROS (Bondy and Naderi, 1994), suggesting that CYP could produce RM with no substrate requirement. The substrate-independent RM production by CYPs supports the apparent uncoupling of NADPH reduction from the subsequent activation and insertion of an oxygen atom into PUFA substrates. The apparent uncoupling is greatest in the

CYP2E1 isoform which was described as a leaky enzyme demonstrating a coupling of NADPH reduction to substrate oxygenation of only 0.5 – 3% (Lu and Cederbaum, 2008). The catalytic production of RM by CYP2E1 contributed significantly to the carbon tetrachloride-induced hepatotoxicity in a murine model of oxidative stress (Park et al., 2010). Several other CYP isoforms in hepatocytes (CYP4A, CYP3A4, 1A1, 1A2, and 2B6) and CYP2C9 in endothelial cells are important lipid metabolizing enzymes and generators of RM (Puntarulo and Cederbaum, 1998, Leclercq et al., 2000, Fleming et al., 2001). These data suggest that the multiplicity of the CYP enzymes generating RM may preclude effective modulation of oxidative stress during disease by targeting specific isoforms. Further, inhibiting CYP isoforms to reduce RM production in acute illness is complicated by generalized suppression of several CYP isoforms (Theken et al., 2011). Therefore, targeting the CYP-derived oxylipids may be more beneficial to limit RM production while preserving essential functions of the CYP enzymes.

Non-ROS oxylipids enhance or diminish production of ROS

Cyclooxygenase-derived oxylipids

Cyclooxygenases exist as the constitutively expressed COX-1 and the inducible COX-2 isoforms. With AA as the PUFA substrate, hydrogen removal and insertion of dioxygen to form the unstable PGG_2 occurs at the oxygenase site followed by translocation to the peroxidase site where reduction to PGH_2 occurs (Liu and Roth, 2016). Subsequently, PGH_2 is converted to downstream prostanoids including PGD_2, PGE_2, PGF_2, PGI_2, and PGJ_2 by various PG synthases as well as conversion into thromboxanes (TX) A_2 and B_2 by thromboxane synthase (O'Donnell et al., 2009). Many studies showed that the increased production of RM following COX2-induction was due to the effects of the COX-derived oxylipids (Cho et al., 2011, Munoz et al., 2015). With the knowledge that COX inhibitors may suppress the constitutive physiological

prostanoid production, targeting the specific oxylipid species may offer better responses and reduce complications related to clinical use of COX 2 blockers.

A major downstream product of PGH_2 during inflammation is PGE_2 which mediates its effects through the PGE_2 prostanoid (EP) receptor subtypes 1, 2, 3 and 4. Production of PGE_2 induces oxidative stress in a receptor-dependent manner in models of neuronal degenerative diseases such as Alzheimer's disease. For example, cerebral PGE_2 production increased ROS formation and development of neuronal oxidative stress detected by increased concentrations of markers including AA-derived F_2-isoprostanes (F_2-IsoP) and DHA-derived neuroprostanes (Montine et al., 2002). Deletion of the EP_2 and EP_3 receptors in the neuronal tissue in mice and neural cell cultures diminished oxidative-stress related changes (Montine et al., 2002, Shi et al., 2012). In contrast, the deletion of EP_2 receptors in a model of intracerebral hemorrhage exacerbated O_2^- production and oxidative carbonylation of proteins (Wu et al., 2016) suggesting that EP2 receptor activation was protective in that model. In neuronal cell cultures exposed to oxygen-glucose deprivation, agonist activation of the EP2 receptor was protective from oxidative stress (McCullough et al., 2004). Thus, the effects of PGE_2 in inducing oxidative stress may be dependent on the stimulus involved. The specific sources of RM after PGE_2 stimulation appears to be the NOX enzymes based on EP_4 receptor activation detected in human hepatocytes in response to LPS and phorbol myristate acetate (PMA) (Sancho et al., 2011). Perhaps, the detrimental effects of PGE2 may be limited by EP receptor antagonists or enhancing the degradative PG dehydrogenase enzymes.

Prostaglandin I_2 is not just a vasodilator but also a modulator of inflammatory processes, particularly in conditions characterized by oxidative stress (Dorris and Peebles, 2012). Overexpression of PGI synthase in murine models of acute lung injury prevented bleomycin-

induced oxidative stress by enhancing the expression of antioxidant enzymes (Zhou et al., 2011). In another model, supplementation of the PGI_2 agonist, beraprost sodium, prevented aluminum-induced hippocampal oxidative stress (Pan et al., 2015) suggesting that relative deficiencies of certain oxylipids promote oxidative stress. A mechanism for the PGI_2 deficiency may be the nitration and inhibition of PGI synthase by peroxynitrite produced by the reaction of O_2^- and nitric oxide, inhibiting the formation of PGI_2 in endothelial and smooth muscle cells (Zou and Ullrich, 1996, Klumpp et al., 2005, Schildknecht and Ullrich, 2009). Oxidative stress, therefore, may have a dual effect on PGI_2 synthesis, first increasing production by indirectly stimulating the COX2 pathway and, secondly, by the direct inhibition of the activity of PGI synthase. The latter is a more likely scenario in cases of oxidative stress dominated inflammatory processes, particularly in cardiovascular conditions in which the TXA_2/PGI_2 ratio is increased. Indeed, human endothelial cells exposed to high glucose experienced oxidative stress and altered eicosanoid biosynthesis characterized by increased TXA_2 and decreased PGI_2 (Cosentino et al., 2003).

Some COX-derived oxylipids have demonstrated roles as antioxidant inducers. For example, 15-$dPGJ_2$, formed from the dehydration of PGD_2 (Shibata et al., 2002) was shown to be protective by activating PPARγ receptors (Haskew-Layton et al., 2013). The antioxidant effects of 15-PGJ_2 were also mediated by activation of the transcription factor NrF2 in glutathione-depleted astrocytes (Kansanen et al., 2009). The activation of NrF2 was mediated by 15-$dPGJ_2$ which mediated an electrophilic attack of the cysteinyl residues on KEAP1 and promoted nuclear translocation of NrF2. Through the activation of antioxidant response elements, 15-$dPGJ_2$ resulted in the induction of several antioxidant enzymes including heme oxygenase-1, SOD, and glutathione synthesizing enzymes (Shibata, 2015). In a murine macrophage cell line, RAW264.7,

15-dPGJ$_2$ inhibited inflammasome activation, which was associated with increased production of RMs during innate immune defenses (Maier et al., 2015). The multiple targets by which 15-dPGJ$_2$ may afford anti-oxidant protection and the inhibition of both NFκB and inflammasome activation, make 15-dPGJ$_2$ an attractive therapeutic target as responses may be cell and tissue specific.

Lipoxygenase-derived oxylipids

Apart from being ROS species themselves, hydroperoxides increased production of other RM from sources including the mitochondria and the NOX enzyme system. For example, the 13-HpODE induced mitochondrial RM production and cellular apoptosis via cytochrome c release, loss of mitochondrial membrane potential, and increased mitochondrial Fe^{2+} uptake in bovine aortic endothelial cells targeted antioxidants (Dhanasekaran et al., 2005). The activation of NOX was linked to subsequent mitochondrial RM production based on the depletion of mitochondrial GSH following NOX activation in endothelial cells (Doughan et al., 2008). Reduction of 15-HpETE to the hydroxy derivative (15-HETE) also induced mitochondrial ROS production in pulmonary endothelial and smooth muscle cells (Li et al., 2016). The possibility of multiple targets by the same hydroperoxides suggests that specifically targeting the pathway of their production may be more efficient in controlling oxidative stress by limiting their overall abundance of hydroperoxides in inflammatory conditions.

Changes in cellular redox status are also involved in the activation of LOX enzymes and may represent a possibility for positive feedback relationships that perpetuate detrimental oxidative damage. The ratio of reduced to oxidized coupled molecules such as reduced GSH to oxidized GSH as well as reduced Trx to oxidized Trx determine the cellular redox status (Go and Jones, 2008). Both GSH and Trx are essential co-factors in the reduction of hydroperoxides and other

RM in reactions mediated by GPx and Trx reductase enzymes, respectively (Mattmiller et al., 2013). In the process, GSH and Trx are converted to oxidized forms which must be reduced by the glutathione reductase and Trx reductase enzymes, respectively (Mattmiller et al., 2013). Maintenance of a normal GSH/GSSG ratio is critical as the depletion of GSH in hepatocytes was associated with increased RM and lipid hydroperoxides (Tirmenstein et al., 2000). The dependence of GSH/GSSG system on the availability of Se means that altered levels of this trace mineral can result in a reduction in the decrease of the GSH/GSSG ratio and the development of oxidative stress. For example, bovine mammary endothelial cells cultured in Se-deficient media showed decreased GPx activity and enhanced 15-HpETE production (Cao et al., 2000a).

The activation of another LOX isoform, 5-LOX, in B-lymphocytes was dependent on the production of O_2^- and hydroperoxides produced from granulocytes (Werz et al., 2000). The metabolism of AA by 5-LOX initially generates 5-hydroperoxyeicosatetraenoic acid (5-HpETE). Sequential reduction of 5-HpETE to the hydroxyl (5-HETE) and dehydrogenation to the ketone derivative (5-oxoETE) both require RM production. The NOX-associated oxidative burst in eosinophils and monocytes, increased the formation of the 5-oxoETE because the NOX enzymes generate NADP in releasing O_2^- (Powell et al., 1994, Erlemann et al., 2007a). Similar oxidative stress-dependent formation of 5-oxoETE formation was also shown in structural cells including human endothelial cells and intestinal and airway epithelial cells (Erlemann et al., 2006, Erlemann et al., 2007b). Because 5-oxoETE is a potent chemoattractant of leukocytes to inflammatory sites, the overproduction of 5-oxoETE could result in uncontrolled infiltration with inflammatory cells. Indirectly, excessive formation of 5-oxoETE may perpetuate the oxidative stress-inflammatory cycle by attracting immune cells with the reactive metabolite production

capacity such as neutrophils and monocytes. Targeting formation of 5-LOX-derived oxylipids may be desirable to break the oxidative stress-oxylipid synthesis cycle during inflammation.

Some LOX-derived oxylipids may indirectly exert anti-inflammatory effects by modulating the oxidative stress. For example, the DHA-derived LOX metabolite, resolvin D1, decreased oxidative stress in a murine LPS-model of acute lung injury, in part, by the reduction in lipid peroxidation, increased SOD activity, and the induction of the antioxidant HO-1 enzyme (Wang et al., 2014a). Another LOX-derived DHA metabolite, protectin, inhibited ROS production in human neutrophils stimulated by PMA by inhibiting the phosphorylation of the NOX enzyme complex (Liu et al., 2014a). Induction of ROS in RAW264.7 murine cells by 3-morpholinosydnonimine hydrochloride was diminished by the downstream LOX metabolites, 9-oxo-ODE and lipoxin A_4 (Mattmiller et al., 2014a). A possible mechanism for LXA_4 may be the demonstrated activation of NrF2 activity in an oxygen-glucose deprivation oxidative stress model in astrocytes (Wu et al., 2015). Several metabolites derived from the LOX metabolism of several PUFA, referred to as special pro-resolving metabolites ameliorate inflammatory conditions in part by diminishing oxidative stress responses (Serhan et al., 2008). Therefore, relative deficiencies of pro-resolving oxylipids may exacerbate the oxidative stress responses in various diseases.

A possible formation of RM related to LOX catalysis is the release of Fe^{2+} from the active site following suicidal inactivation. The inactivation follows the oxidation of the labile histidine residues in the active site that are responsible for chelating Fe^{2+} in place (Cheng and Li, 2007). The released Fe^{2+} becomes available for the generation of ROS including soluble hydroxyl or lipid hydroxyl radicals through the Fenton reaction (Cheng and Li, 2007, Dixon and Stockwell, 2014). The use of inhibitors of ROS generation such as deferoxamine, which chelate transition

metals including Fe^{2+} demonstrated the involvement of free Fe^{2+} in mediating oxidative stress [99]. LOX enzymes are thought to contribute to the labile pools of Fe2+ with consequent increased ROS formation thus perpetuating the oxylipid-ROS generation cycle.

Cytochrome P450-derived oxylipids

Apart from the catalytic formation of RM by CYP enzymes, the concurrent metabolism of PUFA into oxylipids may be more significant in altering cellular redox balance. For example, Hep G2 cells overexpressing the CYP enzyme isoform, 2E1, showed enhanced lipid peroxidation and apoptosis in the presence of AA in contrast to other fatty acids such as oleic acid (Chen et al., 1997). The enhanced toxicity of AA was attributed to its metabolism by the RM produced from the CYP2E1 catalytic cycle (Chen et al., 1997). However, CYP2E1 still metabolizes AA to hydroxyl metabolites despite having a minor role in the formation of CYP-derived oxylipids compared to the 2C subfamily (Rifkind et al., 1995). It is plausible that in diseases where 2E1 becomes enhanced, the capacity for metabolizing oxylipids may increase substantially and impact oxidative stress responses. It is also interesting to note that CYP2E1 demonstrated a substrate preference for n-3 PUFA to AA (Arnold et al., 2010a, Arnold et al., 2010b) and therefore may be exploited for the production of anti-inflammatory n-3-derived oxylipids. Changing the available PUFA may alter the available substrate targeted by the RM with subsequent formation of anti-inflammatory and antioxidant oxylipids.

The CYP2C subfamily has the main PUFA metabolizing isoforms which generate oxylipids whose effects on oxidative stress depend on parent substrate. The 2C9 isoforms enhance ROS production and pro-inflammatory effects of LA in endothelial cells by activating NFκB (Viswanathan et al., 2003). Increased permeability of endothelial cell monolayers to albumin after exposure to LA were predominantly the result of the formation of oxylipids known as

epoxyoctadecenoic acids (EpOME). The endothelial cell permeability was further enhanced by the subsequent conversion of the EpOMEs to dihydroxy metabolites (DiHOMEs) (Slim et al., 2001) by the soluble epoxide hydrolase enzyme (sEH). In contrast, AA epoxygenation by CYP2C9 and CYP2C8 into various epoxyeicosatrienoic acids (EET) isomers resulted in anti-oxidative and anti-apoptotic effects in endothelial cells and other cell lines (Dhanasekaran et al., 2006). The differential effects of metabolites from similar pathways illustrate the complexity of substrate-CYP interaction in modulating oxidative stress. In both AA and LA, the downstream metabolism of both epoxides from AA and LA are in part responsible for the beneficial and enhanced toxicity of these substrates, respectively. Thus by altering the proportions of available substrates, oxidative stress responses may be attenuated in conditions where CYP expression and activity are enhanced. Inhibition of the sEH enzyme could also limit the formation of more toxic oxylipids such as LA-derived DiHOMEs while simultaneously enhancing the beneficial types such as the AA-derived EETs.

The beneficial effects of EETs are mediated, in part, by their modulation of redox-sensitive transcription factors including NFκB, AP-1, NrF2, and c-Fos. Oxidative stress and apoptosis of HUVECs induced by TNFα were prevented by direct exposure to 11,12-EET and transfection with CYP2C8. The effects were attributed to EET-mediated stimulation of the antioxidant regulator, NrF2 (Liu et al., 2015) which in turn decreased TNFα-induced ROS production. Another EET isomer, 14,15-EET, also decreased oxidative stress by suppressing the expression of a transcriptional repressor of the HO-1 antioxidant protein known as Bach (Yu et al., 2015). In HUVECs and macrophages, EETs or transfection with CYP2C8 decreased macrophage chemoattractant protein 1 and interleukin-6 through PPARγ activation and inhibition of NFκB activation (Liu et al., 2014b). Although EETs do not directly activate PPARγ, the activation of

the upstream factors that are dependent on the redox-responsive phosphorylation reactions. For example, activation of signaling proteins upstream of PPARγ activation including GTP exchange factor proteins, MAPK, PI3K, Akt and, protein kinase C was involved in diminishing H_2O_2-induced apoptosis of renal epithelial cells after exposure to 14,15-EET (Chen et al., 2001). A reciprocal relationship also may exist in which activation of transcription factors that promote antioxidant activity also induce the expression of CYPs involved in EETs biosynthesis. For example, the activation of Nrf2 in HepG2 cells induced the expression of CYP2J2 (Lee and Murray, 2010). Thus maintenance of some redox imbalance sufficient to for the production of beneficial oxylipids may be necessary during some inflammatory states.

The effect of oxidative stress on CYP expression is not clear and may vary among animal species, tissue and cell type, the inciting stimulus, and specific CYP isoforms. Carbon tetrachloride-induced oxidative stress in mice was associated with increased CYP2E1 expression and lipid peroxidation (Park et al., 2010), suggesting a direct activation of this CYP isoform. In contrast, the expression of several CYP isoforms was downregulated *in-vivo* during murine LPS-sepsis models with recovery occurring 24 to 48 hours later (Theken et al., 2011). The initial downregulation of the CYP isoforms was attributed to increased cytokine production including TNFα and interleukin 6 (Theken et al., 2011). The redox activation of transcription factor NrF2 by the antioxidant inducer butylated hydroxyanisole caused the dimeric association with c-Jun and subsequent activation of CYP2J2 (Lee and Murray, 2010). The resulting production of EETs, in turn, activates NrF2 in a positive feed-forward manner. The ability of EETs to activate NrF2 was shown in both HUVECs and macrophages (Liu et al., 2015). The differential activation of CYPs in various conditions require further studies to identify optimal periods for

either blocking or enhancing expression of CYP enzymes to promote the production of antioxidant oxylipids.

Oxidative stress conditions are also associated with activation of the sEH enzyme (Zhang et al., 2012) which converts the CYP-generated epoxides to their downstream dihydroxy epoxides. The activation of sEH follows the stimulation of the redox-sensitive transcription factor, AP-1 [111]. Activation of sEH may decrease the beneficial effects of EETs by decreasing EET-dependent activation of PPARγ receptor (Liu et al., 2005). Thus, sEH inhibition is attractive in acute inflammation and chronic cardiovascular based disorders such as hypertension (Schmelzer et al., 2005, Westphal et al., 2015) where its expression is enhanced. The benefits of targeting sEH should also be explored in veterinary medicine where its expression may be enhanced.

Another major CYP-derived oxylipid formed from the hydroxylation of AA to 20-HETE is associated with oxidative stress-related vascular dysfunction in cardiovascular and cerebral circulations (Waldman et al., Lukaszewicz and Lombard, 2013). Several pathways were shown for 20-HETE induced vascular dysfunction including eNOS/HSP90 uncoupling through NFκB activation (Cheng et al., 2010). Increased NFκB following 20-HETE administration was thought to occur via production of cytokines such as TNFα (Ishizuka et al., 2008). Other mechanisms of RM production by 20-HETE involve phosphorylation of the main cytosolic NOX complex components (Medhora et al., 2008, Zeng et al., 2010) and the activation of mitochondrial RM production via the glucose-6-phosphate dehydrogenase involved in the biosynthesis of NADPH which is essential for the NOX-mediated RM production (Lakhkar et al., 2016). The resulting dysfunction in vascular tissues was due to interference with signaling pathways, whereas in cardiomyocytes and renal epithelial cells, 20-HETE-induced cytotoxicity through mitochondrial-dependent apoptosis (Nilakantan et al., 2008, Bao et al., 2011a). Chemical inhibition of 20-

HETE biosynthesis in cerebral ischemia and *in-vivo* models of spontaneous hypertension abolished the oxidative stress mediated pathology (Renic et al., 2012, Han et al., 2013, Toth et al., 2013). Pharmacological inhibition of 20-HETE biosynthesis or use of its mimetics has been utilized in several disease models and promises to be beneficial in part because of its ability to modulate of oxidative stress in many disease syndromes.

The detrimental effects of 20-HETE in chronic inflammatory conditions mediated through oxidative stress are in contrast to some reported effects of 20-HETE in acute inflammatory conditions. For example, the production of 20-HETE was diminished in an *in-vivo* murine LPS-induced sepsis model which is characterized by oxidative stress (Tunctan et al., 2013c). Follow-up studies utilizing 20-HETE mimetics in the sepsis models was shown to improve clinical effects of LPS administration such as the development of hypotension (Tunctan et al., 2013a, Tunctan et al., 2013b, Senol et al., 2016). In contrast, other studies demonstrated that murine acute inflammation models induced by LPS administration or the cecal ligation and puncture technique were associated with several orders of magnitude in the increase of 20-HETE (Willenberg et al., 2015). In particular, the mRNA for 20-HETE producing CYP isoforms were increased within 5 hours (Anwar-mohamed et al., 2010) following LPS administration and persisted up to 24 hours. In dairy cattle with severe *Escherichia coli* (*E. coli*) mastitis, significant 20-HETE production was detected simultaneously with increased oxidative stress as determined by RM production and elevated 15-F_{2t}-Isop lipid peroxidation products (Mavangira et al., 2015, Mavangira et al., 2016a). The differential effects of 20-HETE on oxidative stress in chronic and acute inflammatory require further studies to determine the usefulness of 20-HETE as a therapeutic target in different inflammatory conditions.

Oxylipids are useful biomarkers of oxidative stress

The metabolism of PUFA also occurs non-enzymatically with free radical-mediated hydrogen abstraction, followed by addition of oxygen, and intramolecular rearrangement to stable oxylipid products. The metabolism of AA, for example, generates isomers of prostaglandins known as isoprostanes (IsoPs) (Milne et al., 2011). Isoprostanes exist for each COX-derived prostanoid class of which several diastereomeric metabolites can be produced (Milne et al., 2011). Conversely, intramolecular rearrangements in some isoprostane classes such as IsoPs D_2 and E_2 are possible, adding to the pool of COX-derived oxylipid prostanoids such as PGD_2 and PGE_2 (Gao et al., 2003). The metabolism of other long chain fatty acids such as the n-3 PUFA also involves the formation of isoprostane-like metabolites at much greater rates of reactivity than AA (Milne et al., 2011) because of increasing double bonds.

Isoprostanes are currently considered the gold standard markers of oxidative stress and were utilized in human conditions with oxidative stress acute inflammatory conditions such as sepsis and in chronic diseases like atherosclerosis, coronary heart disease (Milne et al., 2015). The F_2-isoprostanes were shown to reliably detect oxidative stress induced by the free radical generators, carbon tetrachloride induced (Morrow et al., 1992) and 2,2'-azobis-2-methyl-propanimidamide, dihydrochloride (AAPH) (Yoshida et al., 2008), and in LPS-induced sepsis in mice. In neural tissue where there is an abundance of DHA, the equivalent of IsoPs known as neuroprostanes, are oxidative stress markers in neurodegenerative diseases such as Alzheimer's (Milatovic et al., 2005). Recently a specific IsoP (15-F_{2t}-IsoP) was evaluated in dairy cattle with oxidative stress during coliform mastitis (Mavangira et al., 2016b) and in other veterinary medicine species with different disease conditions (Soffler et al., 2010).

In addition to their utility as biomarkers of oxidative stress, IsoPs have potent effects on inflammatory processes, worsening or ameliorating oxidative stress responses depending on the PUFA substrate. For example, F_2-IsoPs from AA exacerbate oxidative stress by mediating TXA_2-like effects through TP receptor activation (Comporti et al., 2008, Bauer et al., 2014). In contrast, AA-derived J_2 and A_2 IsoPs and the EPA-derived F_3-isoprostanes limited proinflammatory responses through the inhibition of NFκB activation by stimuli including LPS, TNFα and IL-1β in macrophages (Musiek et al., 2005, Brooks et al., 2011). Thus, the greater reactivity of n-3 PUFAs relative to n-6 may be utilized to modulate oxidative stress responses during disease. Another significant contribution of the free-radical-mediated peroxidation is the potential contribution to the enzymatically derived oxylipids. For example, PGE_2 and PGD_2 may be biosynthesized independent of the COX pathway from the molecular re-arrangement of the free radical-generated IsoPs of the E and D series, respectively (Gao et al., 2003). Prostaglandin $F_{2\alpha}$ is another prostanoid also produced through free radical peroxidation adding to the enzymatically derived $PGF_{2\alpha}$ (Van't Erve et al., 2016). The combined source of $PGF_{2\alpha}$ may increase its pool which may also be associated with increased oxidative stress (Tian et al., 2011). Thus, in addition to being valuable oxidative stress biomarkers, the formation of some oxylipids may represent alternate pathways of biosynthesis, representing a contribution of previously unrecognized perturbations in the redox and oxidant status in some inflammatory conditions.

Other than the IsoPs, AA- derived and LA- derived hydroxyl metabolites have been utilized as oxidative stress markers. For example, 9-HETE was substantially increased in atherosclerotic plaques from clinically symptomatic coronary heart disease patients (Mallat et al., 1999). Similarly, 9-HODE from LA metabolism was increased at levels even greater than the F_2-IsoPs in unstable atherosclerotic plaques (Jira et al., 1998). These data suggest that some oxylipids may

detect oxidative stress better than IsoPs in some conditions especially in situations of imminent catastrophic pathology. More significantly, the multiplicity of oxylipids identified thus far may broaden the available oxidative stress biomarkers which may further improve detection.

Regulation of Oxylipid Metabolizing Systems – Opportunities for Intervention

The importance of regulating oxidative stress in pathological conditions such as sepsis was recognized for a long time; however, antioxidant supplementation was associated with variable efficacy (Jain and Chandel, 2013). For example, the supplementation of N-acetyl-cysteine in acute respiratory distress syndrome and severe sepsis patients increased plasma levels of reduced GSH; however, there were no improvements in mortality (Jain and Chandel, 2013). Several reasons for the lack of clinical improvement in some studies after antioxidant supplementation included study design limitations where pathology had already occurred, inability to deliver antioxidants at sites where they are needed, and challenges of accurately assessing oxidative stress (Jain and Chandel, 2013; Biswas, 2016). Targeting oxylipid biosynthesis offers an alternative for limiting oxidative stress by either diminishing pro-oxidant or enhancing antioxidant oxylipids during pathology. The regulation of oxylipid biosynthesis occurs at several levels including modification of type and abundance of available substrate, modulation of the lipid biosynthetic pathways through pharmacologic, and the degree of metabolism of specific oxylipids.

Modification of oxylipids through supplementation of PUFA substrate

Changing substrates for oxylipid biosynthesis can be achieved by dietary supplementation. For example, n-3 PUFA were increased in WBCs through dietary supplementation in humans (Calder, 2008). The increased concentrations of supplemented fatty acids translate to the biosynthesis of oxylipids from the PUFA. Similarly, pigs supplemented with AA and DHA had

elevated plasma concentrations of these PUFA and their CYP-derived oxylipids (Bruins et al., 2013). These studies demonstrate the feasibility of modifying substrates for oxylipid biosynthesis to influence the oxylipid profiles. Modification of PUFA metabolism was targeted in many disease conditions in humans and animal models to modulate inflammatory and oxidative stress with beneficial effects in some, but equivocal in others. For example, n-3 PUFA supplementation in humans with diabetic and hypertensive humans was associated with decreased urinary F_2-IsoPs without changing inflammatory cytokines like IL-6 and TNFα (Mori et al., 2003). Similarly, plasma F_2-IsoPs were decreased by EPA and DHA supplementation in overweight and dyslipidemic humans (Mas et al., 2010). In other cases, however, in-utero LPS injection in preterm mice on a fish oil diet and *in-vitro* exposure of RAW 264.7 cells to EPA and DHA were associated with oxidative stress and increased pro-inflammatory cytokine production (Boulis et al., 2014). The challenge in balancing the resulting pro- and anti- oxidative oxylipids following n-3 supplementation may explain the variable results. Much remains to be determined on how substrate supplementation can be fine-tuned to balance the anti-oxidative oxylipids and those with pro-oxidative effects during disease.

Pharmacological partial inhibition and preservation of specific oxylipids

Oxylipids can be modified by pharmacological inhibition of biosynthetic pathways involved; however, use of inhibitors may be associated with the development of complications. For example, prolonged NSAID use was associated with cardiovascular complications, renal tissue damage, and gastrointestinal ulceration (Ghosh et al., 2015). In addition, use of a COX2 inhibitor, rofecoxib, in mice was associated with the accumulation 20-HETE in plasma (Liu et al., 2010), which may provide an alternate explanation for the cardiovascular complications other than the altered PGI_2/TXA_2 ratio due to prolonged NSAID use. The complications associated

with drugs currently used in humans and veterinary medicine may be minimized by using the concept of polypharmacology where drugs are combined at lower doses so that they exert intended effects due to combined pharmacodynamic interactions (Meirer et al., 2014). This approach is expected to ensure partial production of oxylipid species necessary for mediating effective proinflammatory effects as well as those that promote inflammation resolution. Examples of polypharmacological approaches that affect oxylipid biosynthesis include the dual COX2/sEH inhibitor (Hye Khan et al., 2016) that decreased oxidative stress in diabetic rats and a dual COX/5-LOX inhibitor (Kumar et al., 2015) that decreased oxidative stress, inflammatory cytokine production, and improved cognitive function in a mouse model of neurodegeneration. Further studies are required to determine whether improved oxidative responses are the result of oxylipid profile changes and determine optimal drug combinations for different inflammatory states.

Modification of oxylipid production via modulation of other biosynthetic pathways

Evidence exists suggesting that enhancing production of oxylipids in one pathway will influence the production of oxylipids via other pathways. For example using sEH inhibitors prolongs the presence of EETs that are beneficial in both being anti-oxidative and anti-inflammatory during murine LPS-induced sepsis (Schmelzer et al., 2005). In turn, the elevated EETs were associated with decreased proinflammatory oxylipids including PGE_2 and TXB_2 (Schmelzer et al., 2005). In other diseases, humans with severe asthma characterized by oxidative stress had decreased concentrations of the anti-inflammatory and anti-oxidative lipoxin A_4 (Ono et al., 2014). Whole blood leukocytes and bronchoalveolar lavage fluid cells collected from asthmatic patients incubated with sEH inhibitors demonstrated increased production of lipoxin A_4 (Ono et al., 2014). Another useful approach is a modification of COX2 enzymes by acetylation of the active

site using aspirin to switch from PGH_2 to 15*R*-HETE which is further converted to a more potent isomer of LXA_4, 15-epi-LXA_4, by WBCs (Serhan, 1997). Thus pharmacological inhibitors can be used to preferentially promote the production of oxylipids with anti-oxidant properties while simultaneously inhibiting those with pro-oxidant properties.

Influencing the profiles of oxylipid metabolism through regulatory mechanisms

Another level for influencing oxylipid biosynthesis is targeting pathways through modifying cellular redox status. Redox regulation of oxylipid biosynthesis was recently reviewed by Mattmiller *et al.* with particular emphasis on the role played by the trace mineral Se (Mattmiller et al., 2013). Selenium is essential for maintaining the glutathione-peroxidase system vital for cellular redox balance (Mattmiller et al., 2013). Dairy cows consuming insufficient dietary Se had increased proinflammatory oxylipid production (Maddox et al., 1990). In vitro, Se deficiency of various cells altered redox tone and oxylipid biosynthesis (Cao et al., 2000b, Weaver et al., 2001, Sordillo et al., 2005, Mattmiller et al., 2014b). Supplementation of other antioxidants such as vitamins C and E in mice fed low and high fat diets decreased F_2-IsoP and 9-HETE concentrations while increasing CYP-derived and LOX-derived oxylipids (Picklo and Newman, 2015). Thus, antioxidants can be utilized to counter the production of RM directly, and also promote the production of anti-oxidative oxylipids.

The positive feedback link between oxylipid production and oxidative stress is illustrated classically by the dependency of the LOX pathway on cellular redox status. Depletion of Se in RAW264.7 cells modulated the production of several oxylipids (Mattmiller et al., 2014a) suggesting that Se represents a viable target for controlling oxidative stress in diseases. In turn, the LOX-derived oxylipids induce oxidative stress by activating several ROS producing pathways and activation of redox-sensitive transcription factors such as activator protein 1 (AP-

1) (Rao et al., 1996). Thus understanding the changes in the LOX-derived oxylipid metabolite profiles in inflammatory diseases is crucial to determine whether interventions should target the production of and limiting the degradation of the anti-oxidative oxylipids.

Conclusions and Future Directions

The accumulated evidence on the roles of PUFA oxidizing pathways and the metabolic products produced in enhancing ROS production provides insights on opportunities for modulating oxidative status in several pathologies. Approaches to enhancing oxylipids with antioxidant benefits include substrate modification, pharmacological inhibition of metabolic pathways, and targeting regulatory aspects of oxylipid biosynthesis such as Se-dependent regulation. The success of any of these approaches in diminishing oxidative stress depends on understanding many aspects of oxylipid biosynthesis during disease. First, defining the roles of individual oxylipids during disease is critical to determine the utility of targeting the given metabolite. Second, changes of oxylipid profiles in different diseases should be evaluated based on the knowledge that oxylipid profiles will differ among the various pathophysiological states. Knowledge of disease-specific oxylipid profiles will not only allow customized interventions but also provide other diagnostic metabolites that can be used for the detection of oxidative stress. Evidence has shown that the commonly used isoprostane oxylipids as gold standard oxidative stress biomarkers in humans may not always detect oxidative stress responses suggesting that other oxylipids must be explored. Combination strategies such as utilizing PUFA supplementation and combined pharmacological modification of pathways may be the more efficacious at altering oxylipid profiles to impact oxidative stress responses.

Finally, the continual improvements in diagnostic methods such as the mass spectrometry and nuclear magnetic resonance techniques will be useful in defining interactions of relevant oxylipid

biosynthetic pathways during oxidative stress. Several metabolomics approaches in disease frequently evaluate nucleic acid, protein, and carbohydrate metabolism but omit the metabolites produced through the oxylipid biosynthesis and consequently their contribution to pathological processes during disease. The comprehensive metabolomics approaches may be utilized to determine the contributions of various metabolites in oxidative stress and particularly explore the roles played by oxylipids to identify opportunities for limiting inflammatory pathology in humans and animals.

Acknowledgments

The authors acknowledge research support from the Agriculture and Food Research Initiative Competitive Grants Program (2011-67015-30179) from the USDA National Institute of Food and Agriculture, and an endowment from the Matilda R. Wilson Fund (Detroit, MI, USA).

CHAPTER 2

POLYUNSATURATED FATTY ACIDS INFLUENCE DIFFERENTIAL BIOSYNTHESIS OF OXYLIPIDS AND OTHER LIPID MEDIATORS DURING BOVINE COLIFORM MASTITIS

Vengai Mavangira,[1] Jeffery C. Gandy,[1] Chen Zhang,[2] Valerie E. Ryman,[1] A. Daniel Jones,[2,3] and Lorraine M. Sordillo*[1]

[1]Department of Large Animal Clinical Sciences, College of Veterinary Medicine, [2]Department of Chemistry, and [3]Department of Biochemistry and Molecular Biology, Michigan State University, East Lansing 48824

***Corresponding author**

Dr. Lorraine M. Sordillo,

Department of Large Animal Clinical Sciences

College of Veterinary Medicine

Michigan State University

sordillo@msu.edu

Tel: (517) 432-8821

Fax: (517) 432-8822

Publication in the Journal of Dairy Science, 2015, 98: 6206-6215. See appendix for copyright

Abstract

Coliform mastitis is a severe and sometimes fatal disease characterized by an unregulated inflammatory response. The initiation, progression, and resolution of inflammatory responses are regulated, in part, by potent oxylipid metabolites derived from polyunsaturated fatty acids. The purpose of this study was to characterize the biosynthesis and diversity of oxylipid metabolites during acute bovine coliform mastitis. Eleven cows diagnosed with naturally occurring acute systemic coliform mastitis and 13 healthy control cows, matched for lactation number and days in milk, were selected for comparison of oxylipid and free fatty acid concentrations in both milk and plasma. Oxylipids and free fatty acids were quantified using liquid chromatography-tandem mass spectrometry. All polyunsaturated fatty acids quantified in milk were elevated during coliform mastitis with linoleic acid being the most abundant. Oxylipids synthesized through the lipoxygenase and cytochrome P450 pathways accounted for the majority of the oxylipid biosynthesis. This study demonstrated a complex and diverse oxylipid network, most pronounced at the level of the mammary gland. Substrate availability, biosynthetic pathways, and degree of metabolism influence the biosynthesis of oxylipids during bovine coliform mastitis. Further studies are required to identify targets for novel interventions that modulate oxylipid biosynthesis during coliform mastitis to optimize inflammation.

Key words: inflammation, mastitis, oxylipid, lipids

Introduction

Gram-negative bacteria are a predominant cause of clinical mastitis infections in dairy cows (Erskine et al., 1988; Oliveira et al., 2013). Whereas some infections are subclinical and self-limiting, a proportion of affected cows develop an acute and severe systemic disease resulting in significant decrease in milk production and sometimes death (Erskine et al., 1988; Hogan and Smith, 2003). Subclinical and self-limiting infections are associated with a controlled inflammatory response with a prompt return to normal tissue homeostasis and milk production (Vangroenweghe et al., 2005). Acute gram-negative mammary infections, however, are characterized by dysregulated inflammatory responses elicited by LPS (Sordillo et al., 2009). Binding of LPS to toll-like receptor 4 (**TLR4**) results in activation of nuclear factor κB (**NF-κB**) with subsequent transcription and translation of proteins important for inflammatory mediator biosynthesis. Potent phospholipid mediators crucial for onset and progression of inflammation following LPS exposure also are released including platelet activating factor and oxidized lipids known as oxylipids (Corl et al., 2008).

The biosynthesis of oxylipids is preceded by release of their PUFA precursors, including linoleic acid (**LA**), arachidonic acid (**ArA**), eicosapentaenoic acid (**EPA**), and docosahexaenoic acid (**DHA**) from the *sn*-2 esterification site in the phospholipid glycerol backbone (Rosenthal et al., 1995). The abundance of PUFA in phospholipids is dependent on and can be modified by dietary FA composition in several species (Calder, 2008; Childs et al., 2008). Metabolism of PUFA may occur in situ on esterified forms in phospholipids or, more commonly, following their release and availability as FFA in the cytosol (Kuhn et al., 2015). The release of PUFA as free or pre-oxygenated fatty acids from the *sn*-2 ester linkage is mediated by phospholipase enzymes (Murakami et al., 2011). Several classes of phospholipase enzymes are known, but the cytosolic

PLA_2 (**$cPLA_2$**) is the predominant isoform class responsible for *sn*-2 ester linkage hydrolysis (Buczynski et al., 2009). The activation of $cPLA_2$ is mediated by an increase in intracellular calcium in response to several stimuli, including LPS from gram-negative bacteria (Rosenthal et al., 1995). Activation of other classes of lipases releases other bioactive lipid mediators from cell membrane phospholipids, including endocannabinoids (Zubrzycki et al., 2014a).

Regardless of PUFA type, oxygenation can occur through enzymatic pathways such as cyclooxygenase (**COX**), lipoxygenase (**LOX**), or cytochrome P450 (**CYP**) and nonenzymatic auto-oxidation mediated by some reactive metabolites (Buczynski et al., 2009). The COX enzymes are bifunctional, initially abstracting a hydrogen atom mediated by a tyrosine radical at the oxygenase site and followed by addition of dioxygen to generate prostaglandin (**PG**) G_2 (Wu et al., 2011). Then, PGG_2 is reduced at the peroxidase site of COX into the more stable PGH_2, which undergoes further metabolism by various prostaglandin synthases to a variety of bioactive prostanoids. Lipoxygenases utilize their non-heme Fe^{2+} to form ferrous hydroxide, which subsequently abstracts a hydrogen atom followed by insertion of molecular oxygen, forming a peroxy radical that is further converted to peroxy fatty acids (Kuhn et al., 2015). Similarly, cytochrome enzymes use their non-heme Fe^{2+} in mediating the oxidation, peroxidation, and hydroxylation of PUFA and some of the COX-derived prostaglandins including PGE_2 and PGD_2 (Spector et al., 2004).

The nonenzymatic oxidation of PUFA is primarily orchestrated by pro-oxidant metabolites such as reactive oxygen species (**ROS**) that include superoxide and hydrogen peroxide. Although physiologically important at low levels, ROS concentrations exceeding the cellular antioxidant capacity can induce oxidative stress where there is peroxidation of cell membrane PUFA

(Sordillo et al., 2009). In dairy cows, the transition period is associated with oxidative stress related to increased ROS production by enhanced mitochondrial metabolism (Bernabucci et al., 2005). The induction of the oxidative burst mechanism used by leukocytes in killing bacteria is another major source of ROS during infections such as mastitis (Sordillo et al., 2009). The highly reactive unpaired electrons of ROS free radicals target the double bonds in PUFA and generate oxylipids, including hydroperoxy fatty acids and isoprostanes. Such auto-oxidation of PUFA differs from the enzymatic-derived pathways, by producing an assortment of both positional and enantiomeric isomeric products because of lack of specificity as exhibited by enzymes (Milne et al., 2011).

The initial oxygenation FA products from either enzymatic or nonenzymatic oxidation are subjected to further downstream metabolism to form a diverse network of oxylipids. Prostaglandin H_2 metabolites are converted to downstream prostaglandins by specific prostaglandin synthases. For example, specific prostaglandin synthases metabolize PGH_2 to prostaglandins D_2, E_2, $F_{2\alpha}$, and I_2. The LOX-derived peroxy FA are further converted into leukotrienes, lipoxins, resolvins, and protectins (Kuhn et al., 2015), whereas CYP-derived fatty acid epoxides are further converted to fatty acid diols by soluble epoxide hydrolases. At least 140 oxylipids have been characterized to date, most with potent regulatory effects on inflammation (Tam, 2013).

Oxylipid biosynthesis is complex and is regulated by available PUFA substrates, activation of oxygenation pathways, and the extent to which initial oxygenation products are metabolized. A broader understanding of oxylipid diversity, changes in patterns of oxylipid accumulation, and their direct effects on inflammatory responses during bovine mastitis is required to enable

evaluation of efficacious intervention modalities that promote resolution of inflammation. The purpose of this study, therefore, was to investigate the biosynthesis of oxylipid metabolites during acute naturally occurring coliform mastitis infection in dairy cows. Based on previous studies documenting increased FFA during mastitis (Atroshi et al., 1989a,b), the hypothesis for this study was that oxylipid biosynthesis would be correlated with their FFA substrates in both milk and plasma during naturally occurring bovine coliform mastitis.

Materials and Methods

Chemicals

Acetonitrile, methanol, and formic acid of liquid chromatography-mass spectrometry grade were purchased from Sigma-Aldrich (St. Louis, MO). Deuterated and nondeuterated oxylipid standards were purchased from Cayman Chemical (Ann Arbor, MI). Butylated hydroxy toluene was purchased from ACROS (Thermo Fisher, Fair Lawn, NJ), EDTA and triphenylphosphine were purchased from Sigma-Aldrich, and indomethacin was purchased from Cayman Chemical.

Animals

This study was approved by the Michigan State University Institutional Animal Care and Use Committee (IACUC) and cows were enrolled with client consent. The study was conducted at a commercial dairy operation in Michigan with about 3,300 lactating cows with an approximate rolling herd average milk production of 12,250 kg. Cows were housed in free stall barns and grouped according to lactation number, DIM, and milk yield. Cows were milked 2 times daily. Diets were formulated to meet the energy requirements based on production (Table 1) and feed was delivered 2 times/d as TMR.

Study Design

Twenty-four multiparous dairy cows of at least third lactation were enrolled and divided into coliform mastitis (n = 11) and healthy control (n = 13) groups. The coliform mastitis group cows had cultured positive for *Escherichia coli* in milk samples and exhibited signs of systemic clinical disease. Negative bacterial cultures on milk, absence of overt clinical signs, and an SCC of <250,000 cells/mL on last test day were required for the healthy control group. Bacterial milk cultures were performed on blood agar and selective media for coliform bacteria according to the National Mastitis Council guidelines (Hogan et al., 1999). Briefly, individual mammary gland quarter milk (10 μL) was streaked onto a sheep blood agar and selective media using a sterile loop inoculator. Cultures were incubated at 37°C, read at 24 and 48 h, and considered positive for coliform growth based on presence of 3 or more colonies on both blood and selective media. Clinical signs for diagnosis of acute systemic coliform mastitis included elevated rectal temperature (>39.2°C), tachycardia (heart rate >80 beats/min), tachypnea (respiratory rate >30 breaths/min), episcleral injection, local signs of mammary gland inflammation including discoloration, swelling, heat, pain on palpation, and typical serum-like watery milk. Cows in the mastitis group had heavy coliform bacterial growth (>100 cfu) on milk culture and at least 2 of the clinical signs of systemic disease. Milk and blood samples were collected at the same time from each cow within 12 h following a clinical diagnosis of systemic coliform mastitis and from the lactation and DIM matched healthy control cows.

Lipidomics

Targeted PUFA, MUFA, SFA, and oxylipids were quantified using liquid chromatography tandem mass spectrometry (LC-MS/MS). Plasma from whole blood collected in EDTA anticoagulant and milk samples were mixed with an antioxidant reducing agent mixture to

prevent degradation of preformed oxylipids and prevent ex vivo lipid peroxidation (O'Donnell et al., 2009). The antioxidant reducing agent mixture consisted of 50% methanol, 25% ethanol, and 25% water with 0.9 m*M* butylated hydroxy toluene, 0.54 m*M* EDTA, 3.2 m*M* triphenylphosphine, and 5.6 m*M* indomethacin. Samples were flash frozen in liquid nitrogen and stored at −80°C until analyses.

Internal Standards

A mixture of internal standards containing 5(S)-hydroxyeicosatetraenoic-d_8 acid [5(S)-HETE_d_8], 15(S)-hydroxyeicosatetraenoic-d_8 acid [15(S)-HETE_d_8], 8(9)-epoxyeicosatrienoic-d_{11} acid [8(9)-EET_d_{11}], prostaglandin E2-d_9 (PGE2_d_9), 8,9-dihydroxyeicosatrienoic-d_{11} acid (8,9-DHET_d_{11}), arachidonic acid-d_8 (AA_d_8), 2-arachidonoyl glycerol-d_8 (2-AG_d_8), and arachidonoyl ethanolamide-d_8 (AEA_d_8) was prepared to final concentrations of 0.25, 0.25, 0.5, 0.5, 0.25, 50, 2, and 0.25 µ*M*, respectively. The internal pure standards mixture was added into each sample and used to generate a 6-point standard curve ranging from 500 to 0.001 µ*M* in concentration of unlabeled fatty acid and oxylipid standards.

Sample Processing

Frozen plasma and whole milk samples were thawed on ice and processed as follows: 4 mL of milk was combined with 9.15 mL of 4°C acetonitrile, and 2 mL of plasma was combined with 5 mL of 4°C methanol and 2 µL of 88% formic acid. To each sample mixture, 15 µL of internal standard cocktail was added, and the sample was vortexed for 2 min, incubated at room temperature for 15 min, and centrifuged at 4,816 × *g* for 20 min at 4°C. For plasma, the supernatant was diluted with 95 mL of HPLC-grade water and 95 µL of formic acid, and

supernatant in milk samples was diluted with 170 mL of HPLC-grade water and 170 µL of formic acid.

Solid-Phase Extraction

Solid-phase extraction was performed for each sample with Oasis HLB 12cc (500 mg) LP Extraction Columns (Waters, Milford, MA). Columns were conditioned with 6 mL of methanol followed by 6 mL of HPLC water. Extracts were loaded onto the columns, which were then washed with 6 mL of 20% methanol and dried under full vacuum for 4 min. Analytes were eluted with 6 mL of methanol:acetonitrile 50:50 (vol:vol). The volatile solvents were removed under vacuum using a Savant SpeedVac (ThermoQuest, Holbrook, NY). The residues were reconstituted in 100 µL of methanol and transferred to a microcentrifuge tube containing 50 µL of water. The mixture was centrifuged at 14,000 × *g* for 10 min at 4°C and then the supernatant was transferred to an auto-sampler vial with a low volume insert and stored at −20°C until analyzed.

LC-MS/MS Analyses

The quantification of metabolites was accomplished on a Waters Acquity UPLC coupled to a Waters Xevo TQ-S triple quadrupole mass spectrometer (Waters) using multiple reaction monitoring. Chromatography separation was performed with an Ascentis Express C18 HPLC column, 10 cm × 2.1 mm, 2.7 µm (Supelco, Bellefonte, PA) held at 50°C. The autosampler was held at 10°C. Mobile phase A was water with 0.1% formic acid, and mobile phase B was acetonitrile. Flow rate was fixed at 0.3 mL/min. Liquid chromatography separation took 15 min with linear gradient steps programmed as follows (A:B ratio): time 0 to 0.5 min (99:1), to (60:40) at 2.0 min; to (20:80) at 8.0 min; to (1:99) at 9.0 min; 0.5 min held at (1:99) until min 13.0; then

return to (99:1) at 13.01 min, and held at this condition until 15.0 min. All oxylipids and fatty acids were detected using electrospray ionization in negative-ion mode, whereas the endocannabinoids were detected using positive-ion mode. Cone voltages and collision voltages were optimized for each analyte using Waters QuanOptimize software (see Table 2 for multiple reaction monitoring parameters).

Statistical Analyses

Statistical analyses were performed using SAS software (version SAS 9.4; SAS institute Inc., Cary, NC). Data were expressed as means ± standard errors of the mean and tested for normality. Where Gaussian distribution was satisfied, *t*-tests for independent means were performed. Data deviating from the Gaussian distribution were either square root- or log-transformed before analyses. An ANOVA and Tukey test for comparison between means were performed to determine differences among FA concentrations in the same sample type (milk or plasma). Pearson correlations were calculated for multiple relationships among FA substrates; FA substrates and their oxylipid metabolites; related upstream and downstream oxylipid metabolites and concentrations of the same substrate/metabolite in milk versus plasma. The levels of significance for correlation analyses were adjusted for multiple comparisons. Statistical significance was set at $\alpha = 5\%$, and data are presented as means ± SEM.

Results

Fatty acids quantified in milk and plasma included PUFA (ArA, LA, EPA, and DHA), MUFA (oleic acid), and SFA (palmitic and stearic acids). All PUFA concentrations were greater in milk during coliform mastitis; however, only the elevations in LA concentrations were reflected systemically in plasma (Figure 2). Fold differences of PUFA in milk between mastitis and

healthy cows were highest for LA (5.1) followed, in decreasing order, by ArA (3.8), DHA (3.0), and EPA (2.4). Linoleic acid was the most abundant PUFA in both milk and plasma in both mastitis and healthy cows (Figure 2). Higher concentrations of oleic acid in milk during coliform mastitis were reflected systemically in plasma, whereas no differences in the SFA were detected (Figure 3).

A lipidome of 63 oxylipid species was targeted by the LC-MS/MS protocol used in this study. Thirty oxylipids were detected in milk and 27 were detected in plasma. The oxylipids leukotriene B_4 (LTB_4), 8,9-epoxyeicosatrienoic acid (8,9-EET), and 17-hydroxydocosahexaenoic acid (17-HDoHE) were detected in milk only and accounted for the differences in the number of detected oxylipids between milk and plasma. A significantly ($P < 0.05$) higher proportion of the fraction of total oxylipid changes was observed in milk oxylipids (60%) compared with plasma oxylipids (32%) during coliform mastitis. Oxylipids that were not detectable in 50% or more cows in the study groups were excluded from all statistical analyses and are reported together with their corresponding limits of detection (Table 3). The limit of detection was defined as the concentration at which the peak response for an analyte was 3 times that of the noise (signal:noise = 3).

Oxylipids detected were representative of the known enzymatic pathways (COX, LOX, and CYP) and nonenzymatic pathways. The COX pathway was represented by prostaglandin metabolites from ArA metabolism, accounting for only 8 and 9% of the fraction of total oxylipids in milk and plasma, respectively. Concentrations of PGE_2 and 6-keto$PGF_{1\alpha}$ were elevated significantly in milk (Table 4), but only the concentrations of 6-keto$PGF_{1\alpha}$ (a stable metabolite of PGI_2) were reflected systemically in plasma.

Lipoxygenase-derived oxylipids (Table 5) accounted for the highest proportion of the fraction of total oxylipid metabolites detected in both milk (48%) and plasma (45%). The hydroxy metabolite concentrations, 9- and 13-hydroxyoctadecadienoic acids (HODE) from LA and 5- and 15-hydroxyeicosatetraenoic acids (HETE) from ArA were elevated in milk during coliform mastitis; however, their respective downstream ketone derivatives 9- and 13-oxooctadecadienoic acid (oxoODE) from LA and 5- and 15-oxoeicosatetraenoic acid (oxoETE) from ArA were not different. Lipoxygenase-derived LTB_4 and lipoxin A_4 (LXA_4) similarly were elevated in milk, but LXA_4 was significantly lower in plasma during mastitis. The DHA metabolite resolvin D_2 (RvD_2) was significantly decreased in plasma during mastitis.

The CYP enzymatic metabolism of LA, ArA, and EPA generated oxylipids that accounted for 36 and 36% of the fraction of total oxylipids detected in milk and plasma, respectively (Table 6). The epoxidation metabolites of LA, epoxyoctadecenoic acids (9,10- and 12,13-EpOME), were significantly elevated in milk of coliform mastitis cows but the epoxide hydration products (dihydroxyoctadecenoic acids; 9,10- and 12,13-DiHOME) were significantly lower in plasma of mastitis cows. In contrast, the ArA epoxide 11,12-epoxyeicosatrienoic (EET) was elevated in plasma of control cows. The hydroxylation product of ArA, 20-HETE, was elevated in both milk and plasma during coliform mastitis. Although the EPA vicinal diols 14,15- and 17,18-dihydroxyeicosatetraenoic acid (DiHETE) were increased in milk during coliform mastitis, significantly lower concentrations of the 14,15-DiHETE isomer were detected in plasma.

The nonenzymatic metabolites from AA (hydroxyeicosatetraenoic acids; 9- and 11-HETE) were abundant in milk, but not in plasma during mastitis. Consequently, nonenzymatic metabolites accounted for only 8 and 9% of the fraction of total oxylipids in milk and plasma, respectively

(Table 7). The relative contribution of nonenzymatic auto-oxidation of LA into 9- and 13-HODE was not determined.

Relative contributions of metabolic pathways to oxylipid biosynthesis were assessed from ratios of metabolites of different pathways from the same PUFA substrate (Table 8). In both milk and plasma, the lack of differences between mastitis and control cows in the ratios 13-HODE to 9-HODE and 9- and 11-HETE to 15-HETE suggested lack of pathway preference for LA and ArA, respectively. However, there was a shift from epoxidation of ArA toward hydroxylation into 20-HETE in milk during coliform mastitis.

Ratios representing the progressive metabolism of oxylipids such as the conversion of hydroxy oxylipids to ketone derivatives (HODE to oxoODE; HETE to oxoETE) and epoxides to vicinal diols (EpOME to DiHOME) were compared between groups (Table 9). Ratios suggesting greater (when >1) abundance of hydroxy metabolites were detected for both milk and plasma in all cows; however, only the ArA-derived metabolites in coliform mastitis milk samples and 13-HODE:13-oxoODE in plasma of control cows were significant. The within-group epoxide-to-vicinal diol ratios suggested abundant 12,13-EpOME (>1) and lesser 9,10-EpOME (<1) isomers in coliform mastitis cows and greater vicinal diols (<1) in control cows. Numerical values of the epoxide-to-vicinal diol ratios were greater significantly in coliform than in control cows.

Several significant correlations were detected among quantified metabolites (FA, FA and oxylipids, oxylipid to oxylipid) in milk and plasma from coliform mastitis cows (Tables 10, 11, and 12). Interestingly, no correlations could be detected for several metabolites between the milk and plasma samples, especially in the coliform mastitis group. Endocannabinoid metabolites derived from ArA and DHA only were detected with significantly higher concentrations of arachidonyl ethanolamide (mastitis, 1.5 ± 0.2 n*M* vs. control 0.07 ± 0.01 n*M*; $P < 0.0001$) and

docosahexanoyl ethanolamide (mastitis, 1.5 ± 0.05 n*M* vs. control 1.1 ± 0.004 n*M*; $P < 0.001$) in milk, but not in plasma, during coliform mastitis.

Discussion

Polyunsaturated fatty acids are essential substrates that play a critical role in the synthesis of oxylipids during health and inflammatory processes. The elevations of all PUFA assessed in milk in this study agree with previous findings of increased LA, ArA, and EPA in milk from bovine mastitis (Atroshi et al., 1989b). Mastitis in humans is also associated with increased long-chain FA in milk (Hunt et al., 2013). The increased PUFA suggest abundance of oxylipid precursor substrates whose sources may include increased lipolysis, dietary lipids, and de novo biosynthesis from essential FA. Although sources of FA were not evaluated in this study, increased lipolysis related to elevated tumor necrosis factor α (TNFα), may have contributed to increased PUFA substrate (Hoeben et al., 2000). For example, previous studies showed that plasma TNFα concentrations increase significantly with bovine coliform mastitis (Sordillo and Peel, 1992). Experimental injection of TNFα and the associated decrease in DMI increased adipose tissue lipolysis in cows (Kushibiki et al., 2003). Although plasma NEFA, an indicator of lipolysis, were not measured in this study, increased lipolysis could be supported by significant elevations in oleic acid in this study, a known abundant component of plasma NEFA in dairy cows during times of increased lipolysis (Contreras and Sordillo, 2011).

The simultaneous evaluation of metabolites in milk and plasma during coliform mastitis showed substantial differences in oxylipid profiles even with the presence of systemic disease. Similarly, mice with LPS-induced sepsis demonstrated different oxylipid profiles among various tissue locations (Balvers et al., 2012). Consequently, oxylipid concentrations in one biological sample cannot be used to infer oxylipid profiles in a different anatomic area. The lack of correlations in

concentrations of several oxylipids between milk and plasma during mastitis (Table 11) suggests that the microenvironment of the affected tissues can greatly influence oxylipid biosynthesis. Concentrations of milk and plasma PUFA substrates differed during coliform mastitis and can be explained by several factors. First, milk production decreases precipitously during coliform mastitis, resulting in elevated concentrations of milk components, including FFA (Shuster et al., 1991). Second, the disruption of the blood mammary endothelial barrier and increased blood flow to the mammary gland during coliform mastitis could result in increased transfer of long-chain FA into the mammary gland (Wenz et al., 2001). For example, previous studies in mice with LPS-induced peritonitis showed that increased n-3 fatty acids intravenously pre-infused were detected in peritoneal exudates (Kasuga et al., 2008). Increasing plasma concentrations of select PUFA types such as the n-3 FA may be a direct source of PUFA for localized inflammatory sites. Thus, plasma PUFA may be increased by their dietary supplementation or precursor essential FA such as LA and α-linoleic acid to support de novo biosynthesis of PUFA.

The variety of oxylipids expressed in both milk and plasma in this study represented some of the well-known enzymatic and nonenzymatic oxylipid biosynthetic pathways. Earlier studies on bovine coliform mastitis reported a few select prostanoids including PGE_2, $PGF_{2\alpha}$, and thromboxane B_2 in milk using immunoassay based detection techniques (Atroshi et al., 1989a). In the current study, the use of LC-MS/MS provided a more robust methodology to identify an expanded oxylipid network during acute bovine coliform mastitis.

Oxylipids generated from the COX pathway in the current study were represented only by PGE_2 and the inactive downstream metabolite of PGI_2, 6-keto$PGF_{1\alpha}$. Both PGI_2 and PGE_2 are produced by constitutive COX-1 and inducible COX-2 isoforms and are important for the

vasodynamic responses during initial stages of inflammation (Bulger and Maier, 2000). In addition to maintaining basal prostanoid production, COX-1 isoforms are responsible for the initial prostanoid synthesis during inflammation before induction of the transcriptionally and translationally dependent COX-2 isoform (Pober and Sessa, 2007). Previous experimental and natural bovine coliform mastitis studies reported increased concentrations of PGE_2, PGI_2, $PGF_{2\alpha}$, and thromboxane B_2. Inhibition of COX enzymes using nonsteroidal anti-inflammatory drugs (NSAID) reduces prostanoid and thromboxane concentrations, with subsequent improved clinical signs (Anderson et al., 1986). Use of NSAID in veterinary medicine, however, is associated with complications such as abomasal ulceration and renal toxicity (Anderson and Muir, 2005). Defining the variety and temporal generation of COX-derived oxylipids during coliform mastitis may identify optimal times for pharmacologic inhibition of COX enzymes. In acute bovine coliform mastitis, for example, early NSAID use may not be optimal as oxylipid products of COX enzymes mediate crucial processes during early stages of acute inflammation.

The LOX-derived metabolites accounted for the majority of oxylipids detected in the present study. Several lines of evidence showed that LOX generates both pro- and anti-inflammatory oxylipids. For example, development of atherosclerosis in humans is associated with increased 15LOX mRNA expression and hydroxy metabolites including 15-HETE and 9- and 13-HODE (Gertow et al., 2011). Several oxylipids, including lipoxin A_4, resolvins, protectins, and maresins in several murine models of sepsis, are associated with shorter time to inflammation resolution and improved survival (Serhan et al., 2008). In dairy cows, *15LOX1* gene expression was increased in mammary gland tissues during the periparturient period, suggesting a potential contribution to oxidative stress in transition cows (Aitken et al., 2009). Oxidative stress was suggested as contributing to predisposing periparturient cows to dysregulated inflammatory

conditions including mastitis (Sordillo and Mavangira, 2014). Nonspecific inhibition of LOX in combination with flunixin meglumine, a COX inhibitor, was associated with improved bovine mammary gland inflammation (Rose et al., 1991). Taken together, these data demonstrate the need to clearly define the role of LOX-derived oxylipids in the pathophysiology of coliform mastitis to explore potential targets and optimal times for therapy or interventions.

The metabolism of PUFA through CYP enzymes showed significant elevations in various epoxides of ArA, LA, and EPA. Several epoxide metabolites were identified as unexplored targets for therapy with potent anti-inflammatory effects (Morisseau and Hammock, 2013). For example, with LPS-induced peritonitis, inhibiting hydration of epoxides decreased pro-inflammatory cytokines, abrogated hypotension, and diminished mortality compared with control mice (Schmelzer et al., 2005). Furthermore, pro-inflammatory metabolites of COX and LOX pathways such as PGE_2 and 5-HETE, respectively, were decreased, suggesting an indirect influence of CYP epoxides on acute inflammatory pathways (Schmelzer et al., 2005). Conversely, CYP hydroxylation of ArA produces 20-HETE, a potent hypertensive oxylipid during inflammation (Konkel and Schunck, 2011). Epoxides of LA origin are associated with acute respiratory distress syndrome following sepsis in humans (Konkel and Schunck, 2011), suggesting that FA substrate and relative abundance of their derived oxylipids may affect the inflammatory phenotype. Defining the relative contributions of CYP derived epoxides from different PUFA is critical to balance between the beneficial anti-inflammatory species and the pro-inflammatory 20-HETE and LA epoxides. The apparent shift from epoxidation into hydroxylation of ArA (Table 8) in the current study suggests a contribution of pro-inflammatory 20-HETE to the acute inflammatory phase during bovine coliform mastitis. The ability of epoxides to downregulate pro-inflammatory metabolites from other biosynthetic pathways may

make them particularly attractive because of a multimodal mechanism that may be very effective at resolving inflammation.

Several PUFA metabolites exhibit different levels of metabolism producing distinct oxylipid species with specific effects on the inflammatory process. For example, LA is initially oxygenated to hydroperoxy acids (9- and 13-HPODE) that are subsequently reduced by peroxidases to hydroxy acids (9- and 13-HODE). Dehydrogenase enzymes eventually convert the hydroxy acid metabolites into ketone derivatives (9- and 13-oxoODE). The hydroperoxy oxylipid 13-HPODE activates the pro-inflammatory transcription factor NFκB in vascular smooth muscle cells (Natarajan et al., 2001). In addition, another hydroperoxy metabolite, 15HPETE, mediates inflammation and apoptosis in bovine aortic endothelial cells (Sordillo et al., 2005). Hydroxy metabolites (HODE and ArA-derived HETE) are associated with either pro- or anti-inflammatory states in cardiovascular and other diseases (Kuhn et al., 2015). The ketone derivatives have predominantly anti-inflammatory effects. For example, 13-oxoODE reduces pro-inflammatory IL-8 through peroxisome proliferator-activated receptor gamma activation in human colonic epithelial cells (Altmann et al., 2007). Together, these data suggest that the degree of PUFA catabolism during inflammation may affect the duration, phenotype, and outcome of inflammatory process. Although upstream oxylipids were positively correlated with their downstream derivatives in the current study (Tables 10 and 11), the abundance of ArA- and LA-derived hydroxy oxylipids suggests an overproduction or decreased dehydrogenation to the ketone derivatives, indicating a pro-inflammatory oxylipid profile. Studying the temporal patterns of the degree of metabolism of PUFA and the specific effects of their oxylipid metabolites during inflammation may uncover targets for enhancement or blockade of metabolic pathways to modulate inflammation.

The roles for endocannabinoid metabolites from ArA and DHA that accumulated during coliform mastitis are not immediately clear. In a rat model of LPS-induced uveitis, activation of cannabinoid CB2 receptors was associated with reduction in the pro-inflammatory transcription factors, pro-inflammatory cytokines, and leukocyte endothelial adhesion (Toguri et al., 2014). The endocannabinoid system was reviewed recently as a potential inflammation modulatory target in various human diseases (Zubrzycki et al., 2014a,b). In cows, endocannabinoids were detected in milk from healthy animals (Gouveia-Figueira and Nording, 2014). Further investigations may be useful to determine the presence and influence of cannabinoid receptors on mammary gland inflammation.

Conclusions

In conclusion, oxylipid generation during acute bovine coliform mastitis is influenced by substrate availability, multiple biosynthetic pathways, and different degrees of metabolism. The use of LC-MS/MS offers a sensitive and specific technique that can be utilized to evaluate novel targets in oxylipid biosynthesis for diagnostic and therapeutic interventions in inflammatory conditions, including coliform mastitis. Additionally, biomarkers that reflect oxylipid profiles and inflammatory phenotype during disease can be developed. The detection of several localized changes in oxylipid biosynthesis in the presence of systemic disease suggests focusing specifically on the mammary gland environment in developing and evaluating interventions to modulate inflammation during mastitis.

Acknowledgements

The authors acknowledge the staff and resources at the Michigan State Research Technology Support Facility Mass Spectrometry and Metabolomics Core (East Lansing), especially Scott Smith. The Waters Xevo TQ-S mass spectrometer was purchased using funds from the Great Lakes Fishery Commission (Ann Arbor, MI). The authors thank Sasha Kravchenko at the Michigan State Plant, Soil and Microbial Sciences department for assistance with statistical analyses. The authors thank Louis M. Neuder, and Jill Brester (Michigan State University, Teaching Center for Dairy Professionals) and the owners and staff at the participating dairy. This work was funded through the Michigan AgBioResearch project MICL02143 and through grant 2011-67015-30179 from the Agriculture and Food Research Initiative Competitive Grants Programs of the USDA National Institute for Food and Agriculture (Washington, DC).

CHAPTER 3

15-F_{2t}-ISOPROSTANE CONCENTRATIONS AND OXIDANT STATUS IN LACTATING DAIRY CATTLE WITH ACUTE COLIFORM MASTITIS

Vengai Mavangira,[1] Martin J. Mangual,[1] Jeffery C. Gandy,[1] and Lorraine M. Sordillo*[1]

[1]Department of Large Animal Clinical Sciences, College of Veterinary Medicine, Michigan State University, East Lansing 48824

***Corresponding author**

Dr. Lorraine M. Sordillo,

Department of Large Animal Clinical Sciences

College of Veterinary Medicine

Michigan State University

sordillo@msu.edu

Tel: (517) 432-8821

Fax: (517) 432-8822

Publication in the Journal of Veterinary Internal Medicine, 2016, 30: 339-347. Open access

Abstract

Background: Severe mammary tissue damage during acute coliform mastitis in cattle is partially caused by oxidative stress. Although considered a gold standard biomarker in some human conditions, the utility of 15-F_{2t}-Isoprostanes (15-F_{2t}-Isop) in detecting oxidative stress in dairy cattle has not been validated.

Hypothesis: Concentrations of 15-F_{2t}-Isop in plasma, urine, and milk correlate with changes in oxidant status during severe coliform mastitis in cattle.

Animals: Eleven lactating Holstein-Friesian dairy cows in their 3rd–6th lactation.

Methods: A case–control study using cows with acute coliform mastitis and matched healthy controls were enrolled into this study. Measures of inflammation, oxidant status, and redox status in plasma and milk samples were quantified using commercial assays. Plasma, urine, and milk 15-F_{2t}-Isop were quantified by liquid chromatography/tandem mass spectrometry (LC-MS/MS) and ELISA assays. Data were analyzed by Wilcoxon rank sum tests ($\alpha = 0.05$).

Results: Plasma 15-F_{2t}-Isop quantified by LC-MS/MS was positively correlated with systemic oxidant status ($r = 0.83$; $P = .01$). Urine 15-F_{2t}-Isop quantified by LC-MS/MS did not correlate with systemic oxidant status, but was negatively correlated with redox status variables ($r = -0.83$; $P = .01$). Milk 15-F_{2t}-Isop quantified by LC-MS/MS was negatively correlated ($r = -0.86$; $P = .007$) with local oxidant status. Total 15-F_{2t}-Isop in milk quantified by a commercial ELISA (cbELISA) was positively correlated with oxidant status in milk ($r = 0.98$; $P < .001$).

Conclusions and Clinical Importance: Free plasma 15-F_{2t}-Isop quantified by LC-MS/MS and total milk 15-F_{2t}-Isop quantified by cbELISA are accurate biomarkers of systemic and mammary

gland oxidant status, respectively. Establishing reference intervals for free and total 15-F_{2t}-Isops for evaluating oxidative stress in dairy cows should currently be based on the LC-MS/MS method.

Key words: Inflammation, lipid peroxides, oxylipids, oxidative stress, redox status

Introduction

Escherichia coli bacteria are a major cause of clinical coliform mastitis in dairy cattle (Oliveira et al., 2013). Uncontrolled bacterial replication caused by dysfunctional immune responses results in severe mammary tissue damage and death (Frost and Brooker, 1986, Burvenich et al., 2003). Excessive production of reactive metabolites (RM) by phagocytic cells results in oxidative mammary tissue damage observed during coliform mastitis (Burvenich et al., 2004). Increased metabolism of polyunsaturated fatty acids (PUFA) such as arachidonic acid (AA) generates lipid hydroperoxides that contribute to the RM pool (Sordillo and Aitken, 2009). Enhanced mitochondrial metabolism also contributes large amounts of superoxide ions to the toxic pool of RM during inflammation (Sordillo and Aitken, 2009). Oxidative stress occurs when elevated RM overwhelm the antioxidant defenses and induce tissue damage (Lykkesfeldt and Svendsen, 2007). Antioxidants include enzymatic and nonenzymatic systems that quench the damaging effects of RM (Sordillo and Aitken, 2009). The role of oxidative stress in clinical coliform mastitis was demonstrated by the increased severity of disease associated with decreased vitamin C and increased lipid hydroperoxides. In addition, supplementation of vitamin E and selenium in the transition period decreased the severity of clinical disease (Smith et al., Weiss et al., Ranjan et al., 2005). Reliable biomarkers of oxidative stress in cattle are currently lacking despite experimental evidence supporting the critical role of RM in the pathophysiology of coliform mastitis in cattle (Celi, 2011).

Lipids are particularly sensitive to RM attack resulting in generation of lipid hydroperoxides and isoprostanes (Lykkesfeldt and Svendsen, 2007). Isoprostanes are prostaglandin-like metabolites of nonenzymatic peroxidation of AA (Milne et al., 2011). Formation of these chemically stable peroxidation end-products starts with the free radical-mediated generation of an AA peroxyl

radical followed by the cyclization into an F-pentane peroxyl ring that is then immediately reduced to F_2-isoprostanes (Milne et al., 2011). A total of 64 F_2-isoprostane isomeric compounds from AA are generated and can be detected in biological samples by chromatography and mass spectrometry methods (Milne et al., 2015). However, 15-F_{2t}-Isoprostanes (15-F_{2t}-Isop, also known as 8-isoprostanes) were the major isoform validated as gold standard markers of oxidative stress in humans (Morrow et al., 1992b, Milne et al., 2015). Immune-based assays such as ELISAs that are specific to the common pentane ring in isoprostanes are used for 15-F_{2t}-Isop detection in some human biological samples, but are less accurate than the gold standard mass spectrometry techniques (Basu, 1998, Janicka et al., 2013).

The detection of oxidative stress in cattle utilizes lipid hydroperoxides that are quantified by measuring their low molecular weight degradation aldehyde products such as malondialdehyde (MDA) using the thiobarbituric acid reactive substances (TBARS) method (Janero, 1990). The TBARS method, however, lacks specificity to the lipid-derived MDA because they can react with metabolites derived from other macromolecules including DNA and polysaccharides (Celi, 2011). Therefore, determining the utility of 15-F_{2t}-Isop might provide an accurate marker for diagnosis of oxidative stress and monitoring treatment responses in veterinary medicine (Milne et al., 2011).

To date, 15-F_{2t}-Isop was not evaluated as biomarkers of oxidative stress during acute coliform mastitis. The purpose of this study, therefore, was to determine whether 15-F_{2t}-Isop could predict systemic and local mammary gland oxidant status during coliform mastitis using liquid chromatography/tandem mass spectrometry (LC-MS/MS). The potential utility of using commercial ELISA assays**,** validated for use in samples from humans, also were evaluated as

alternative 15-F_{2t}-Isop quantification techniques on bovine samples. The hypothesis for this study was that 15-F_{2t}-Isop in plasma, urine, and milk correlate with the oxidant status associated with severe bovine coliform mastitis. This study determined both the utility of 15-F_{2t}-Isop as a biomarker of oxidative stress and provided a basis for defining reference intervals for evaluating oxidative stress associated with clinical and subclinical coliform mastitis.

Materials and Methods

Animals

Control and coliform mastitis cows in this study (n = 4/group) were randomly selected from larger groups with housing and diet information published elsewhere (Mavangira et al., 2015). Another group of healthy cows (n = 3) was selected for assessment of ELISA assays before utilizing them in analyses of samples from the control and coliform mastitis study groups. This study was approved by the Michigan State University Institutional Animal Care and Use Committee (IACUC) and all cows were enrolled from the same herd with client consent.

Study Design

All cows enrolled in this study were multiparous Holstein dairy cows that ranged from 3rd to 6th lactation and averaged 69 (3–105) days in milk. Cows affected with acute coliform mastitis (n = 4) and matched healthy control (n = 4) made up the 2 experimental groups. The average body condition score was 3.06 (range: 2.75–3.50) for control cows and 3.00 (range: 2.50–3.50) for coliform mastitis cows. Cows in the coliform mastitis group had positive *E. coli* milk cultures (>100 colony forming units) and exhibited at least 2 signs of systemic clinical disease. Signs of acute systemic coliform mastitis included increased rectal temperature (>39.2°C), tachycardia (heart rate > 80 beats/minute), tachypnea (respiratory rate > 30 breaths/minute), episcleral

injection, local signs of mammary gland inflammation including discoloration, swelling, heat and pain on palpation, and typical serum-like watery milk. By the time of sampling, coliform mastitis affected cattle had received at least a single dose of flunixine meglumine (2.2 mg/kg IV), ceftiofur sodium (2.2 mg/kg SC), and oral electrolyte fluids after standard farm treatment protocols. Healthy control cows had negative bacterial milk cultures, absence of overt clinical signs and a somatic cell count of <250,000 cells/mL on the last test day before the start of the study. Bacterial milk cultures were performed according to the National Mastitis Council guidelines (Hogan, 1999). Milk and blood samples were collected at the same time from mastitis and healthy control cows within 12 hours following a clinical diagnosis of systemic coliform mastitis.

Sample Collection and Analyses

Blood samples were collected in serum-separator and EDTA tubes, whereas urine and milk samples were collected in plain 15 mL tubes and processed on the day of collection and stored at −80°C until analyzed. Whole blood aliquot from EDTA tubes was processed, and analyzed for reduced (GSH) and oxidized (GSSG) glutathione as previously described (Sordillo et al., 2007). Plasma and serum were harvested after centrifuging at 711 × *g* for 15 minutes. Plasma, milk, and urine for 15-F_{2t}-Isop quantification were mixed with an antioxidant reducing agent (AOR, 4 μL/mL) as described previously (Mavangira et al., 2015). Using commercial assays, RM were analyzed in plasma and milk with no AOR, whereas, serum amyloid A (SAA) and haptoglobin (Hp) were analyzed in serum. Serum albumin and nonesterified fatty acids (NEFA) were analyzed at the Diagnostic Center for Population and Animal Health (Lansing, MI). Plasma and milk antioxidant potential (AOP) were measured in samples collected without AOR agent as described previously (Re et al., 1999). Briefly, the AOP of a sample was standardized to the

reduction capacity of trolox (synthetic vitamin E analog) in 2,2′-azinobis-3-ethylbenzothiazoline-6-sulfonic acid (ABTS) solution.

15-F_{2t}-Isoprostane Quantification: LC-MS/MS

Details for chemicals, sample processing, sample extraction and the LC-MS/MS protocol for the detection of 15-F_{2t}-Isop in plasma, urine, and milk were as previously described with some modifications (Mavangira et al., 2015). Briefly, modifications included urine sample preparation where the first step was mixing 4 mL of sample with 24 µL of formic acid. Thereafter, urine samples were processed in the same way as plasma samples. Prostaglandin E_2-d_9 (PGE_2_d_9) was the single deuterated standard used as a reference for the quantification of 15-F_{2t}-Isop. Multiple reaction monitoring parameters for 15-F_{2t}-Isop (Cone voltage = 21, collision voltage = 22, parent ion *m/z* = 353.2, and product ion *m/z* = 193) and PGE_2_d_9 (Cone voltage = 21, collision voltage = 16, parent ion *m*/*z* = 360.2, and product ion *m*/*z* = 280) were optimized using MassLynx software (Table 2, Waters Corp, Milford, MA USA).

15-F_{2t}-Isoprostane Quantification: ELISA assays

The ELISA assays validated for human plasma and urine samples from Cell Biolabs (cbELISA) and Cayman Chemicals (ccELISA), were used for quantifying 15-F_{2t}-Isop in milk, plasma and urine samples. Preliminary performance of the ELISA assays was first determined on samples (milk, plasma, and urine) from healthy third lactation cows (n = 3) in the first 30 days in milk. Samples were pooled by type, split into 3 aliquots and assayed independently. Samples were assayed for free (unbound) and for total (free + esterified) 15-F_{2t}-Isop. Total 15-F_{2t}-Isop were measured after alkaline hydrolysis for milk and plasma, and acidic hydrolysis for urine. Hydrolysis of samples was based on the Cell Biolabs protocol with some modifications. Briefly, 200 µL of milk or plasma were combined with 50 µL of 10N sodium hydroxide and incubated at

45°C for 2 hours. For cbELISA analyses, after incubation, 55 µL of 6N hydrochloric acid (HCl) were added and samples were centrifuged for 5 minutes at 4,816 × *g* and room temperature. Finally, a 1:2 sample dilution with neutralization solution to achieve a pH between 6 and 8 was performed. For ccELISA analyses, after incubation, plasma and milk samples were diluted to 1:6 using acetonitrile with 1% formic acid and centrifuged (4,816 × *g*, room temperature for 5 minutes). The supernatant was eluted through 1 mL Phenomenex solid phase extraction columns and dried in a SpeedVac (55°C, 2 hour). Residues were suspended in ccELISA buffer. For acidic hydrolysis, 200 µL of urine were combined with 50 µL of 6N HCL until a pH < 3.0 was reached and then diluted 1:6 with phosphate buffered saline. A final 1:3 urine sample dilution was performed with neutralization solution. In addition, a 10 ng quantity of a 15-F_{2t}-Isop standard was added to samples to assess the effect of the various sample preparation methods on 15-F_{2t}-Isop recovery. All ELISA assays were performed in duplicate following manufacturers' recommendations.

Statistical Analyses

No assumptions for normality of data were made because of the small sample size. All variables were expressed as median (range) concentrations and analyzed using the Wilcoxon rank sum procedure ($\alpha = 0.05$) using the SAS software. Spearman correlations between plasma and urine 15-F_{2t}-Isop concentrations to systemic inflammatory, oxidant status and redox status parameters were calculated. Similarly, Spearman correlations between milk 15-F_{2t}-Isop and the oxidant status and redox status parameters for the local environment in the mammary gland were calculated. For correlations, all data were combined to obtain a range of values for a given variable from normal to severely diseased cows. The ELISA assays were also compared for the detection and quantification of 15-F_{2t}-Isop concentrations in similarly processed samples.

Results

All 4 coliform mastitis cows exhibited local mammary gland signs of inflammation as well as signs of systemic involvement including tachycardia, tachypnea, pyrexia, and scleral injection. Within the coliform mastitis group, 3 cows died on days 1, 3, and 8 post sampling and 1 cow was still present in the herd at 105 days post sampling. Cows with naturally occurring coliform mastitis, in this study, had significant differences in the acute phase proteins with greater SAA and Hp (P = .014) and lower albumin (P = .043) concentrations than control cows. Serum NEFAs also were increased significantly (P = .029) in coliform mastitis cows compared to control cows (Table 13). Although AOP did not differ between experimental groups in milk or plasma, RM concentrations were greater in plasma (P = .029) and milk (P = .014) from coliform mastitis than control cows (Table 14). Concentrations of reduced glutathione (GSH) were lower (P = .014), whereas concentrations of the oxidized form (GSSG) were greater (P = .057) in coliform mastitis than control cows. The ratio of reduced to oxidized glutathione (GSH:GSSG) was lower in mastitis than control cows (P = .051) (Table 14). Plasma RM correlated positively with SAA (r = 0.69, P = .058) and Hp (r = 0.67, P = .071) and NEFAs (r = 0.31, P = .456) but negatively with serum albumin (r = −0.85, P = .008).

LC-MS/MS Based 15-F_{2t}-Isop Concentrations in Plasma, Urine and Milk

Cows with coliform mastitis had relatively greater 15-F_{2t}-Isop in plasma and urine (P = .057) than control cows (Table 14). Plasma 15-F_{2t}-Isop concentrations correlated positively with plasma RM (P = .010). The plasma RM were not significantly correlated with urine 15-F_{2t}-Isop concentrations (Table 15). Both plasma and urine 15-F_{2t}-Isop concentrations negatively correlated with GSH levels, however, only urine 15-F_{2t}-Isop significantly correlated with the GSH:GSSG ratio (Table 15). Milk 15-F_{2t}-Isop concentrations were lower in coliform mastitis

than control cows (P = .014, Table 14) and negatively correlated with the RM (P = .007) (Table 15). Although measures of oxidant status were significantly correlated between plasma and milk (RM: r = 0.83, P = .010), the 15-F_{2t}-Isop in plasma and milk were inversely correlated (r = −0.76, P = .028).

ELISA Based 15-F_{2t}-Isop Quantification in Plasma, Urine and Milk

Using the cbELISA, total 15-F_{2t}-Isop were greater (P = .05) in milk and plasma than the free 15-F_{2t}-Isop in samples (Figure 4A and B). For free 15-F_{2t}-Isop, spiking resulted in greater 15-F_{2t}-Isop (P = .05) compared to non-spiked and was associated with recovery rates of 73, 69 and 118% in milk, plasma, and urine, respectively. In spiked milk and plasma samples, hydrolysis resulted in greater total 15-F_{2t}-Isop (P = .05) with recovery rates of 106 and 291%, respectively. Using the ccELISA, there was no difference between free and total 15-F_{2t}-Isop (P = .20) in both milk and plasma (Figure 5A and B). For free 15-F_{2t}-Isop, spiking resulted in greater 15-F_{2t}-Isop (P = .05) compared to non-spiked and was associated with recovery rates of 102, 362 and 154% in milk, plasma, and urine, respectively. In spiked samples, hydrolysis resulted in greater total 15-F_{2t}-Isop (P = .05) in plasma with a recovery rate of 552%. Interestingly, hydrolysis of spiked milk samples resulted in significant (P = .05) lower 15-F_{2t}-Isop concentrations representing a 60% loss of the spiked amount.

Based on significant differences between free and total 15-F_{2t}-Isop, milk and plasma samples were analyzed for both free and total 15-F_{2t}-Isop for the cbELISA. Only free 15-F_{2t}-Isop were analyzed by ccELISA in plasma and milk based on the lack of differences from total 15-F_{2t}-Isop. Following manufacturers' recommendations, urine samples for cbELISA were analyzed for both free and total 15-F_{2t}-Isop, whereas only free 15-F_{2t}-Isop were quantified by ccELISA.

Total 15-F_{2t}-Isop in plasma and urine samples quantified by cbELISA did not differ significantly between control and mastitis cows, whereas greater 15-F_{2t}-Isop concentrations were detected in milk from coliform mastitis than control cows (Table 16). Free 15-F_{2t}-Isop quantified by cbELISA in urine and milk did not differ significantly between the mastitis and control group (Table 16). The cbELISA estimated significantly greater (P = .014) free 15-F_{2t}-Isop concentrations in urine relative to the ccELISA within each of the mastitis and control cow groups (Table 16).

Free 15-F_{2t}-Isop concentrations quantified by both cbELISA and ccELISA in nonhydrolyzed urine samples did not correlate with plasma oxidant or redox status parameters (Table 17). Similarly, free 15-F_{2t}-Isop concentrations quantified by cbELISA in milk did not correlate with milk oxidant status parameters (Table 17). Total plasma and urine 15-F_{2t}-Isop concentrations quantified by cbELISA in hydrolyzed samples did not correlate with oxidant status or redox status in plasma (Table 18). Total milk 15-F_{2t}-Isop concentrations quantified by cbELISA were positively correlated with milk oxidant status variables (Table 18).

Discussion

Plasma and urine 15-F_{2t}-Isop concentrations are well established oxidative stress markers in several human diseases (Morrow et al., 1992b). Cows suffering from naturally occurring acute systemic coliform mastitis in the current study provided an effective model, as supported by the changes in acute phase proteins and NEFAs, to evaluate the utility of 15-F_{2t}-Isop as a biomarker of oxidative stress. Using the gold standard method of LC-MS/MS for quantifying 15-F_{2t}-Isop, both plasma and urine 15-F_{2t}-Isop increased during mastitis. These findings agree with animal models of oxidant injury and severe sepsis with multi-organ damage in humans (Morrow et al.,

1992b, Ware et al., 2011). Plasma 15-F_{2t}-Isop are validated as indicating endogenous production in different tissues and the renal excretion closely reflects plasma levels (Halliwell and Lee, 2010). In humans with acute respiratory distress syndrome (ARDS), exhaled breadth condensate and plasma 15-F_{2t}-Isop concentrations correlated significantly with urinary levels (Carpenter et al., 1998). Plasma and urine samples are thus acceptable for evaluating 15-F_{2t}-Isop during oxidative stress in humans. In this study, both plasma and urine 15-F_{2t}-Isop correlated negatively with GSH, however, only plasma 15-F_{2t}-Isop significantly correlated with the systemic oxidant status. Reduced glutathione (GSH) is an important donor of thiol groups involved in scavenging of oxidants and maintaining redox balance (Trachootham et al., 2008, Sordillo and Aitken, 2009). A decrease in the GSH:GSSG ratio indicating depletion of the thiol donor is considered a useful measure of oxidative stress in sepsis-induced ARDS in humans (Guo and Ward, 2007). On the basis of increased 15-F_{2t}-Isop that correlated positively with oxidant status and negatively with GSH, plasma is ideal for quantifying 15-F_{2t}-Isop reflective of systemic oxidant status in bovine coliform mastitis.

The lack of significant correlation of urine 15-F_{2t}-Isop with oxidant status was unexpected as the renal excretion of 15-F_{2t}-Isop is related directly to its plasma concentrations. For example, a murine model of ischemia-reperfusion injury showed that renal excretion of 15-F_{2t}-Isop was increased by up to 300% (Takahashi et al., 1992). In the same study, intrarenal infusion of 15-F_{2t}-Isop was associated with diminished glomerular filtration rate in a dose dependent manner suggesting a possible contribution of 15-F_{2t}-Isop in the pathogenesis of renal failure (Takahashi et al., 1992). Renal failure is common in humans with sepsis and the association with plasma 15-F_{2t}-Isop is direct evidence for oxidative stress mediated damage (Ware et al., 2011). Renal failure frequently occurs in cows with severe coliform mastitis (George et al., 2008) and would be

expected to increase the rate of 15-F_{2t}-Isop excretion. The observation that increases in plasma free 15-F_{2t}-Isop lag behind the rise in esterified 15-F_{2t}-Isop in murine models of oxidative stress (Morrow et al., 1992a) might explain the lack of significance in urine 15-F_{2t}-Isop and oxidant status in this study. The strong correlations of urine 15-F_{2t}-Isop to redox status parameters (GSH, GSSG, and GSH : GSSG ratio) might indicate depletion of an early line of antioxidant defense before overall changes in AOP as suggested by lack of differences in plasma AOP in this study. Evaluating the temporal changes in 15-F_{2t}-Isop excretion as the disease progresses might uncover the relationship between plasma and urine 15-F_{2t}-Isop during coliform mastitis.

The lower concentrations of 15-F_{2t}-Isop and its inverse correlation with the abundance of RM in milk was unexpected because oxidative stress mediates mammary gland damage, especially during coliform mastitis (Aitken et al., 2011). The presence of increased PUFA substrates in the same local environment of the mammary with excess RM could be expected to also generate increased 15-F_{2t}-Isop. A recent study found that several PUFA substrates were increased in milk during coliform mastitis in tandem with some nonenzymatic derived oxylipids including hydroperoxy acids from AA (Mavangira et al., 2015). The formation of 15-F_{2t}-Isop, which occurs predominantly, while AA is esterified to phospholipids, (Milne et al., 2011) could explain the lack of prediction of oxidant status by free 15-F_{2t}-Isop quantified by LC-MS/MS in milk. The concentrations of free 15-F_{2t}-Isop in milk also were inversely correlated with free 15-F_{2t}-Isop concentrations in plasma suggesting that differential release from esterification sites might exist across compartments. The 15-F_{2t}-Isop initially formed in situ esterified to phospholipids are subsequently hydrolyzed to yield free 15-F_{2t}-Isop by phospholipase (PL) enzymes (Morrow et al., 1992a). Differential PL activity was detected in humans where the activity in plasma was greater with more 15-F_{2t}-Isop hydrolysis compared to intracellular PL (Stafforini et al., 2006).

The concept of differential hydrolysis was supported by the use of a hydrolysis method and analyzing for total 15-F_{2t}-Isop by 1 of the 2 ELISA assays (cbELISA) in this study which yielded greater concentrations that positively correlated with milk oxidant status. Therefore, it appears that predictive ability of 15-F_{2t}-Isop concentrations on local mammary gland oxidant status during coliform mastitis can be improved by performing sample hydrolysis. Further research is required to understand the counterintuitive decrease in 15-F_{2t}-Isop concentrations in the presence of increased RM especially when other nonenzymatic oxylipid metabolites were detected in nonhydrolyzed samples.

An alternate approach to LC-MS/MS for the quantification of 15-F_{2t}-Isop is by use of immunoassays such as ELISA (Milne et al., 2015). Despite the reported accuracies of plasma and urine 15-F_{2t}-Isop quantified by ELISAs of 95–101%, ELISAs are often affected by cross-reactivity from prostaglandin and other isoprostane metabolites because they target a single metabolite (Basu, 1998, Milne et al., 2015). Free 15-F_{2t}-Isop in milk and urine as well as total 15-F_{2t}-Isop in plasma and urine, analyzed by cbELISA, failed to predict oxidant status. Only the total 15-F_{2t}-Isop quantified in milk by cbELISA demonstrated potential reliability that was supported by the accurate recovery (106%) of the spiked 15-F_{2t}-Isop standard (Figure 4A). Variable performances of ELISAs in quantifying 15-F_{2t}-Isop were previously reported in studies in veterinary species and humans that reported poor correlations with GC/MS or LC-MS/MS as well as between different ELISA assays (Soffler et al., 2010, Klawitter et al., 2011, Smith et al., 2011). Results of this study showed that, despite acceptable recovery rates by the ccELISA (102%) on free milk 15-F_{2t}-Isop and cbELISA (118%) on free urine 15-F_{2t}-Isop, there was no correlation with oxidant status. Further, the variable performances of the ELISAs as shown by both overestimation (plasma, cbELISA, Figure 4; plasma and urine, ccELISA, Figure 5) and

underestimation (milk, ccELISA Figure 4) make it impossible for general recommendations for using ELISA in quantifying 15-F_{2t}-Isop in bovine samples. A recent study reported a positive linear correlation between milk and plasma 15-F_{2t}-Isop by utilizing an ELISA based (ccELISA) assay. The investigators of that study suggested that milk was a possible alternate route of 15-F_{2t}-Isop excretion (Vernunft et al., 2014). The inverse correlation between free 15-F_{2t}-Isop in plasma and milk using LC-MS/MS in this study does not support the possibility of milk as a route of excretion for 15-F_{2t}-Isop. An expanded lipidomic profile during coliform mastitis showed lack of correlation among several oxylipids suggesting that oxylipid biosynthesis, including isoprostanes, between plasma and milk could be independent of each other (Mavangira et al., 2015). The difference in the correlation with the present findings might be the use of a disease model associated with high degree of oxidative stress, as well as different sample extraction methods. It is unclear whether the study (Vernunft et al., 2014) analyzed free or total 15-F_{2t}-Isop in both milk and plasma. The performance of ELISA assays in quantifying 15-F_{2t}-Isop in bovine samples should be validated with the gold standard mass spectrometry-based methods such as the LC-MS/MS.

In conclusion, results of this study show that free plasma 15-F_{2t}-Isop concentrations are predictive of systemic oxidant status during acute coliform mastitis. Free 15-F_{2t}-Isop in urine and milk were not predictive of systemic or local mammary gland environment oxidant status, respectively. Quantification of total 15-F_{2t}-Isop in milk by cbELISA is an accurate alternative to LC-MS/MS and suggests that milk samples should be hydrolyzed when determining 15-F_{2t}-Isop associated with oxidant status in the mammary gland. The lack of significance for some variables in this study might have been because of the small number of experimental animals in this study. Findings of this study can thus be used as a basis for further studies designed to provide broader

scope inferences. Establishing threshold concentrations for 15-F_{2t}-Isop during clinical coliform mastitis will provide a basis for formulation and application of practical interventions to control oxidative stress in dairy cows and currently should be based on gold standard methods such as LC-MS/MS.

Acknowledgements

Michigan State University (MSU) Mass Spectrometry Core facility, MSU Center for Statistical consulting and MSU Teaching Center for Dairy Professionals. This work was funded through grant 2011-67015-30179 from the Agriculture and Food Research Initiative Competitive Grants Programs of the USDA National Institute for Food and Agriculture, an endowment from the Matilda R. Wilson Fund (Detroit, MI) and the College of Veterinary Medicine Endowed Research Grants, Sterner Fund, 2015

CHAPTER 4

20-HYDROXYEICOSATRIENOIC ACID ALTERS ENDOTHELIAL CELL INTEGRITY BY AN OXIDATIVE STRESS-MEDIATED MECHANISM

Vengai Mavangira[1] and Lorraine M. Sordillo*[1]

[1]Department of Large Animal Clinical Sciences, College of Veterinary Medicine, Michigan State University, East Lansing 48824

***Corresponding author**

Dr. Lorraine M. Sordillo,

Department of Large Animal Clinical Sciences

College of Veterinary Medicine

Michigan State University

sordillo@msu.edu

Tel: (517) 432-8821

Fax: (517) 432-8822

Abstract

Unregulated inflammation during diseases, including bovine mastitis, is characterized by oxidative stress-induced tissue damage. Vascular dysfunction is frequently the result of oxidative stress in severe coliform mastitis. We recently demonstrated increased production of 20-hydroxyeicosatetraenoic acid (20-HETE), a cytochrome P450-derived oxylipid that correlated with oxidative stress during severe bovine coliform mastitis. The hypothesis for this study was that 20-HETE-induced oxidative stress causes apoptosis, which disrupts endothelial cells barrier function. Our results showed that 20-HETE decreased endothelial barrier integrity which was associated with increased reactive metabolite production and decreased redox status. Vitamin E partially delayed the loss in endothelial resistance by 5 hours, after that, the endothelial resistance decreased to the same extent as treatment with 20-HETE alone. The loss in barrier resistance was not associated with apoptosis. Specific mechanisms by which 20-HETE alters vascular barrier integrity require further investigation to identify targets for diminishing oxidative stress during inflammatory conditions characterized by enhanced CYP450 activity.

Key words: 20-Hydroxyeicosatetraenoic acid, oxidative stress, oxylipids, oxidants, antioxidants, isoprostanes.

Introduction

Severe bovine coliform mastitis is characterized by an unregulated inflammatory response that causes severe tissue pathology (Aitken et al., 2011a). The severe tissue damage occurs, in part, due to the accompanying oxidative stress. Oxidative stress refers to the damage that occurs to cellular macromolecules (including lipids, proteins, and DNA) as a consequence of an imbalance between oxidants and antioxidants (Valko et al., 2007). Oxidants comprise reactive oxygen species (ROS) which can be free radicals or non-radicals capable of oxidizing macromolecular substrates (Villamena, 2013). Physiological concentrations of ROS produced by the mitochondria and the nicotinamide adenine dinucleotide phosphate oxidase enzymes (NOX) play important roles in normal cellular processes by participating in intracellular signaling pathways (Valko et al., 2007). Production of ROS increases during inflammation due to enhanced mitochondrial metabolism and the activation of NOX during the oxidative burst mechanism in leukocytes. Additionally, some ROS sources include inducible enzymes such as cyclooxygenases (COX), lipoxygenases (LOX), and cytochrome P450 (CYP) enzymes involved in lipid metabolism (Huet et al., 2009). The overproduction of ROS can overwhelm cellular antioxidant defenses resulting in oxidative stress.

Defense against the excessive production of oxidants is accomplished by antioxidants that have the capacity to scavenge pre-formed ROS or to delay the formation of these pro-oxidants (Valko et al., 2007). Vitamin E is a dietary antioxidant which scavenges pre-formed radical oxidants in cellular membranes and forms a stable radical in the process (Yamauchi, 1997). Vitamin E is regenerated from the stable radical form by the activity of peroxidase enzymes such as the selenium-dependent glutathione peroxidase (GPx), in the presence of reduced glutathione (GSH) (Nwose et al., 2008). Vitamin E-mediated decrease in ROS formation also involves other

mechanisms including inhibition of the phosphorylation of p47phox protein which is essential for NOX activity (Cachia et al., 1998) and the activation of transcription factors that enhance antioxidant enzymes (Ruiz et al., 2013). The importance of antioxidant defenses in disease was demonstrated by the decreased clinical severity and duration of bovine coliform mastitis following dietary supplementation with Vitamin E and selenium (Weiss et al., 1997). Decreased disease severity was likely due to limited RM production and the vascular dysfunction which frequently occur during sepsis (Huet et al., 2009). The vascular dysfunction is characterized by increased permeability, excessive leukocyte transmigration, and thrombosis as a consequence of oxidative stress-induced endothelial cell damage.

Polyunsaturated fatty acids (PUFA) are highly susceptible to oxidation during oxidative stress which can lead to cellular death and organ dysfunction and can also initiate oxidative stress (Milne et al., 2011). Oxidation of lipids occurs through enzymatic metabolism through cyclooxygenases (COX), LOX, and cytochrome P450 (CYP) enzymes (O'Donnell et al., 2009). Metabolism also occurs via non-enzymatic pathways which are mediated by the free radical oxidants (Milne et al., 2011). Some initial oxylipid products such as the hydroperoxides are potent ROS capable of inducing cellular damage. For example, 15-hydroxyeicosatetraenoic acid (15-HpETE) from LOX-mediated oxygenation of arachidonic acid (AA) induces endothelial cell oxidant stress and apoptosis (Sordillo et al., 2005). Endothelial cell apoptosis and loss of barrier integrity were also shown for 13-hydroperoxyoctadecadienoic acid (13-HpODE), an oxylipid derived from both non-enzymatic and the LOX pathway metabolism (Ryman et al., 2016). Alternatively, oxylipid metabolites can act as indirect inducers of oxidative stress by stimulating excessive production of ROS from sites including the mitochondria. For example, the CYP-derived 20-hydroxyeicosatereaenoic acid (20-HETE) activates the NOX pathway inducing ROS

production in cardiomyocytes (Han et al., 2013). Thus, the production of some oxylipids can contribute to the oxidative stress-mediated pathology during inflammation.

We recently demonstrated the elevation of milk and plasma concentrations of 20-HETE during severe bovine coliform mastitis (Mavangira et al., 2015). Concurrently, several oxidative stress biomarkers including 15-F_{2t}-isoprostane (15-F_{2t}-IsoP) were elevated, (Mavangira et al., 2016a) and correlated strongly with the 20-HETE. The 15-F_{2t}-IsoP is an arachidonic acid-derived metabolite generated by free radical ROS and is a useful biomarker of oxidative stress in humans (Milne et al., 2011). In many chronic conditions including hypertension, 20-HETE concentrations were increased and correlated with oxidative stress occurrence (Lukaszewicz and Lombard, 2013). The mechanisms by which 20-HETE induced oxidative stress included uncoupling of endothelial nitric oxide synthase (eNOS) (Cheng et al., 2008), NOX activation (Han et al., 2013), and increased mitochondrial ROS production (Lv et al., 2008). Despite the convincing evidence of 20-HETE-induced vascular dysfunction in chronic conditions (Dunn et al., 2008), the role in acute inflammation is contradictory among studies. For example, in lipopolysaccharide (LPS)-induced sepsis of mice, the use of 20-HETE mimetics ameliorated several clinical signs including hypotension and mortality suggesting insufficient 20-HETE concentrations in acute inflammation (Tunctan et al., 2012, Tunctan et al., 2013a, Tunctan et al., 2013b). In other studies, however, CYP isoforms involved in the biosynthesis of 20-HETE were elevated during LPS-induced murine sepsis with consequent production of 20-HETE (Anwar-mohamed et al., 2010, Willenberg et al., 2015). Our preliminary studies and others showing acute increases in the concentrations of 20-HETE suggest that this oxylipid participates in either the development or resolution of pathology during acute inflammation.

Targeting of the vascular endothelium by 20-HETE may compromise the endothelial barrier integrity contributing to immunopathology due to increased permeability, excessive leukocyte transmigration, and thrombosis. Endothelial cells transduced with CYP4A1, an isoform that generates 20-HETE, were characterized by increased ICAM 1 and interleukin 8 (Ishizuka et al., 2008) which may account for excessive leukocyte migration. Thrombus formation was accelerated in mice administered with 20-HETE (Wang et al., 2015). The treatment of HUVECs with 20-HETE induced von-Willebrand's factor formation and platelet adhesion (Wang et al., 2015) suggesting that overproduction may promote excessive thrombosis and pathology in acute inflammation. Previously, 20-HETE was also shown to induce mitochondrial-dependent apoptosis in neonatal murine cardiomyocytes (Bao et al., 2011b), however, it is not known if the pro-oxidant effects of 20-HETE are sufficient enough to disrupt the barrier function of the vascular endothelium. Based on the high concentrations of 20-HETE and the severity of clinical disease in bovine coliform mastitis, we hypothesized that 20-HETE would disrupt endothelial cells barrier integrity by mediating cellular apoptosis through an oxidative stress-dependent mechanism.

Materials and Methods

Reagents

High performance liquid chromatography (HPLC) grade acetonitrile, HPLC-grade methanol, formic acid, glycerol, transferrin, insulin, heparin, sodium selenite, Hanks buffered salt solution (HBSS) powder, collagenase, lipopolysaccharide (O111:B4), paraformaldehyde, potassium hydroxide, N-acetyl cysteine (NAC), Trolox (6-Hydroxy-2,5,7,8-tetramethylchromane-2-carboxylic acid), tempol (4-Hydroxy-2,2,6,6-tetramethylpiperidine 1-oxyl), triphenylphosphine were purchased from Sigma-Aldrich (St. Louis, MO). Oxylipid standards, deuterated and non-

deuterated, indomethacin, 20-hydroxyeicosatetraenoic acid (20-HETE), HET0016 [N-hydroxy-N'-(4-n-butyl-2-methylphenyl) formamidine], and AAPH (2,2'-azobis-2-methyl-propanimidamide, dihydrochloride) were purchased from Cayman Chemical (Ann Arbor, MI). Butylated hydroxy toluene and hydrochloric acid were purchased from ACROS (Thermo Fisher, Fair Lawn, NJ). Fetal bovine serum was purchased from Hyclone Laboratories, Inc. (Logan, Utah) and HEPES buffer and DMSO (dimethyl sulfoxide) were purchased from Corning Inc. (Corning, NY). HAM's F-12k was purchased from Irvine Scientific (St. Santa Ana, CA). Antibiotics/antimycotics, trypsin-EDTA, bovine collagen, and ProLong-Gold antifade were from Life Technologies (Carlsbad, CA). Predesigned and custom-made bovine TaqMan primers were purchased from Applied Biosystems (Foster City, CA). CellROX^{TM} Deep Red reagent and DAPI (4,6-Diamidino-2-phenylindole, dihydrochloride) were purchased from Molecular Probes (Eugene, OR). Vitamin E (DL-α-tocopherol) was purchased from Millipore (Billerica, MA). Von Willebrand's factor was purchased from Agilent Technologies (Santa Clara, CA)

Cell culture

Primary bovine aortic endothelial cells (BAEC) were isolated from aorta sections collected from freshly slaughtered mature dairy cattle, and processed using a method previously described by our group (Aitken et al., 2011b). Briefly, bovine aorta sections were collected and stored in cold Hanks buffered saline solution (HBSS) and transported on ice for processing in the laboratory. The endothelial surface was exposed to a collagenase and solution for 10 minutes at 37^{o}C, washed in F12K cell culture media supplemented with 10% irradiated fetal bovine serum, selenium (sodium selenite, 10 ng/mL), heparin sulphate (100 µg/mL), transferrin (5 µg/mL), and insulin (10 µg/mL), then cultured in T25 tissue culture flasks. Upon confluency, the single cell dilution technique was used to achieve a seeding density of 1-2 endothelial cells in a single well

in a 96-well plate to establish single colony cell cultures of BAECs. Finally, uniform colonies were frozen in media made by combining F12K media with 10% FBS, fetal bovine serum, and dimethyl sulfoxide (DMSO) at 5:4:1 (*v:v:v*). For experiments, frozen cells were thawed, grown in F12K media with 10% FBS, transferrin, insulin and heparin until confluency. For purity, BAEC were stained for the endothelial cell marker, Von Willebrand's factor expression evaluated by fluorescence microscopy using the Zeiss inverted microscope. Experiments were performed with cells from passage 6 to passage 9.

Cell viability

Cell viability was determined based on ATP production using the Promega CellTiter-Glo viability Assay (Promega Corp., Madison, WI), following manufacturer's instructions and as previously described by our group (Contreras et al., 2012b). The assay is based on amount of ATP directly generated is proportional to the number of viable cells. Luminescence was measured using a plate reader (Tecan Infinite 200 PRO, Switzerland). A complimentary OxiSelect calorimetric assay (Cell Biolabs, San Diego, CA) which measures released lactate dehydrogenase enzyme (LDH) was also used to assess cell viability. The assay is based on the calorimetric reaction whose signal intensity is proportional to the amount of LDH release, hence cell death.

Oxidative stress induction

The free radical generator, AAPH, was used to induce oxidative stress in BAEC and also assessed in cells treated 20-HETE by measuring reactive metabolite production, redox status, quantification of lipid peroxidation products, and protein carbonyls. For these experiments, cells were initially seeded in and incubated under humid conditions at 37^{o}C, 5% CO_2 and natural air in F12K media containing 5% serum, antibiotic/antimycotic solution, transferrin, heparin and

insulin. After 24 hours, cells were acclimation to serum-free media for a period of 4 – 6 hours before treatments with AAPH or 20-HETE and appropriate controls were added in for indicated times.

Reactive metabolites determination

Reactive metabolite production was measured using 2 methods using different probes that are oxidized by RM to fluorescent probes; the CellROX^{TM} Deep Red reagent and DFCH-DA probe. The CellROX^{TM} Deep Red reagent assay was evaluated by the inverted Zeiss fluorescent microscopy. For this procedure, BAEC were seeded on sterile light microscope slide coverslips placed in a 6 well plate at 1.5 – 2 x 10^5 cells/slide in 200 µL of media and allowed to stand for 1 minute before topping off with 2 mL of media followed by 24 hour incubation. Initial experiments evaluated RM induction by exposure of BAEC to AAPH to the culture media at a dose and duration determined based on viability assays detailed below. For 20-HETE treatments, the positive control treatment with AAPH was performed at the time of exposure of BAEC to acclimation serum-free medium for 6 hours before 20-HETE was added for up to 1 hour. CellROX^{TM} Deep Red reagent was added (4 µL) to the wells 30 minutes before the end of the incubation period. Cells were then washed in 1X PBS, fixed in 1 mL of 3.7% paraformaldehyde dissolved in 1X PBS (15 min at 37^{o}C) and counterstained with the DAPI nuclear stain (2 µL, 15 min at room temp). Coverslips were air dried and mounted on microscope slides using the Prolong Gold anti-fade reagent (5 µL). Fluorescence measurements were determined using an inverted microscope (Axiovert 200M; Zeiss). Images were analyzed in gray-scale using the image J software (Schneider et al., 2012)

An alternate method utilized for quantifying reactive metabolite production was the OxiSelect flourometric assay (Cell Biolabs, San Diego, CA). This method uses a non-fluorescent probe,

2′,7′-dichlorodihydrofluorescin diacetate (DCFH-DA) which is cleaved by cellular deacetylases and is oxidized by RM to the fluorescent and stable 2′,7′-Dichlorodihydrofluorescein (DCF) product. For this assay, BAEC were initially seeded at 2 x 10^4 cells/well in 100 µL of media. Reactive metabolites were quantified following manufacturers recommendation. Briefly, BAEC were cultured for 24-hours in 96-well black walled and clear bottom, plates suitable for fluorescence measurements. Cells were then preloaded with DCF-DA at 100 µM in 0% FBS for 15 minutes before treatments were added. Temporal measurements of ROS/RNS production were determined by measuring fluoresce using a plate reader (Tecan Infinite 200 PRO, Switzerland) at 480 nm excitation and 530 nm emission wavelengths. Pre-incubation of cells with antioxidants was performed to titrate doses tolerable by cells at concentrations effective for reducing agonist-induced ROS/RNS production before being evaluated for their ability to protect BAEC against compromised barrier integrity. Results were analyzed as fold change in fluorescence signal over untreated controls.

Redox status

The redox status of BAEC under different treatment conditions was evaluated using the concentrations of reduced glutathione (GSH), oxidized (GSSG) glutathione, and their ratio (GSH/GSSG) using the Promega GSH/GSSG-Glo™ assay (Promega, Madison, WI). Total glutathione concentrations were also quantified using the OxiSelect™ assay kit (Cell Bio Labs, San Diego, CA). For the GSH/GSSG-Glo™ assay, cells were seeded at 2 x 10^4 cells/well in a white wall clear bottom 96 well plates and incubated with media and treatments as previously described. After incubation with treatments, total glutathione standards from 0 – 16 µM, were added to wells previously with no cells or media and all media was replaced with either total or oxidized glutathione lysis reagent and incubated for 30 minutes at room temperature with

constant shaking. The luciferin signal generation reagent was added to the samples at a volume ratio of 1:1, briefly shaken for 30 seconds and incubated at room temperature for 15 minutes. Luminescence was read using the Tecan Pro 200 plate reader. Results were expressed as either µM concentrations of total, reduced or oxidized glutathione, as well as the ratio of GSH/GSSG. For the total glutathione OxiSelect^{TM} assay, cells were seeded at 3 x 10^6cells/100 mm dish and incubated with media and treatments as previously described. After treatment duration, culture media was discarded and cells were washed once with HBSS buffer, detached by incubation with 1 mL of 0.05% EDTA-trypsin for 2 minutes at 37oC and quenched with 2 mL of 5% serum-containing F12K media. Cells were then processed for quantification of total GSH following manufacturer's instructions.

Oxidant damage

Oxidant damage of cultured cells was determined by lipid and protein oxidation metabolites. Lipid oxidation metabolites were evaluated as part of a broader but targeted oxylipid profile using liquid chromatography-tandem mass spectrometry (LC-MS/MS) section below. Protein oxidation was determined using an ELISA for the detection of protein carbonyls following oxidative damage to proteins following manufacturer's instructions. Briefly, cultured cells in 100 mm dishes or 150 mm dishes for LC-MS/MS procedure below were collected by scrapping using cell lifters from culture dishes, washed with 1X PBS solution before being sonicated (2 minutes, amplitude 10 at 5^{o}C) in 1X PBS buffer with anti-protease inhibitor. Sample protein concentrations, oxidized and reduced bovine serum albumin (BSA) were determined and adjusted to 10 µg/mL solution. The concentrations of protein carbonyls were determined from the linear portion of an absorbance standard curve determined by a combination of the reduced and oxidized BSA read using Tecan Infinite 200 PRO plate reader.

Sample preparation for LC-MS/MS

A targeted oxylipid metabolites in cell pellets and culture media were separately subjected to solid phase extraction and quantification using LC-MS/MS. Cells were seeded at either 3 x 10^6 cells and 8 mL of media or 5 x 10^6 cells with 15 mL of media in 100 mm or 150 mm dishes, respectively. At the end of experiments culture media and cell pellets were collected and mixed with an antioxidant mixture and internal standards. The antioxidant reducing agent mixture consisted of final concentrations of 0.9 mM butylated hydroxytoluene, 0.54 mM EDTA, 3.2 mM triphenylphosphine, and 5.6 mM indomethacin. A mixture of internal standards containing 5(S)-hydroxyeicosatetraenoic-d_8 acid [5(S)-HETE_d_8], 15(S)-hydroxy eicosatetraenoic-d_8 acid [15(S)-HETE_d_8], 8(9)-epoxyeicosatrienoic-d_{11} acid [8(9)-EET_d_{11}], prostaglandin E2-d_9 (PGE2_d_9), 8,9-dihydroxy eicosatrienoic-d_{11} acid (8,9-DHET_d_{11}), arachidonic acid-d_8 (AA_d_8), 2-arachidonoyl glycerol-d_8 (2-AG_d_8), and arachidonoyl ethanolamide-d_8 (AEA_d_8) as prepared to final concentrations of 0.25, 0.25, 0.5, 0.5, 0.25, 50, 2, and 0.25 µM, respectively. The internal pure standards mixture was added into each sample and used to generate a 6-point standard curve ranging from 500 to 0.001 µM in the concentration of unlabeled fatty acid and oxylipid standards. Both media and cell pellets were brought up to 60% methanol and additionally, for media alone, acidified to 0.1% formic acid. Samples were stored at -80^{o}C until analyzed.

Sample extraction for LC-MS/MS

Media samples collected from culture experiments, previously stored at -80oC, were thawed while protected from light, centrifuged (4,000 x *g*, 30 minutes, 4 ^{o}C), and combined with HPLC-grade water and formic acid to achieve 20% methanol and maintain 0.1% formic acidification, respectively. Samples were eluted in SPE cartridges (Waters Oasis HLB 12cc, 500 mg LP) preconditioned with methanol followed by HPLC-grade water, washed with 20% methanol

solution and cartridges were dried for 15 minutes under full vacuum. A 7.5 mL 1:1 mixture of methanol and acetonitrile was used to elute extracted samples from the cartridges into glass tubes pre-coated with 10 µL of 20% glycerol in methanol followed by a 30 second drying under full vacuum. Samples were dried in a Savant SpeedVac with an initial heating phase at 45 ^{o}C, residues suspended in 150 µL of a 2:1 (v:v) methanol and water mixture, and centrifuged (14,000 x *g*, 5 minutes, 4 ^{o}C). A 120 µL supernatant was transferred to an autosampler vial with a low volume insert and stored at -80 ^{o}C before LC-MSMS analyses. Cell pellets were processed similar to media samples with modifications. After samples were thawed, samples were incubated with a 3M potassium hydroxide solution at 45 ^{o}C for 45 minutes, allowed to cool to room temperature before being acidified with hydrogen chloride to a pH range of 2 – 3. Prior to extraction in Phenomenex 8B-S100-FCH extraction cartridges, cell pellet samples were centrifuged at 4816 x *g* for 45 minutes at 4 ^{o}C. The acetonitrile/methanol mixture for eluting samples was 6 mL.

LC-MS/MS

The liquid chromatography and mass spectrometry analyses of all media and cell pellet samples were performed using a method we have previously utilized before. (Mavangira et al., 2015) The quantification of metabolites was accomplished on a Waters Acquity UPLC coupled to a Waters Xevo TQ-S triple quadrupole mass spectrometer (Waters) using multiple reaction monitoring. Chromatography separation was performed with an Ascentis Express C18 HPLC column, 10 cm × 2.1 mm, 2.7 µm (Supelco, Bellefonte, PA) held at 50°C. The autosampler was held at 10°C. Mobile phase A was water with 0.1% formic acid, and mobile phase B was acetonitrile. Flow rate was fixed at 0.3 mL/min. Liquid chromatography separation took 15 min with linear gradient steps programmed as follows (A:B ratio): time 0 to 0.5 min (99:1), to (60:40) at 2.0 min;

to (20:80) at 8.0 min; to (1:99) at 9.0 min; 0.5 min held at (1:99) until min 13.0; then return to (99:1) at 13.01 min, and held at this condition until 15.0 min. All oxylipids and fatty acids were detected using electrospray ionization in negative-ion mode, whereas the endocannabinoids were detected using positive-ion mode. Cone voltages and collision voltages were optimized (Table 2) for each analyte using Waters QuanOptimize software and reported previously (Mavangira et al., 2015).

mRNA quantification in BAEC

The quantification of gene expression of target genes was performed as previously described by our group (Aitken et al., 2011b). Initially total RNA was isolated from BAEC treated in 6-well plates at a seeding density of 1 x 10^6 cells/well using the RNeasy Mini KIT (Qiagen, Venlo, Limburg) following manufacturer's instructions. Using predesigned and custom-designed TaqMan minor groove binding primers with FAM probe from Applied Biosystems, quantitative real-time (qRT-PCR) was performed. The qRT-PCR was performed in triplicate for each sample using reaction mixtures containing phosphoglycerate kinase 1 (PGK1), TATA-box binding protein (TBP) and ribosomal protein S9 (RPS9) as endogenous controls. The COX2, vascular cell adhesion molecule 1 (VCAM-1), CYP 3A4, 4F2, and 4A11 were the target genes (Table 19). The thermal cycling conditions for fast 2-step PCR were used: stage1 enzyme activation, 95 ◦C for 20s; stage 2, 95ºC for 3s; stage 3, 60 ◦C for 30 s; with 40 replications through stages 2 and 3. The abundance of target genes was normalized to endogenous control genes and calculated using the ΔCt method for statistical analyses and the $2^{-\Delta\Delta Ct}$ method for relative expression was used for graphical display of the data (Aitken et al., 2011b).

Apoptosis

BAEC were cultured in 96 well plates at $1x10^4$ cells/well in F12K media supplemented with 5% FBS, insulin, transferrin and heparin for approximately 15 hours. After that, cells were incubated with 0% FBS media for about 4-6 hours before treatments were added similar to the barrier integrity experiments. Apoptosis was determined by reading luminescence with a plate reader after the addition of the Caspase-Glo assay reagent (Promega, Madison, WI). Results were evaluated as fold change in luminescence over untreated control samples.

Endothelial Cell-substrate Impedance Sensing (ECIS)

Barrier integrity of BAEC was performed using a protocol previously described by our group (Ryman et al., 2016) Briefly, BAEC were cultured in 8-well arrays with 10+ electrode system until confluency. Cell culture media was changed to 0% approximately 4 – 6 hours before adding treatments. For treatments with antioxidants, media for seeding at the beginning of the experiment and the 0% FBS containing media change before adding treatments included the antioxidants, N-acetyl cysteine (NAC, 5 mM), tempol (4-Hydroxy-2,2,6,6-tetramethylpiperidine 1-oxyl, 10 mM), or vitamin E (DL-α-Tocopherol, 10 μM). Resistance to electrical passage across the confluent monolayer was monitored throughout the duration of the experiment using the Electric Cell-Substrate Impedance Sensing system (ECIS, Applied Biophysics, Inc., Troy, NY). Resistance measurements immediately before treatment additions were used to normalize all subsequent values.

Statistical analyses

For statistical analyses, one- or two-way ANOVA were performed using the proc mixed procedure with or without repeated measures where appropriate using the SAS software (SAS 9.4, Cary Inc., NC). A Tukey adjustment for multiple comparisons was performed with a $P \leq$

0.05 considered significant. For statistical analyses, undetected measures of variables in a treatment class were presented as undetected and assigned a zero value for statistical analyses.

Results

Exposure of BAEC to AAPH induced oxidative stress

Previous studies showed that activation of endothelial cell markers occurs by at least 4 – 12 hours after agonist treatment (Aitken et al., 2011b, Contreras et al., 2012a). Therefore, a period between 6 – 12 hours was targeted to capture effects of induced oxidative stress in BAEC. Exposure of BAEC to the free radical generator, AAPH, showed a dose (Figure 6A) and time (Figure 6B) dependent decrease in cell viability relative to untreated controls. Thus, a dose of 5 mM for an 8-hour incubation was selected for positive induction of oxidative stress for subsequent experiments. Exposure of BAEC to AAPH time-dependently increased ROS/RNS production, which peaked at 4 hours and remained elevated for the duration of the experiment (Figure 7A). Increased ROS/RNS was accompanied by decreases in the total glutathione concentrations (Figure 7B). The changes in oxidant and redox status were associated with increased production of lipid peroxidation markers, 15-F_{2t}-IsoP (Figure 8A) and 11-HETE (Figure 8B).

Induced oxidative stress in BAEC does not result in the production of 20-HETE

To evaluate the production of 20-HETE during oxidative stress conditions, BAEC were exposed to AAPH with and without the CYP hydroxylase inhibitor, HET0016 at 10 nM. The 10 nM HET0016 dose used to selectively inhibit CYP hydroxylases activity is at least 1000-fold less than doses required to inhibit epoxygenation activity of CYP enzymes (Nakamura et al., 2003). No significant changes in 20-HETE concentrations were detected with or without HET0016 in BAEC treated with AAPH or LPS (Figure 9A). However, the AAPH dose of 5 mM induced

significant mRNA expression for COX2 but not VCAM-1 in BAEC (Figures 9B and 9C). In another bovine cell line, MDBK cells, AAPH induced significant ROS/RNS production (Figure 9D), and mRNA expression of CYP3A4 but not CYP4F2 (Figures 9E and 9F).

Exposure of BAEC to LPS with or without HET0016 did not alter 20-HETE production relative to non-treated control (Figure 9A); however, there was a dose-dependent induction of COX2 and VCAM-1 mRNA expression (Figure 9B and 9C). In MDBK cells, LPS doses of 1- and 10 ng/mL for 24 hours failed to induce ROS/RNS production (Figure 9E) or mRNA expression for either CYP3A4 or CYP4F2 (Figures 9E and 9F). The CYP isoform, CYP4A11, was not detectable for any of the treatments or cells.

The CYP hydroxylase inhibitor decreased AA-derived epoxides and LA-derived hydroxy-oxylipids

The formation of the oxylipids when BAEC were exposed to AAPH or LPS with or without HET0016 was quantified by LC-MS/MS and data analyzed as fold change in AAPH or LPS treated BAECs relative to untreated controls (Table 20). Treatment of BAEC with AAPH or LPS alone did not affect the production of the quantified targeted lipidome. Treatment of BAEC with AAPH and LPS in the presence of HET0016 decreased the proportion of 8,9-EET, 14,15-EET, 9-HODE and 13-HODE relative to control. Of these 4 oxylipids, only 14,15-EET was not significantly different between control+HET0016 and AAPH+HET0016 treatments.

Exposure of BAEC to 20-HETE induces oxidative stress

Exposure of BAEC to 20-HETE dose- and time-dependently increased ROS/RNS production which peaked at 30 minutes (Figures 10A and 10B). From 90 mins onwards, the RNS/ROS fluorescence signal lost significance for the remainder of the experimental duration. A significant decrease in the GSH/GSSG ratio was detected at 90 minutes (Figure 10C). Neither 15-F_{2t}-IsoP

nor protein oxidation markers, protein carbonyls, was changed by BAEC exposure to 20-HETE (Appendix, Figure 14).

20-HETE induced loss in endothelial resistance by an oxidative stress mechanism

The dose of 100 μM for 20-HETE induced significant decreases in the BAEC barrier integrity (Figure 11A) similar to treatments with 5 mM AAPH (Figure 11B). Several antioxidants were tested to determine if the endothelial barrier integrity loss was due to oxidative stress, including the SOD mimetic (tempol), GSH precursor (N-acetyl cysteine, NAC), and DL-α-tocopherol (Vitamin E). Antioxidant doses used were determined based on the effect of each antioxidant alone on cell viability, production of ROS/RNS, and the ability to decrease AAPH-induced ROS/RNS formation. Doses selected for evaluation on endothelial barrier integrity were 5 mM NAC and 10 μM vitamin E. Antioxidants were added simultaneously with 20-HETE as a treatment to the immediate induction of oxidant stress by 20-HETE. For NAC, 5 and 10 mM had an adequate viability of at least 90% (Figure 11C and 11D) and significantly decreased the production of AAPH-induced reactive metabolites (Figure 11E). Co-treatment of BAEC with 5 mM of NAC and 20-HETE induced loss of barrier integrity to the same extent as or worse than 20-HETE alone (Figure 11F). Vitamin E at 10 μM had adequate viability (Figure 12A) but did not affect the AAPH-induced RM production (data not shown). Barrier integrity upon exposure to Vitamin E alone did not differ from the untreated controls (Figure 12B). Co-exposure of BAEC to 20-HETE and vitamin E simultaneously resulted in an increased lag time to the development of barrier integrity loss which became significant at 8 hours as opposed to 3 hours induced by 20-HETE alone (Figure 12C). From hour 9 until the end of the experiment, loss of barrier integrity was similar for 20-HETE alone and 20-HETE+vitamin E, and both were significantly different from untreated controls (Figure 12C).

Decrease in endothelial resistance by AAPH and 20-HETE is not mediated by apoptosis

Exposure of BAEC to 20-HETE or AAPH alone did not induce significant changes in caspase 3/7 activity (Figure 13A, 13B, and 13C). The addition of NAC to BAEC treated simultaneously with 20-HETE induced apoptosis similar to that produced by NAC alone (Figure 13A). Pre-incubation of BAEC with NAC for 12 hours before the addition of 20-HETE also increased apoptosis compared to negative control, AAPH or 20-HETE alone (Figure 13A). There was no effect on apoptosis in BAEC pre-exposed to vitamin E for 12 hours before the addition of 20-HETE for a further 8 hours (Figure 13B). Relative to untreated controls, there was no evidence of apoptosis in BAEC exposed to the following treatments: Vitamin E alone, Vitamin E+20-HETE simultaneously, and 12-hour pre-incubation with vitamin E followed by 20-HETE (Figure 13C). An LDH-release assay was performed to examine whether cellular necrosis played a role in the decreased barrier integrity. The LDH-release assay showed that cell death was induced only by co-exposure of BAEC to NAC and 20-HETE (figure 13D).

Discussion

Our most recent studies on bovine coliform mastitis showed overproduction of 20-HETE that was correlated strongly with concurrent oxidative stress (Mavangira et al., 2015, Mavangira et al., 2016b). Based on oxidative stress-dependent cellular injury studies in human microvascular endothelial cells (Scarpato et al., 2011), we developed an oxidative stress model as a reference for evaluating the effects of 20-HETE on endothelial barrier integrity. Oxidative stress was induced using AAPH, which thermally decomposes in aqueous solution to generate free radicals (Scarpato et al., 2011). In our model, AAPH successfully induced oxidative stress by overproduction of RM, decreased total glutathione and increased lipid peroxidation. Our findings agree with previous studies that used AAPH to induce oxidative stress in various cells including

endothelial cells, hepatocytes, and liposarcoma cells (Plumb et al., 1997, Roche et al., 2009, Scarpato et al., 2011). Further, AAPH was shown to induce *in-vivo* oxidative stress in mice as detected by increased 15-F_{2t}-IsoP (Yoshida et al., 2008). The 15-F_{2t}-IsoP have recently also been utilized in cell culture systems to demonstrate oxidative stress (Labuschagne et al., 2013). In our model, concentrations of 15-F_{2t}-IsoP and another lipid oxidation metabolite elevated in various in-vivo disease with marked oxidative stress, 11-HETE (Mallat et al., 1999), showed the successful induction of oxidant damage. Thus, our oxidative stress model provided a sufficient reference for testing the links that may exist between LPS, 20-HETE and the development of oxidative stress during acute inflammation.

Previous studies showed that acute inflammation depresses CYP gene expression and the subsequent production of CYP-derived oxylipids including eicosatetratrienoic acids (EETs) and 20-HETE in various organs (Theken et al., 2011). Our studies showing increased 20-HETE in bovine mastitis are in agreement with the LPS- and cecal ligation and puncture murine sepsis models in which 20-HETE production increased by up to 300% in some organs (Anwar-mohamed et al., 2010, Willenberg et al., 2015). Thus, we expected that the stimulation of BAEC with LPS would result in the endogenous production of 20-HETE. In fact, it appears that oxidative stress mechanism may not be a requirement since AAPH did not change the 20-HETE production despite induction of oxidative stress in BAEC. Alternatively, aortic-derived endothelial cells may be devoid of CYP hydroxylation capacity because ionophore stimulation of BAECs failed to induce 20-HETE production (Cheng et al., 2010). Additionally, murine studies showed that CYP hydroxylase mRNA expression increased with decreasing systemic arterial vessel diameter with initial identification in the mesenteric artery (Marji et al., 2002). The lack of increase in 20-HETE following AAPH or LPS treatment was not related to the potency of the

doses utilized because BAEC were sufficiently activated based on the mRNA expression for COX2 and VCAM-1. Studies have shown that activation of HUVECs as evidenced by tumor necrosis factor alpha production following exposure to LPS was associated with increased mRNA expression of the CYP-epoxygenase isoform, CYP2J2 (Askari et al., 2014). Utilizing another bovine cell line, MDBK, same AAPH doses and even lower doses of LPS (1 and 10 ng/mL) for 24-hour duration showed differential responses of CYP isoforms with no changes detected for the canonical CYP hydroxylases. Our study, therefore, suggests that AAPH and LPS do not induce significant expression of the CYP-hydroxylases or 20-HETE production in BAEC compared to untreated control.

The lack of increase in 20-HETE concentrations after pre-exposure to the CYP-hydroxylase inhibitor, HET0016, further supported the deduction that BAEC were not a significant source of 20-HETE in our model. In vivo studies in which overproduction of 20-HETE and oxidative stress are key for pathology, show protection from oxidative damage when treated with HET0016 (Dunn et al., 2008). Similarly, cell cultures in several models of cellular damage due to 20-HETE-induced oxidative stress including the oxygen-glucose deprivation in hippocampal slices, renal epithelial cells, and neonatal myocardial murine cells were protected by HET0016 (Nilakantan et al., 2008, Bao et al., 2011a, Renic et al., 2012). Although the 10 nM dose utilized in our study is at least 1000 fold less than doses that would affect epoxygenase isoforms (Nakamura et al., 2003), a few oxylipids were decreased significantly suggesting a potential influence on the oxylipid profile which can affect the overall oxidant phenotype in agonist-treated cells. Further studies with an expanded lipidome profile may be needed to understand the implications of 20-HETE biosynthesis inhibition.

Previous studies in HUVECs transduced with CYP-hydroxylase isoforms, 4A1 and 4A2, showed that increased concentrations of 20-HETE could induce oxidative stress (Ishizuka et al., 2008). In this study, we also demonstrated that BAEC exposed to 20-HETE increased RM production accompanied decreased GSH/GSSG ratio, an acceptable marker of oxidative stress. The induced oxidative stress was accompanied by a significant loss in endothelial barrier resistance as early as the 3rd hour of incubation in a very similar manner to AAPH, thus implicating an oxidative stress-dependent mechanism. In bovine retinal microvascular endothelial cells treated with 12-HETE, 15-HETE or hydroperoxides, pre-exposure to NOX inhibitors rescued the loss of endothelial resistance (Othman et al., 2013). The NOX enzyme system may be a relevant source of reactive metabolites in our study since previous studies showed that 20-HETE upregulated NOX activity (Han et al., 2013). The NOS enzyme and mitochondria may be additional reactive metabolite sources previously implicated in other studies with 20-HETE (Cheng et al., 2008, Dunn et al., 2008). Increased mitochondrial ROS in HUVECs stimulated with the cytokine tumor necrosis factor-α was linked through ceramide to initial NOX-mediated ROS formation (Chen et al., 2008). Further metabolism by endothelial cells may also play a role in the ability and duration of oxidative stress induced by 20-HETE. For example, 20-HETE metabolism by COX into 20-hydoxy-PGG_2, PGH_2, and PGE_2 was required to cause vasodilation of the basilar artery from rats (Fang et al., 2006). Alternatively, 20-HETE is converted to 20-COOH-AA by alcohol dehydrogenase for the vasodilatory activity (Fang et al., 2006). Alcohol dehydrogenase 4 mediated this conversion and was identified in the cerebral microvascular endothelium (Collins et al., 2005). The possibility that 20-HETE is metabolized to products that are ultimately responsible for the loss of endothelial resistance requires further investigation.

Oxidative damage stress induced by 20-HETE caused cellular apoptosis in renal kidney cells, cardiomyocytes, and HUVECs transduced with CYP hydroxylase. On that basis, we investigated the potential for 20-HETE to mediate loss of barrier resistance through endothelial cell apoptosis. Antioxidants were ineffective at completely rescuing the loss in barrier integrity. Of the antioxidants tested, NAC, tempo, and vitamin E, only NAC decreased AAPH-induced ROS production. Some studies have shown that cells cultured in hypoxic conditions have increased ROS production and undergo enhanced apoptosis when supplemented with NAC (Qanungo et al., 2004). The pre-incubation of BAECs with serum-free media likely placed the cells at increased risk for NAC-induced apoptosis. In other cells, NAC induced non-ROS mediated apoptosis (Wu et al., 2014), a mechanism that may be dependent on induction of reductive stress due to over-supplementation with antioxidants (Zhang et al., 2012). Combining serum-free media and lack of supplemental Se may have increased endothelial cells susceptibility to 20-HETE-induced dysfunction because of increased ROS production. The partial protection afforded by vitamin E could be explained by rapid utilization of Vitamin E which is not regenerated because of lack of Se. The Se-dependent glutathione reductase enzymes participate in the regeneration of vitamin E in the presence of reduced GSH (Ho and Chan, 1992). Our study showed that 20-HETE diminished reduced GSH in culture conditions with no supplemental Se. Our group previously showed that lack of Se supplementation decreased the activity of GPx enzymes (Sordillo et al., 2008). Loss of endothelial resistance in the presence of antioxidants might also be due to the failure of antioxidants to reach the site of highest ROS production, presumably the mitochondria. In HUVECs stimulated with H_2O_2, targeting both tempo and vitamin E to the mitochondria protected against endothelial apoptosis compared to their untargeted forms (Dhanasekaran et al., 2004). Surprisingly, neither 20-HETE nor AAPH induced

endothelial apoptosis despite altering the oxidative stress parameters and evidence of inducing lipid peroxidation in AAPH treatments. Thus, the loss in endothelial resistance in our model does not depend on cell death upon exposure to 20-HETE. In pulmonary endothelial cells, 20-HETE protected against apoptosis from stimuli including serum starvation, LPS, and hypoxia (Dhanasekaran et al., 2009), an effect explained by the differential effects of 20-HETE in different vascular beds. For example, 20-HETE induces vasodilation in pulmonary vasculature but causes constriction in the systemic vasculature. In the endothelial resistance loss induced by AAPH, our studies showed that necrosis plays a role.

The loss in barrier integrity in the absence of cell death in our studies suggest that other mechanisms may be involved. In podocytes, 20-HETE increased permeability to calcium ions by opening calcium channels thus increasing electrical conductivity (Roshanravan et al., 2016). Calcium may participate in the contraction of the intracellular microtubules resulting widening of cellular gap junctions. Another potential mechanism for the 20-HETE-induced loss in endothelial permeability might have been the phosphorylation of small GTPase proteins, including Rho kinase (Randriamboavonjy et al., 2003). Other lipid metabolites, 12- and 15-HETE were also shown to directly affect cell junctional protein expression including zona occludens protein 1 in an NOX-dependent manner (Othman et al., 2013), a mechanism that may be relevant for 20-HETE. Future studies are required to elucidate the mechanisms involved in the 20-HETE-induced loss of endothelial barrier resistance.

Conclusions

In conclusion, the results of this study showed that 20-HETE affects the barrier integrity of endothelial cells as demonstrated by the decreased electrical resistance. The loss of endothelial barrier integrity is consistent with changes in some oxidative stress parameters; however, no

definitive evidence of oxidant damage occurred in 20-HETE treatments. Co-treatment of BAEC with antioxidants did not prevent the loss of barrier integrity. The loss in endothelial barrier integrity induced by 20-HETE was not dependent on cell death. Although endothelial cells are targets for 20-HETE-induced dysfunction, BAECs are not a primary source of 20-HETE production. Further studies should explore the precise mechanisms by which vascular barrier integrity is disrupted by 20-HETE.

Acknowledgements

The authors wish to thank members of the Meadow Brook laboratory at Michigan State University including Jeffrey C. Gandy and Jennifer De Vries for their technical assistance. This work was funded through grant 2011-67015-30179 from the Agriculture and Food Research Initiative Competitive Grants Programs of the USDA National Institute for Food and Agriculture

CHAPTER 5

SUMMARY AND CONCLUSIONS

The broad goal of this dissertation was to determine the contribution of the CYP-derived oxylipid metabolite, 20-HETE, to the vascular endothelial barrier dysfunction which is a significant pathological manifestation in acute and severe inflammatory conditions such as sepsis. The rationale for focusing on 20-HETE came from preliminary data presented in chapter 2 in which several perturbations in the production of oxygenated lipid metabolites (oxylipids) were detected. Previous studies by our group and others showed that oxylipid production was altered in dairy cows with coliform infection in the mammary gland (Maddox et al., 1990, Maddox et al., 1991). As the knowledge of oxylipid production in many diseases of humans and animals has increased rapidly over the last few decades, the changes of the oxylipid profiles in severe coliform mastitis were unknown (Dennis and Norris, 2015). Therefore, in Chapter 2, oxylipid profiles in severe bovine coliform mastitis showed that increased PUFA substrate availability, activation of multiple biosynthetic pathways, and the degree of oxylipid metabolism contributed in defining the observed oxylipid profiles (Mavangira et al., 2015). A significant finding, reported for the first time in coliform mastitis, was the consistent elevation in the CYP-derived oxylipid, 20-HETE in plasma and milk from cows with severe coliform mastitis. With the knowledge that clinical severity of coliform mastitis is partly dependent on concurrent oxidative stress development, a panel of biomarkers for the detection of oxidative stress were employed in the cows with severe coliform mastitis. Based on the limitations of many of the currently used biomarkers of oxidative stress in veterinary medicine, especially in ruminants (Celi, 2011), the study in Chapter 3 evaluated the utility of a biomarker that is considered as a gold standard biomarker (Milne et al., 2015) of oxidative stress in humans. The biomarker, an

oxylipid derived from the free radical metabolism of AA known as 15-F_{2t}-isoprostane (15-F_{2t}-IsoP), was correlated with the changes in oxidant and redox status that are consistent with the occurrence of oxidative stress (Mavangira et al., 2016). The findings in the study reported in Chapter 3, therefore, recapitulated the observations from previous studies that oxidative stress was related to the severity of clinical disease in coliform mastitis of dairy cattle. Further analyses showed significant correlations between 20-HETE and the oxidative stress biomarkers suggesting that a cause-effect relationship may exist among these variables and potentially influence disease outcome. Thus, the study in Chapter 4 was performed with the goal of assessing potential pathological consequences of increased 20-HETE production during inflammation. We showed that 20-HETE disrupted barrier integrity but contrary to our hypothesis, cell death did not appear to play a role. Antioxidants evaluated failed to prevent or significantly improve the loss in barrier integrity; instead, the combination of two of the antioxidants, N-acetyl cysteine and tempo (superoxide dismutase mimetic), with 20-HETE tended to exacerbate the loss of endothelial barrier integrity.

Chapter 2

Oxylipids regulate all parts of the inflammatory response, from initiation, to progression, and to its resolution (Dennis and Norris, 2015). Production of oxylipids was previously reported in cows with coliform mastitis with a predominance of proinflammatory metabolites such as the prostaglandins (PG) E_2 and $F_{2\alpha}$ and thromboxane (TX) B_2. These findings were the basis of for the use of NSAIDs in coliform mastitis; however, there are several complications associated with NSAID use including abomasal ulceration and renal necrosis as well as minimal evidence of efficacy. The study reported in Chapter 2 described the patterns and diversity of oxylipid metabolites occurring during severe bovine coliform mastitis using liquid chromatography/mass

spectrometry (LC-MS/MS) for detection and quantification. We showed that both concentration and number of individual oxylipid species produced differed between the site of infection, the local mammary gland, and systemic production. A major strength of the study was the use of a naturally occurring disease model which captured changes that would allow practical use of the knowledge gained. However, the study had notable limitations. The use of a single time point sample/cow does not allow for defining the overall inflammatory phenotype associated with oxylipid changes. We were also unable to follow the temporal changes in oxylipids and correlate the changes to clinical signs. In taking into account the costs of LC-MS/MS and the goal of the study as a pilot evaluation of oxylipid profiles, the study design was justified and significant for defining the oxylipid profile much more comprehensively for the first time in dairy cattle. There are several reasons explain the variability in the data obtained, including pathogen load at infection, variation in response to infection, lag times from onset of disease to diagnosis, and the effect treatments like NSAIDs that influence COX2-dependent oxylipid biosynthesis. An attempt was not made to assess the effects of treatments with NSAIDs or antibiotics because of lack of reliable clinical records. The ability to evaluate treatment effects would have been informative because NSAIDs may shuttle PUFA substrates to non-COX pathways and impact oxylipid profiles. Studies have demonstrated that COX-metabolism can be modified by acetylsalicylate to produce 15R-HpETE, which can be converted to anti-inflammatory LXA4. Perhaps this information could have been determined by partitioning clinical cases into NSAID-treated and non-treated, specifically with aspirin. Another important information that could have been addressed by this study is the influence of diet on fatty acid composition in the plasma and milk samples. Diet affects PUFA composition in the many cells and fluid compartments of the body. Oxylipid data could have been correlated to dietary PUFA concentrations to account for diet as a

source of the elevated PUFA detected in milk and plasma from mastitis cows. Related to this fact is also the lack of non-esterified fatty acid data in plasma which would have added more to the speculation that lipid mobilization played a role in increasing the PUFA substrate available for oxylipid biosynthesis. Despite the shortcomings of the study, many significant findings were important first reports in bovine mastitis: 1st, the consistently increased 20-HETE concentrations; 2nd, the expanded lipidomic profile showing differential effects of the compartment with several changes in the mammary gland compared to systemic. Because of the challenge regarding limited effective anti-inflammatories and the need to reduce antibiotic use in treatment and prevention of diseases in food-producing animals, the oxylipids may represent novel alternate targets for treatment approaches and the study in Chapter 2 provides specific examples of metabolites and pathways that can be explored. Because oxylipids may mediate their effects through various mechanisms including oxidative stress, Chapter 3 examined oxidative stress occurring during bovine coliform mastitis to determine if one of the oxylipid metabolites could be useful in the detection of oxidative stress.

Chapter 3

Oxidative stress plays a major role in many human and animal diseases, but its detection continues to be a challenge, particularly in veterinary medicine (Celi, 2011). The supplementation of selenium and vitamin E was also shown to reduce the severity and duration of clinical signs due to bovine coliform mastitis (Weiss et al., 1997). The diagnosis of oxidative stress was based on non-specific measures such as ROS production (Kizil et al., 2007). In human, however, products of free radical-mediated peroxidation of PUFA generate isoprostanes that have been used as gold standard biomarkers of oxidative stress (Milne et al., 2011). Thus, we evaluated and concluded that 15-F_{2t}-IsoP is a viable biomarker of oxidative stress in severe

bovine coliform mastitis using LC-MS/MS and also explored the usefulness of commercial assays with reference to LC-MS/MS. The utility of the 15-F_{2t}-IsoP during the oxidative stress of bovine coliform mastitis is especially impressive given the limited number of experimental animals in our study (total n = 8). The small n is also a major limitation of the study. Using the 15-F_{2t}-IsoP data obtained from this study, at least n = 15/group would be required to accurately detect the specific differences in 15-F_{2t}-IsoP concentrations identified in Chapter 3. A series of studies recently suggested that the COX2 enzymes can generate 15-F2t-IsoP and that 15-F_{2t}-IsoP concentrations should be interpreted in the context of prostaglandin $F_{2\alpha}$ (van 't Erve et al., 2015, van't Erve et al., 2016). $PGF_{2\alpha}$ was not measured in our study and it is possible that the overestimation of 15-F_{2t}-IsoP by the ELISA assays evaluated was because of the cross-reactivity with $PGF_{2\alpha}$. Because the accurate determination of 15-F_{2t}-IsoP currently relies on mass spectrometry methods which are expensive and technically challenging, more work is required to develop user-friendly diagnostic methods that accurately quantify 15-F_{2t}-IsoP and to determine the relationship between 15-F_{2t}-IsoP and $PGF_{2\alpha}$ in dairy cattle. An interesting finding was the positive correlation between the 15-F_{2t}-IsoP and the oxylipid, 20-HETE, identified in chapter 2 which formed the basis for proposing a causal link between 20-HETE and oxidative stress. Therefore, an oxidative stress model was developed to determine the role of 20-HETE in the development of oxidative stress and its associated pathological consequences.

Chapter 4

Although previously recognized in chronic inflammatory conditions of humans including hypertension, diabetes and some acute conditions like cerebral ischemia, the relevance of 20-HETE in acute inflammatory conditions is equivocal. For example, in many studies, Tunctan *et al*. showed that treatment of LPS-induced murine sepsis with 20-HETE mimetics resulted in

improved clinical signs including blood pressure, weight loss, and reduced mortality rates. The basis for these studies, therefore, was that 20-HETE production in acute inflammatory conditions was reduced. Studies of LPS-induced murine sepsis showing suppressed CYP gene expression post sepsis induction supported the findings by Tunctan *et al*. (Theken et al., 2011). In contrast, significant increases in CYP4 hydroxylase gene expression and 20-HETE production after LPS- and cecal ligation and puncture (CLP-) in mice were reported (Anwar-mohamed et al., 2010, Willenberg et al., 2015). The studies demonstrating increased 20-HETE agree with the abundance of 20-HETE in our study using severe bovine coliform mastitis. Therefore we investigated the potential pathological contribution of 20-HETE using an in-vitro model of oxidative stress.

First, we developed a model for inducing oxidative stress using primary bovine aortic endothelial cells (BAECs). The model employed used a free radical generator that undergoes temperature-dependent thermal decomposition in aqueous solution generating radicals for a prolonged duration of time ($t_{1/2}$ = 175 hours). Previously, AAPH was shown to induce oxidative stress in human endothelial and other cells (Plumb et al., 1997, Scarpato et al., 2011). In addition, we also utilized a culture media devoid of selenium (Se) supplementation. Previously, our lab showed that insufficient Se in culture media for many cell lines including BAECs, bovine mammary endothelial cells (BMECs), and murine raw cell line 264.7, induced oxidative stress-related changes (Cao et al., 2000, Cao et al., 2001, Mattmiller et al., 2014). Therefore, the combination of a free radical inducer (AAPH) and non-Se media provided conditions for the development oxidative stress. In this model, we showed increased markers of oxidative stress that we previously showed in-vivo, including robust RM production, altered redox state by decreasing total glutathione (GSH) concentrations and the induction of macromolecular damage as shown

by 15-F_{2t}-IsoP. Protein carbonyls did not show any changes of oxidant damage which may be explained by either the poor sensitivity of protein oxidation as a marker of oxidant damage in cell culture. In addition, our agonists may not have been potent enough to cause detectable changes in oxidized proteins. Exogenous 20-HETE (Cayman, Ann Arbor, MI) was used in culture medium with no serum (0% fetal bovine serum, FBS) supplementation. The use of 20-HETE in 0% FBS media is standard practice, as is with using other oxygenated lipids because serum contents including albumin, serum fat acid binding proteins, and phospholipids can bind and interfere with the effects of oxylipids. Conversely, serum may contain components that may induce oxidation of the lipid mediators, for example, the presence of free iron in serum or released from iron in transferrin added to culture medium. The challenge with using 0% FBS is that lack of serum in culture medium in itself induces reactive metabolite production. Our studies showed that 0% FBS media induced significant ROS production, but the levels were less than those induced by 20-HETE and AAPH.

Determining the source of 20-HETE that becomes injurious to the vascular endothelium is important in particular regarding the targeting of therapies for the modulation of disease outcomes. The targets for 20-HETE in the endothelial cells include the endothelial nitric oxide synthase (eNOS) and nicotinamide adenine dinucleotide phosphate-oxidase (NOX) (Cheng et al., 2008, Han et al., 2013). In some studies, 20-HETE was shown to be a substrate for further metabolism through the dehydrogenases (Collins et al., 2005), lipid metabolizing enzymes including Cyclooxygenases (COX) and non-hydroxylating CYP isoforms (Fang et al., 2007). Further metabolism by COX was required for physiological effects. For example, vasodilation of mouse basilar arteries required the formation of prostaglandin derivatives of 20-HETE, 20-hydroxy-PGE_2 (Fang et al., 2007). Therefore, understanding if BAECs are a source of 20-HETE

is important in understanding how overproduction of 20-HETE may interact with other metabolizing pathways thus far detected in endothelial cells. The eNOS and NOX enzymes are targets for many agonists and are required for many physiological processes implying that they may not be the best targets as they may interfere with the normal physiological process. The effect of uncoupling eNOS by 20-HETE raises interesting questions, for example, in diseases characterized by inducible NOS (iNOS) occurs, does 20-HETE also target iNOS and induce more severe oxidative stress? Previous studies showed that in large arteries, endothelial cells do not have significant CYP hydroxylase expression (Marji et al., 2002) and that incubation of BAEC with AA and stimulation with calcium ionophore (Cheng et al., 2010) failed to induce 20-HETE production. Perhaps more physiological studies can be performed by utilizing endothelial cells from vascular beds known to express hydroxylating isoforms of CYPs. Although not physiological, endothelial cells may be engineered by using techniques such as transfection to induce the capacity to induce 20-HETE biosynthesis. The success of such approaches will enable studying the regulation and the pathological mechanisms of 20-HETE production in endothelial cells.

In light of the lack of 20-HETE production by BAECs, we utilized exogenous 20-HETE. The concentration of 100 μM used in our barrier integrity studies were several orders of magnitude greater than a 100 nM dose initially evaluated for ROS production in BAEC. Many studies demonstrating pathological effects of 20-HETE have used concentrations ranging from 5 nM – 20 μM (Cheng et al., 2010, Roshanravan et al., 2016). We evaluated doses from 100 nM – 100 μM, and although we had increased ROS production across the spectrum of doses tested, disruption of barrier function only occurred at 100 μM. Subsequently, the 100 μM dose was utilized in the remainder of the experiments. A concern becomes the possibility of using non-

physiologic and even much greater concentrations than observed in pathological states and therefore inducing concentration-dependent toxicity of 20-HETE to BAECs. Although not investigated in this study, the lack of both apoptosis or necrosis of the BAEC after a 24-hour exposure suggests that there were no lipotoxicity effects. Further studies, however, can examine closely related metabolites at the same doses as 20-HETE (100 μM) to rule out lipotoxicity effects. An example would be to use 19-HETE, the ω-1 hydroxylation metabolite of AA which was found to antagonize the pathological effects of 20-HETE (Elkhatali et al., 2015).

Although 20-HETE induced changes consistent with oxidative stress including RM production, decreased GSH/GSSG ratio, the lack of significant changes in LDH release or caspase enzyme activity suggest that cell death is not involved in the observed endothelial barrier disruption that occurred in our model. Some studies have shown that 20-HETE induces contraction in vascular smooth muscle cells by increasing the permeability to calcium (Ge et al., 2014). In addition, 20-HETE was shown to mediate the phosphorylation of cellular contractile microtubules by phosphorylation of intracellular filament subunits in a mechanism that requires ROS production and activation of GTPase (Kizub et al., 2016). Therefore, observations of vascular barrier dysfunction in our study may be due to induction of contraction of the cellular microfilaments and widening of gap junctions reducing the electrical barrier resistance. Further studies are needed to determine the integrity of gap junctions during BAEC exposure to 20-HETE. The inability of the antioxidants tested in our study to prevent or improve the decrease in barrier integrity could be due to a few possible reasons. First, the duration of the experiment could have been such that the antioxidants were used up in the presence of excess concentrations of 20-HETE. Based on our studies, NAC decreased ROS production whereas Vitamin E delayed the decrease in endothelial cell electrical resistance; therefore, 20-HETE may have been present in

concentrations that overwhelmed the antioxidants. Second, BAEC may lack efficient mechanisms to metabolize 20-HETE to inactive metabolites by dehydrogenation, for example; that may inactivate and reduce the detrimental effects of 20-HETE. If this is true, excess 20-HETE may be channeled towards pathways that may be responsible for the biological effects of 20-HETE like the previously mentioned COX or dehydrogenases. Third, the presence of 20-HETE may disrupt cellular membrane permeability by modifying the lipid content of cell membranes. Coronary artery endothelial cells are known to incorporate 20-HETE when supplemented (Kaduce et al., 2004). Finally, the loss in barrier integrity may not be entirely dependent on oxidative stress changes.

There is a need to evaluate the effects of 20-HETE on endothelial resistance with better antioxidants treatments. First, antioxidants should be targeted to the mitochondria as they are a major source of ROS. Studies in HUVECs treated with H_2O_2 showed that targeting vitamin E and tempo to the mitochondria protected from apoptosis than when the same antioxidants were used in an untargeted fashion (Dhanasekaran et al., 2004). Further, other studies show that stressing cells with hypoxic conditions, for example, makes them susceptible to antioxidant-induced apoptosis. This may explain the increased cell death we saw with NAC (Qanungo et al., 2004). Future studies will establish sufficient antioxidant treatments including supplementing selenium to culture media and longer pre-incubation of cells with antioxidants to allow for sufficient cellular uptake of antioxidants before treatments with positive oxidative stress inducer or 20-HETE are used. Alternatively, it may be possible that 20-HETE has protective effects and that the endothelial cell-substrate impedance sensing may not be the best way to evaluate dysfunction due to 20-HETE

APPENDICES

Appendix A. Authorization to publish manuscript as Chapter 2 in dissertation

ELSEVIER ORDER DETAILS

Oct 14, 2016

Order Number	501192923
Order date	Oct 14, 2016
Licensed Content Publisher	Elsevier
Licensed Content Publication	Journal of Dairy Science
Licensed Content Title	Polyunsaturated fatty acids influence differential biosynthesis of oxylipids and other lipid mediators during bovine coliform mastitis
Licensed Content Author	Vengai Mavangira,Jeffery C. Gandy,Chen Zhang,Valerie E. Ryman,A. Daniel Jones,Lorraine M. Sordillo
Licensed Content Date	September 2015
Licensed Content Volume Number	98
Licensed Content Issue Number	9
Licensed Content Pages	14
Start Page	6202
End Page	6215
Type of Use	reuse in a thesis/dissertation
Portion	full article
Format	electronic
Are you the author of this Elsevier article?	Yes
Will you be translating?	No
Order reference number	
Title of your thesis/dissertation	CYTOCHROME P450 OXYLIPIDS MODULATE OXIDATIVE STRESS-INDUCED VASCULAR DYSFUNCTION
Expected completion date	Dec 2016
Estimated size (number of pages)	200
Elsevier VAT number	GB 494 6272 12
Requestor Location	Vengai Mavangira Michigan State University 736 Wilson Road Room D202 EAST LANSING, MI 48824 United States Attn: Vengai Mavangira
Total	Not Available

Appendix B. Tables

Table 1. Nutrient composition (% of DM unless otherwise noted) of the diet for the experimental animals[1]

Item	Nutrient analysis
DM	47.64
Forage DM	40.87
CP	17.23
MP	11.97
ME, Mcal/kg	2.98
NEL,> Mcal/kg	1.79
ADF	16.23
NDF	29.56
Forage ADF	10.92
Forage NDF	17.46
NFC	42.36
Starch (nonsugar)	29.85
Fat	4.34

[1]Supplemented with: vitamin A, 8,369 IU/kg, vitamin D, 1,455 IU/kg, and vitamin E, 33 IU/kg; minerals (% of DM): 1.04 Ca, 0.48 P, 1.1 K, 0.34 Mg, 0.26 S, 0.56 Na, 0.32 Cl, 0.35 Salt; Ca:P ratio = 2.17; trace minerals (mg/kg): 51.8 Zn, 7.6 Fe, 11.5 Cu, 37.0 Mn, 0.6 Co, 0.6 I, 0.37 Se; DCAD = 27.6 mEq/100 g; Rumensin 9.3 g/t (Elanco, Indianapolis, IN).

Table 2. Optimized multiple reaction monitoring parameters for metabolites

Metabolite[1]	Parent ion (m/z)	Product ion (m/z)	Cone voltage	Collision energy	Precursor[2]	Class
12 HHTrE	279.2	179	45	10	ArA	Alcohol
20-HETE	319.2	245	55	16	ArA	Alcohol
15-HETE	319.2	219	45	10	ArA	Alcohol
11-HETE	319.2	167	51	16	ArA	Alcohol
9-HETE	319.2	151	15	10	ArA	Alcohol
5-HETE	319.2	115	33	10	ArA	Alcohol
14,15-DHET	337.2	207	33	16	ArA	Diol
11,12-DHET	337.2	167	51	22	ArA	Diol
8,9-DHET	337.2	127	15	22	ArA	Diol
AEA	348.2	62	21	16	ArA	Endocannabinoid
2-AG	379.3	287	45	16	ArA	Endocannabinoid
14,15-EET	319.2	219	33	10	ArA	Epoxide
11,12-EET	319.2	179	27	10	ArA	Epoxide
8,9-EET	319.2	155	27	10	ArA	Epoxide
8 iso PGF2α	353.2	193	21	22	ArA	Isoprostane
8 iso PGA2	333.2	175	55	22	ArA	Isoprostane
8 iso PGA1	335.2	235	39	16	ArA	Isoprostane
LTB4	335.2	195	21	16	ArA	Leukotriene
5(S),6(R)-Lipoxin A4	351.2	115	55	16	ArA	Lipoxin
15-OxoETE	317.2	113	45	16	ArA	Ketone
5-OxoETE	317.2	203	45	22	ArA	Ketone
6-keto-PGF1α	369.3	163	21	22	ArA	Prostanoid
PGE2	351.2	271	55	16	ArA	Prostanoid
PGD2	351.2	189	55	22	ArA	Prostanoid
15d-PGJ2	315.2	271	39	10	ArA	Prostanoid
TXB2	369.2	169	51	16	ArA	Thromboxane
17-HDoHE	343.2	281	45	10	DHA	Alcohol
19,20-DiHDPA	361.2	273	27	16	DHA	Diol
10,17-DiHDoHE	359.2	153	15	16	DHA	Protectin
7,17-dh-DPA	361.2	143	27	16	DHA	Protectin
Resolvin D2	375.2	175	21	22	DHA	Resolvin
17,18-DiHETE	335.2	247	39	16	EPA	Diol
14,15-DiHETE	335.2	207	27	16	EPA	Diol
17,18-EpETE	317.2	255	15	10	EPA	Epoxide
14,15-EpETE	317.2	207	27	10	EPA	Epoxide
13-HODE	295.2	195	30	16	LA	Alcohol
9-HODE	295.2	171	45	16	LA	Alcohol

Table 2. (cont'd)

12,13-DiHOME	313.2	183	45	22	LA	Diol
9,10-DiHOME	313.2	201	27	22	LA	Diol
12,13-EpOME	295.2	195	30	16	LA	Epoxide
9,10-EpOME	295.2	171	45	16	LA	Epoxide
13-OxoODE	293.2	113	15	22	LA	Ketone
9-OxoODE	293.2	185	27	16	LA	Ketone
LTD4	495.3	177	51	22	ArA	Leukotriene
Resolvin D1	375.2	141	21	10	DHA	Resolvin
LA	279.2	59	45	16		PUFA
ArA	303.2	259	21	10		PUFA
Eicosapentaenoic acid	301.2	257	39	10		PUFA
Docosahexaenoic acid	327.2	283	51	10		PUFA
Stearic acid	283	283	33	22		SFA
Oleic acid	281	281	45	22		MUFA
Palmitic acid	255	255	33	22		SFA
PGE2_d9	360.2	280	21	16		
8,9-DHET_d11	348.3	127	55	22		
15-HETE_d8	327.2	226	15	10		
8,9-EET_d11	330.3	268	15	10		
AEA_d8	356.3	63	33	10		
2-AG_d8	387.3	294	21	16		
γ-Linoleic acid	277.2	233	27	10		
AA_d8	311.2	267	21	10		
5-HETE_d8	327.3	116	55	16		
7-Maresin1	359.2	177	51	16	DHA	

[1]HHTrE = hydroxyheptadecatrienoic acid; HETE = hydroxyeicosatetraenoic acid; DHET = dihydroxyeicosatrienoic acid; AEA = arachidonoyl ethanolamide; AG = arachidonoyl glycerol; EET = epoxyeicosatrienoic acid; PG = prostaglandin; LTB_4 = leukotriene B_4; oxoETE = oxoeicosatetraenoic acid; 15d-PGJ_2 = 15-deoxyprostaglandin J_2; TXB2 = thromboxane B2; HDoHE = hydroxydocosahexaenoic acid; DiHDPA = dihydroxydocosapentaenoic acid; DiHDoHE = dihydroxydocosahexaenoic acid; 7,17-dh-DPA = 7,17-dihydroxydocosapentaenoic acid; DiHETE = dihydroxyeicosatrienoic acid; EpETE = epoxyeicosatetraenoic acid; HODE = hydroxyoctadecadienoic acid; DiHOME = dihydroxyoctadecenoic acid; EpOME = epoxyoctadecenoic acid; oxoODE = oxooctadecadienoic acid; LTD4 = leukotriene D4; PGE_2_d_9 = prostaglandin E2-d9; 8,9-DHET_d_{11} = dihydroxyeicosatrienoic-d11 acid; 15-HETE_d_8 = hydroxyeicosatetraenoic-d8 acid; 8,9-EET_d_{11} = epoxyeicosatrienoic-d11 acid; AEA_d_8 = arachidonoyl ethanolamide-d8; 2-AG_d_8 = 2-arachidonoyl glycerol-d8; AA_d_8 = arachidonic acid-d8; 5-HETE_d_8 = hydroxyeicosatetraenoic-d8 acid.
[2]ArA = arachidonic acid; DHA = docosahexaenoic acid; EPA = eicosapentaenoic acid; LA = linoleic acid.

Table 3. Concentrations and limits of detection (mean ± SEM; n*M*) for oxylipids inconsistently detected in milk and plasma from coliform mastitis (total n = 11) and control (total n = 13) cows

		Mastitis group			Control cows			
Sample	Oxylipid[1]	No./total (%) of cows	Mean	SEM	No./total (%) of cows	Mean	SEM	LOD[2]
Milk	14,15-EET	0/11 (0)	—	—	0/13 (0)	—	—	0.94
	8,9-EET	5/11 (45)	0.15	0.1	0/13 (0)	—	—	0.02
	19,20-EpDPE	2/11 (18)	0.87	0.16	0/13 (0)	—	—	0.6
	15-dPGJ2	2/11 (18)	0.1	0.02	0/13 (0)	—	—	0.05
	14,15-EpETE	2/11 (18)	0.06	0.06	0/13 (0)	—	—	0.01
Plasma	LTB4	0/11 (0)	—	—	0/13 (0)	—	—	0.003
	14,15-EET	0/11 (0)	—	—	0/13 (0)	—	—	0.94
	8,9-EET	0/11 (0)	—	—	0/13 (0)	—	—	0.02
	19,20-EpDPE	0/11 (0)	—	—	1/13 (8)	0.76	0	0.6
	17-HDoHE	5/11 (45)	0.3	0.11	0/13 (0)	—	—	0.11
	6-ketoPGF1α	5/11 (45)	1.1	0.23	0/13 (0)	—	—	0.44
	15-dPGJ2	2/11 (18)	0.07	0.01	0/13 (0)	—	—	0.05
	14,15-EpETE	1/11 (9)	0.01	0	0/13 (0)	—	—	0.01

[1]EET = epoxyeicosatrienoic acid; EpDPE = epoxydocosapentaenoic acid; 15-dPGJ2 = 15-deoxyprostaglandin J2; EpETE = epoxyeicosatetrae- noic acid; LTB4 = leukotriene B4; HDoHE = hydroxy-docosahexaenoic acid; 6-ketoPGF1α = 6-keto prostaglandin F1α.
[2]Limit of detection.

Table 4. Cyclooxygenase-derived oxylipids in milk and plasma from coliform mastitis (n = 11) and mid-lactation control (n = 13) cows (mean ± SEM; nM)

			Mastitis		Control		
Sample	Oxylipid[1]	Substrate[2]	Mean	SEM	Mean	SEM	Significance
Milk	6-KetoPGF1α	ArA	1.19	0.36	0.44	0	*
	PGE2	ArA	2.28	0.56	0.05	0.06	***
Plasma	6-KetoPGF1α	ArA	0.74	0.21	0.44	0	*
	PGE2	ArA	0.24	0.06	0.2	0.07	

[1]Data log-transformed; results expressed as geometric mean ± SEM; PGE2 = prostaglandin E2; 6-ketoPGF1 α = 6-keto prostaglandin F1 α .
[2]ArA = arachidonic acid.
*$P < 0.05$; ***$P < 0.001$.

Table 5**.** Lipoxygenase-derived oxylipids in milk and plasma from coliform mastitis (n = 11) and mid-lactation control (n = 13) cows (mean ± SEM; n*M*)

			Mastitis		Control		
Sample	Oxylipid[1]	Substrate[2]	Mean	SEM	Mean	SEM	P-value
Milk	13-HODE	LA	32.6	9	6.8	1.7	*
	9-HODE[3]	LA	5.9	0.29	2	0.29	*
	13-oxoODE[3]	LA	1.6	0.47	0.67	0.22	
	9-oxoODE[3]	LA	1.3	0.4	0.67	0.37	
	15-oxoETE[3]	ArA	0.03	0.63	0.019	0.58	
	5-oxoETE[3]	ArA	0.04	0.8	0.01	0.61	
	5-HETE[3]	ArA	0.23	0.28	0.06	0.17	***
	LTB_4[3]	ArA	0.07	1.03	0.003	0	**
	LXA_4[3]	ArA	0.09	0.45	0.01	0.3	**
	15-HETE[3]	ArA	3	0.26	0.07	0.27	***
	17-HDoHE[3]	DHA	0.26	0.22	0.11	0	
	RvD_2[3]	DHA	0.02	0.8	0.02	0.3	
Plasma	13-HODE[3]	LA	4.27	0.17	4.61	0.16	
	9-HODE[3]	LA	1.34	0.21	1.41	0.2	
	13-oxoODE	LA	0.38	0.05	0.51	0.16	
	9-oxoODE	LA	0.86	0.17	1.3	0.34	
	15-oxoETE	ArA	0.02	0.005	0.03	0.01	
	5-oxoETE	ArA	0.01	0.002	0.02	0.005	
	5-HETE[3]	ArA	0.06	0.32	0.08	0.29	
	LXA_4[3]	ArA	0.01	0.12	0.04	0.41	**
	15-HETE[3]	ArA	0.36	0.3	0.2	0.27	
	RvD_2[3]	DHA	0.003	0.02	0.1	0.08	*

[1]HODE = hydroxyoctadecadienoic acid; oxoODE = oxooctadecadienoic acid; oxoETE = oxoeicosatetraenoic acid; HETE = hydroxyeicosatetraenoic acid; LTB4 = leukotriene B4; LXA4 = lipoxin A4, HDoHE = hydroxydocosahexaenoic acid; RvD2 = resolvin D2.
[2]ArA = arachidonic acid; LA = linoleic acid; DHA = docosahexaenoic acid.
[3]Data log-transformed, results expressed as geometric mean ± SEM.
*$P < 0.05$; **$P < 0.01$; ***$P < 0.001$.

Table 6**.** Cytochrome P450-derived oxylipids in milk and plasma from coliform mastitis (n = 11) and midlactation control (n = 13) cows (mean ± SEM; n*M*)

			Mastitis		Control		
Sample	Oxylipid[1]	Substrate[2]	Mean	SEM	Mean	SEM	P-value
Milk	9,10-DiHOME[3]	LA	2	0.54	6.6	0.17	
	12,13-DiHOME[3]	LA	2.7	0.45	5	0.37	
	9,10-EpOME	LA	0.95	0.2	0.46	0.05	*
	12,13-EpOME	LA	2.3	0.57	0.4	0.06	**
	11,12-EET[3]	ArA	0.02	0.28	0.01	0	
	8,9-EET[3]	ArA	0.05	0.43	0.02	0	
	20-HETE[3]	ArA	0.72	0.66	0.01	0.24	***
	14,15-DiHETE	EPA	1.1	0.2	0.1	0.01	***
	17,18-DiHETE	EPA	4.2	0.87	0.16	0.02	**
Plasma	9,10-DiHOME	LA	2.1	0.5	19.3	2	***
	12,13-DiHOME[3]	LA	0.8	0.2	10.9	0.44	***
	9,10-EpOME	LA	1	0.25	1.9	0.46	
	12,13-EpOME[3]	LA	1	0.26	1.8	0.24	
	11,12-EET	ArA	0.02	0.003	0.05	0.01	*
	20-HETE[3]	ArA	0.53	0.31	0.24	0.15	*
	14,15-DiHETE	EPA	1.1	0.19	1.5	0.16	
	17,18-DiHETE	EPA	8	1.3	19.6	3.3	**

[1]DiHOME = dihydroxyoctadecenoic acid; EpOME = epoxyoctadecenoic acid; EET = epoxyeicosatrienoic acid; HETE = hydroxyeicosatetraenoic acid; DiHETE = dihydroxyeicosatrienoic acid.
[2]LA = linoleic acid; ArA = arachidonic acid; EPA = eicosapentaenoic acid.
[3]Data log-transformed, results expressed as geometric mean ± SEM.
*$P < 0.05$; **$P < 0.01$; ***$P < 0.01$.

Table 7**.** Nonenzymatic-derived oxylipids in milk and plasma from coliform mastitis (n = 11) and mid-lactation control (n = 13) cows (mean ± SEM; n*M*)

			Mastitis		Control		
Sample	Oxylipid[1]	Substrate[2]	Mean	SEM	Mean	SEM	P-value
Milk	11-HETE[3]	ArA	0.57	0.62	0.04	0.22	**
	9-HETE[3]	ArA	0.1	0.61	0.02	0.36	**
Plasma	11-HETE	ArA	0.2	0.05	0.14	0.02	
	9-HETE	ArA	0.06	0.02	0.03	0.004	

[1]HETE = hydroxyeicosatetraenoic acid.
[2]ArA = arachidonic acid.
[3]Data log-transformed, results expressed as geometric mean ± SEM.
**$P < 0.01$.

Table 8. Milk and plasma oxylipids in coliform mastitis (n = 11) and mid-lactation control (n = 13) cows expressed as ratios of select pathways based on substrate

Sample	Ratio[1]	Substrate[2]	Mastitis cows	Control cows	P-value
Milk	13-HODE[3]/9-HODE[4]	LA	4.12 ± 0.13	2.60 ± 0.26	
	Sum EET/20-HETE	ArA	0.10 ± 0.51	5.32 ± 0.71	**
	(9-HETE + 11-HETE)[5]/15-HETE[3]	ArA	0.25 ± 0.65	0.84 ± 0.12	
Plasma	13-HODE/9-HODE	LA	3.28 ± 0.26	3.50 ± 0.36	
	(9-HETE + 11-HETE)/15-HETE	ArA	0.59 ± 0.08	0.60 ± 0.07	

[1]HODE = hydroxyoctadecadienoic acid; EET = epoxyeicosatrienoic acid; HETE = hydroxyeicosatetraenoic acid.
[2]ArA = arachidonic acid; LA = linoleic acid.
[3]Predominantly enzyme derived.
[4]Both enzymatic and nonenzymatic derived.
[5]Predominantly nonenzymatic derived.
$^{**}P < 0.01$.

Table 9. Milk and plasma oxylipids in coliform mastitis (n = 11) and mid-lactation control (n = 13) cows expressed as ratios of select upstream:downstream metabolites based on substrate

			Mastitis		Control		
Sample	Ratio[1]	Substrate[2]	Mean	SEM	Mean	SEM	P-value
Milk	5-HETE/5-oxoETE[3]	ArA	37.2	1.08	8.9	0.43	*
	15-HETE/15-oxoETE	ArA	277.7	81.73	6.12	2.44	**
	9-HODE/9-oxoODE[3]	LA	5.7	0.45	4.4	0.41	
	13-HODE/13-oxoODE[3]	LA	18.22	0.56	8.74	0.32	*
	9,10-EpOME/9,10-DiHOME[3]	LA	0.42	0.1	0.07	0.02	**
	12,13-EpOME/12,13-DiHOME[4]	LA	0.94	0.34	0.07	0.33	***
Plasma	5-HETE/5-oxoETE	ArA	10.18	1.65	7.44	1.33	
	15-HETE/15-oxoETE	ArA	88.5	27.82	56.86	19.7	
	9-HODE/9-oxoODE	LA	1.97	0.21	1.61	0.25	
	13-HODE/13-oxoODE	LA	14.26	2.62	40.19	13.4	*
	9,10-EpOME/9,10-DiHOME	LA	0.57	0.1	0.09	0.01	***
	12,13-EpOME/12,13-DiHOME	LA	1.46	0.25	0.23	0.05	***

[1]HETE = hydroxyeicosatetraenoic acid; oxoETE = oxoeicosatetraenoic acid; HODE = hydroxyoctadecadienoic acid; oxoODE = oxooctadecadienoic acid; EpOME = epoxyoctadecenoic acid; DiHOME = dihydroxyoctadecenoic acid.
[2]ArA = arachidonic acid; LA = linoleic acid.
[4]Square-root transformed data reported as geometric mean ± SEM.
[4]Log transformed data reported as geometric mean ± SEM.
*$P < 0.05$; **$P < 0.01$; ***$P < 0.001$.

Table 10. Correlations between FA substrates and their oxylipid metabolites in milk and plasma from coliform mastitis cows

	Milk		Plasma	
Substrate and metabolite[1]	r	P-value	r	P-value
ArA vs. 15-oxoETE	0.921	**		
EPA vs. 14,15-DiHETE			0.863	**
EPA vs. 17,18-DiHETE			0.756	*

[1]ArA = arachidonic acid; oxoETE = oxoeicosatetraenoic; EPA = eicosapentaenoic acid; DiHETE = dihydroxyeicosatrienoic acid.
*$P < 0.05$; **$P < 0.01$.

Table 11. Correlations between degree of metabolism for select oxylipids in milk and plasma from coliform mastitis cows

		Milk		Plasma	
Substrate[1]	Degree of metabolism[2]	r	P-value	r	P-value
LA	13-HODE vs. 9-HODE	0.864	*	0.834	*
LA	13-HODE vs. 13-oxoODE	0.736	*	0.26	NS
LA	9-HODE vs. 9-oxoODE	0.791	*	0.882	**
LA	9,10-DiHOME vs. 9,10-EpOME	0.724	*	0.387	NS
LA	12,13-EpOME vs. 12,13-DiHOME	0.382	NS	0.75	*
ArA	5-HETE vs. 5-oxoETE	0.639	*	0.678	*
ArA	15-HETE vs. 15-oxoETE	0.639	NS	0.531	NS

[1]ArA = arachidonic acid; LA = linoleic acid.
[2]HODE = hydroxyoctadecadienoic acid; oxoODE = oxooctadecadienoic acid; DiHOME = dihydroxyoctadecenoic acid; EpOME = epoxyoctadecenoic acid; HETE = hydroxyeicosatetraenoic acid; oxoETE = oxoeicosatetraenoic acid.
*$P < 0.05$; **$P < 0.01$.

Table 12. Correlations between fatty acid:fatty acid substrate and oxylipid:oxylipid between samples (e.g., milk LA correlated with plasma LA) within each experimental groups

		Mastitis group		Control group	
Substrate[1]	Oxylipid metabolite[2]	r	P-value	r	P-value
LA				0.843	***
ArA				0.903	***
EPA		0.789	**	0.755	**
LA	13-HODE			0.844	***
LA	9-oxoODE			0.976	***
LA	13-oxoODE			0.793	**
LA	12,13-EpOME			0.753	**
LA	9,10-DiHOME	0.73	*		
LA	12,13-DiHOME	0.906	***	0.841	***
ArA	15-HETE	0.751	**		
ArA	15-oxoETE			0.845	**
ArA	2-AG			0.758	**

[1]LA = linoleic acid; ArA = arachidonic acid; EPA = eicosapentaenoic acid.
[2]HODE = hydroxyoctadecadienoic acid; oxoODE = oxooctadecadienoic acid; EpOME = epoxyoctadecanoic acid; DiHOME = dihydroxyoctadecenoic acid; HETE = hydroxyeicosatetraenoic acid; oxoETE = oxoeicosatetraenoic acid; AG = arachidonoyl glycerol.
*$P < 0.05$; **$P < 0.01$; ***$P < 0.001$.

Table 13. Median (range) concentrations of acute phase proteins and non-esterified fatty acids from coliform mastitis and control cows (n = 4/group)

Variable	Control	Mastitis	P-Value
Acute phase proteins			
Serum Hp, mg/mL	0.003 (0.0005–0.01)	0.49 (0.05–1.7)	0.014
Serum SAA, μg/mL	68.0 (12–218)	1395.9 (1,139–1853)	0.014
Serum albumin, g/dL	3.0 (2.9–3.2)	2.8 (2.6–2.9)	0.043
Lipid mobilization			
Serum NEFA, mEq/L	0.08 (0.06–0.13)	0.62 (0.12–1.2)	0.029

Hp, haptoglobin; SAA, serum amyloid A; NEFA, non-esterified fatty acids.
Statistical analyses: Wilcoxon rank sum test, $\alpha = 0.05$.

Table 14. Median (range) concentrations and ratios for oxidant status, redox status and 15-F_{2t}-isoprostanes in samples from coliform mastitis and control cows (n = 4/group)

Variable	Control	Mastitis	P-value
Milk RM,[a] RFU × 1,000/μL	4.1 (3.5–4.8)	26.6 (14.0–36.7)	0.014
Milk AOP[b]	7.7 (4.9–10.2)	4.8 (4.4–11.4)	NS
Plasma RM,[a] RFU/μg protein	0.30 (0.28–0.51)	0.67 (0.46–0.88)	0.029
Plasma AOP[b]	5.5 (4.7–6.2)	4.9 (4.1–5.8)	NS
Blood GSH, μM	471.5 (455.1–577.4)	403.9 (141.2–417.4)	0.014
Blood GSSG, μM	3.2 (2.1–22.9)	15.8 (4.7–38.7)	0.057
GSH : GSSG ratio	147.5 (17.9–268.6)	47.5 (1.6–87.3)	0.051
Urine 15-F_{2t}-Isop, ng/mg Cr	0.05 (0.02–0.89)	1.5 (0.7–5.2)	0.057
Plasma 15-F_{2t}-Isop, ng/L	2.2 (1.0–6.3)	10.0 (5.1–27.6)	0.057
Milk 15-F_{2t}-Isop, ng/L	1177.5 (436–1,535)	182.4 (87–317)	0.014

RM, reactive metabolites represent reactive oxygen species and reactive nitrogen species; AOP, antioxidant potential; 15-F_{2t}-Isop, 15-F_{2t}-isoprostane; Cr, creatinine; GSH, reduced glutathione; GSSG, oxidized glutathione; NS, not significant.

[a]RFU, relative fluorescence units per μL (milk) and per μg of protein (plasma).

[b]AOP expressed as sample antioxidant concentrations with ABTS- radical reducing power equivalent to standard vitamin E (Trolox) concentrations.

Statistical analyses: Wilcoxon rank sum test, $\alpha = 0.05$.

Table 15. Correlations of non-esterified fatty acids, oxidant status and redox status with the LC-MS/MS quantified 15-F_{2t}-isoprostane concentrations in samples from coliform mastitis and control cows (n = 4/group).

Variable	15-F_{2t}-Isop		
	Milk	Plasma	Urine
Lipid mobilization			
Serum NEFA	−0.48	0.14	0.38
Oxidant status			
Plasma RM	−	0.83[a]	0.52
Plasma AOP	−	−0.57	−0.17
Milk RM	−0.86[a]	−	−
Milk AOP	0.5	−	−
Redox status			
Blood GSH	−	−0.71[a]	−0.81[a]
Blood GSSG	−	0.55	0.83[a]
GSH : GSSG ratio	−	−0.55	−0.83[a]

NEFA, non-esterified fatty acids; RM, reactive metabolites represent reactive oxygen species and reactive nitrogen species; AOP, antioxidant potential; GSH, reduced glutathione; GSSG, oxidized glutathione; 15-F_{2t}-Isop, 15-F_{2t}-isoprostane.
[a]$P < .05$ (Spearman correlation, $\alpha = 0.05$).

Table 16. Median (range) concentrations of 15-F_{2t}-isoprostanes quantified by ELISA in samples from coliform mastitis and control cows (n = 4/group)

Variable	Control	Mastitis	P-Value
cbELISA[a]			
Plasma 15-F2t-Isop, μg/L	24.6 (21.4–27.3)	30.5 (7.6–45.2)	NS
Urine 15-F2t-Isop, ng/mg Cr	11.0 (7.1–19.4)	16.2 (8.1–34.9)	NS
Milk 15-F2t-Isop, μg/L	5.0 (4.6–6.8)	20.6 (7.5–42.8)	0.014
cbELISA[b]			
Milk 15-F2t-Isop, μg/L	0.81 (0.77–0.81)	0.74 (0.15–1.10)	NS
Urine 15-F2t-Isop, ng/mg Cr	11.8 (7.9–14.3)[a]	20.5 (7.7–45.1)[a]	NS
ccELISA[b]			
Urine 15-F2t-Isop, ng/mg Cr	1.8 (1.3–3.3)[b]	3.2 (2.5–4.4)[b]	0.056

ccELISA, Cell Biolabs ELISA; ccELISA, Cayman Chemical ELISA; 15-F_{2t}-Isop, 15-F_{2t}-isoprostane; Cr, creatinine; NS, not significant.
[a]Total 15-F_{2t}-Isop in hydrolyzed samples
[b]Free 15-F_{2t}-Isop in non-hydrolyzed samples.
Statistical analyses: Wilcoxon rank sum test, $\alpha = 0.05$.
Values with letter superscripts (a,b) denote the only comparison in the same column (group) and different superscripts denote statistical difference (Wilcoxon rank sum, $P = .014$).

Table 17. Correlations of nonesterified fatty acids, oxidant status and redox status with ELISA quantified free 15-F_{2t}-Isop concentrations in samples from coliform mastitis and control cows (n = 4/group)

Variable	15-F2t-Isop		
	cbELISA		ccELISA
	Milk	Urine	Urine
Lipid mobilization			
NEFA	−0.26	0.24	−0.60
Oxidant status			
Plasma RM	–	0.02	−0.57
Plasma AOP	–	−0.405	−0.17
Milk RM	−0.43	–	–
Milk AOP	0.66	–	–
Redox status			
Blood GSH	–	−0.55	0.36
Blood GSSG	–	0.55	−0.07
GSH : GSSG ratio	–	−0.55	−0.07

NEFA, nonesterified fatty acids; RM, reactive metabolites represent reactive oxygen and nitrogen species; AOP, antioxidant potential; GSH, reduced glutathione; GSSG, oxidized glutathione; 15-F_{2t}-Isop, 15-F_{2t}-isoprostane; cbELISA, Cell Biolabs ELISA; ccELISA, Cayman Chemicals ELISA.
Spearman correlations, $\alpha = 0.05$.

Table 18. Correlations of nonesterified fatty acids, oxidant status and redox status with ELISA quantified total 15-F_{2t}-Isop concentrations in samples from coliform mastitis and control cows (n = 4/group)

Variable	cbELISA 15-F2t-Isop		
	Milk	Plasma	Urine
Lipid mobilization			
NEFA	0.67	−0.31	0.52
Oxidant status			
Plasma RM	–	0.14	0.29
Plasma AOP	–	0.02	0.26
Milk RM	0.98a	–	–
Milk AOP	−0.19	–	–
Redox status			
Blood GSH	–	−0.21	−0.54
Blood GSSG	–	0.31	0.54
GSH : GSSG ratio	–	−0.31	−0.55

NEFA, nonesterified fatty acids; RM, reactive metabolites represent reactive oxygen and nitrogen species; AOP, antioxidant potential; GSH, reduced glutathione; GSSG, oxidized glutathione; cbELISA, Cell Biolabs ELISA; 15-F_{2t}-Isop, 15-F_{2t}-isoprostane.
[a]$P < .001$ (Spearman correlation, $\alpha = 0.05$).

Table 19. Bovine primers for qRT-PCR.

Gene[a]	Reference sequence	TaqMan assay ID[b]
PGK1	NM_001034299.1	Bt03225857_m1
RPS9	NM_001101152.2	Bt03272016_m1
TBP	NM_001075742.1	Bt03241946_m1
COX2	NM_174445.2	Bt03214492_m1
VCAM-1	NM_174484.1	Bt03279189_m1
CYP4A11	NM_001077908.1	Bt03243984_m1
CYP4F2	NM_001035042.1	Bt03245658_m1

[a]PGK1, phosphoglycerate kinase; RPS9, ribosomal protein s9; TBP, TATA-box binding protein; COX-2, cyclooxygenase-2; VCAM-1, vascular adhesion molecule-1; CYP4A11, Cytochrome P450-4A11; CYP4F2, Cytochrome P450-4F2.
[b]Applied Biosystems Foster City, CA.

Table 20. Influence of cytochrome P450 hydroxylase inhibitor (HET0016) on oxylipid biosynthesis in endothelial cells under oxidative stress, n = 4. Data are expressed as mean ± SEM of the fold changes relative to control.

		- HET0016			**+ HET0016**		
Major Pathway	Oxylipid	Control	LPS	AAPH	Control	LPS	AAPH
CYP:							
Hydroxylases	20-HETE	1.00	1.57 ± 1.02	3.84 ± 2.39	1.00	0.69 ± 0.32	0.77 ± 0.33
Epoxygenases	8,9-EET	1.00	4.85 ± 2.58	5.92 ± 2.90	1.00	0.34 ± 0.18[a]	0.24 ± 0.13[a]
	14,15-EET	1.00	1.95 ± 0.77	1.66 ± 0.81	1.00[b]	0.42 ± 0.08[a]	0.51 ± 0.22[a,b]
	9,10-EpOME	1.00	1.63 ± 0.87	1.72 ± 0.83	1.00	5.12 ± 2.44	2.79 ± 1.00
	11,12-EpOME	1.00	4.57 ± 2.64	3.84 ± 2.18	1.00	4.44 ± 1.71	3.62 ± 1.14
	11,12-EET	1.00	7.94 ± 5.53	7.20 ± 6.19	1.00	0.88 ± 0.53	2.41 ± 2.20
	8,9-DHET	1.00	1.08 ± 0.34	0.78 ± 0.21	1.00	3.42 ± 1.89	3.16 ± 1.36
	11,12-DHET	1.00	1.19 ± 0.90	1.22 ± 0.47	1.00	19.75 ± 8.74	30.55 ± 12.75
	14,15-DHET	1.00	0.48 ± 0.08	0.72 ± 0.39	1.00	3.29 ± 1.05	4.75 ± 1.87
	11,12-DiHOME	1.00	1.15 ± 0.67	0.63 ± 0.33	1.00	3.41 ± 1.61	2.61 ± 1.10
LOX:							
5-LOX	5-HETE	1.00	1.38 ± 1.01	3.64 ± 1.55	1.00	0.37 ± 0.21	0.58 ± 0.29
15-LOX	15-HETE	1.00	2.53 ± 1.66	5.50 ± 1.15	1.00	0.27 ± 0.19	0.45 ± 0.32
	9-HODE	1.00	9.01 ± 8.42	19.35 ± 15.68	1.00	0.25 ± 0.17[a]	0.30 ± 0.19[a]
	13-HODE	1.00	3.36 ± 2.61	8.25 ± 4.75	1.00	0.29 ± 0.13[a]	0.38 ± 0.21[a]
	9-oxo-ODE	1.00	0.60 ± 0.34	9.85 ± 8.42	1.00	1.04 ± 0.39	1.19 ± 0.42
	13-oxo-ODE	1.00	0.55 ± 0.23	2.14 ± 0.89	1.00	1.98 ± 0.94	1.20 ± 0.24
Non-enzymatic	9-HETE	1.00	1.62 ± 0.90	2.79 ± 1.15	1.00	0.46 ± 0.23	0.94 ± 0.49
	11-HETE	1.00	2.14 ± 1.15	3.85 ± 1.32	1.00	0.38 ± 0.18	0.62 ± 0.32

CYP – cytochrome P450, LOX – lipoxygenase, LPS – lipopolysaccharide, AAPH - 2,2-azobis(2-amidinopropane) dihydrochloride, HET0016 – N-hydroxy-N'-(4-n-butyl-2-methylphenyl) formamidine, HETE – hydroxyeicosatetraenoic acid, EET – epoxyeicosatrienoic acid, EpOME - epoxyoctadecenoic acid, DHET – dihydroxyeicosatrienoic acid, DiHOME – dihydroxyoctadecenoic acid, HODE – hydroxyoctadecadienoic acid; oxo-ODE – oxooctadecadienoic acid

[a]Different letters denote fold changes that differ from each other in either HET0016 or non-HET0016 treated BAECs

Appendix C. Figures

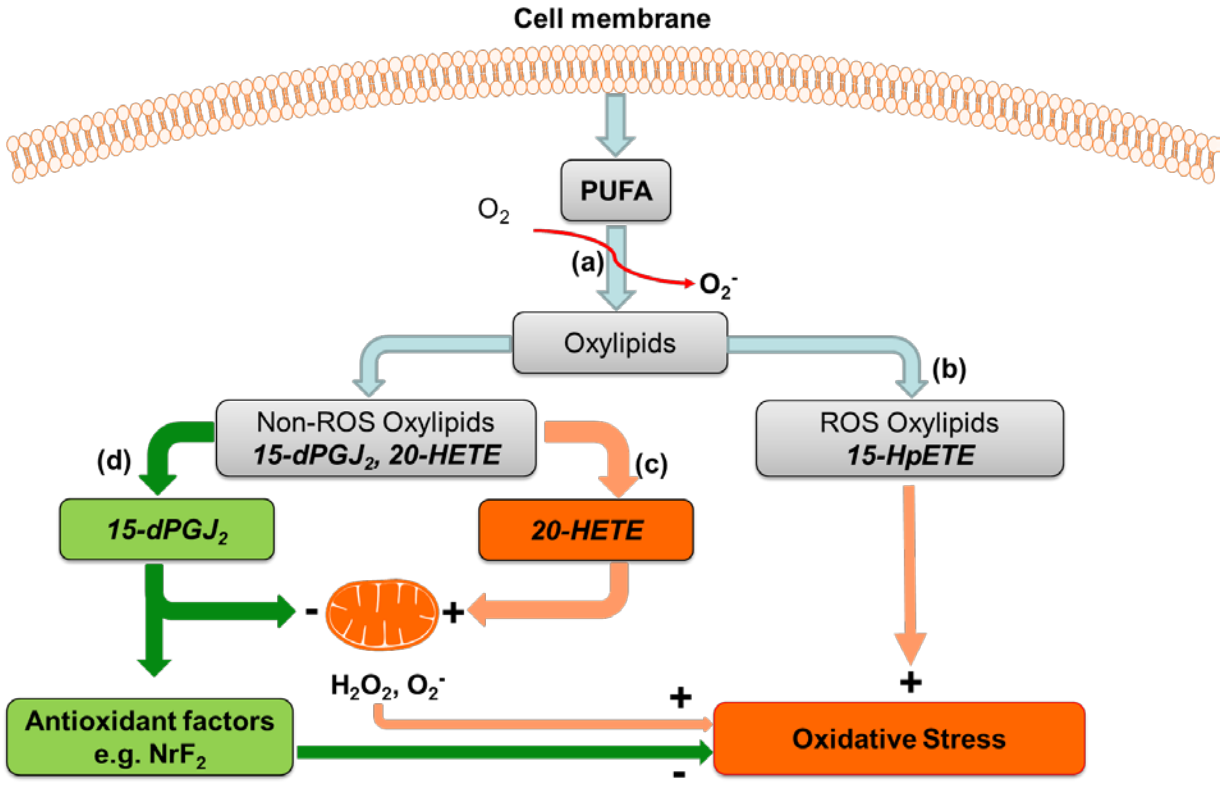

Figure 1. (a) Polyunsaturated fatty acids (PUFA) released from the cell membrane phospholipids are metabolized enzymatically to produce oxylipids with the production reactive oxygen species (ROS) such as superoxide (O_2^-) in the process. (b) Some of the primary oxylipids are potent ROS such as the arachidonic acid-derived 15-hydroperoxyeicosatetraenoic acid (15-HpETE) that can directly damage cellular macromolecules. Other oxylipid metabolites target sites of reactive metabolite production like the mitochondria to induce production (c) such as is the case of the cytochrome P450-derived 20-hydroxyeicosatetraenoic acid (20-HETE). (d) Other oxylipids such as the dehydration product of prostaglandin D2 (15-dPGJ$_2$) decrease reactive metabolite production by directly decreasing production or by stimulating antioxidant factors such as nuclear factor E2-related factor 2 (Nrf$_2$). + induce production; - decrease production; green arrows – antioxidant pathways; red arrows, pro-oxidant pathways.

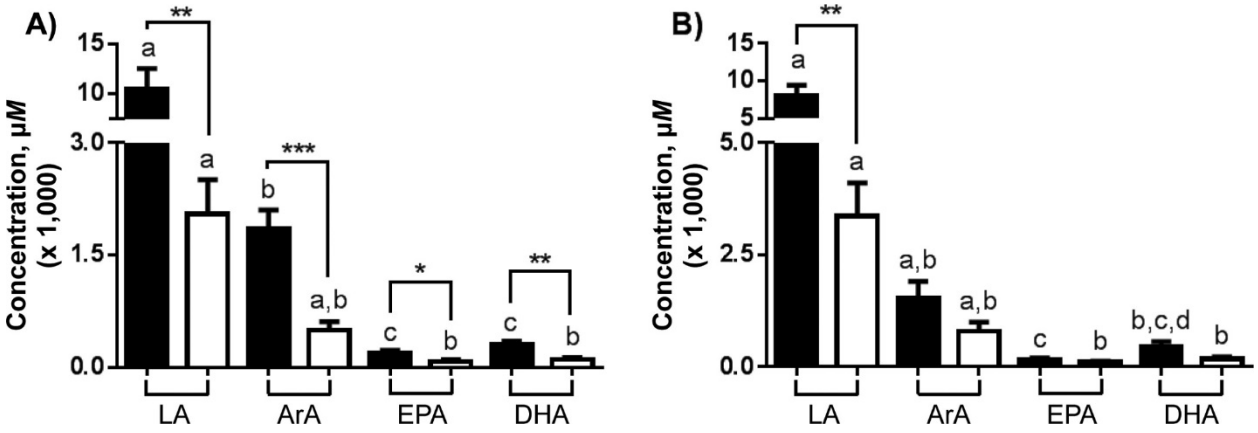

Figure 2. Concentrations (mean ± SEM, µ*M*) of PUFA differed for all PUFA in milk (A) but only for linoleic acid (LA) in plasma (B) between coliform mastitis (solid bars) and healthy control (open bars) cows. Linoleic acid was most abundant among PUFA but similar to arachidonic acid (ArA) in control milk and plasma and mastitis plasma) within an experimental group; EPA = eicosapentaenoic acid, DHA = docosahexaenoic acid. **P* < 0.05, ***P* < 0.01, ****P* < 0.001; bars with different letters (a–d) differ (*P* < 0.05) among PUFA within an experimental group (mastitis or control).

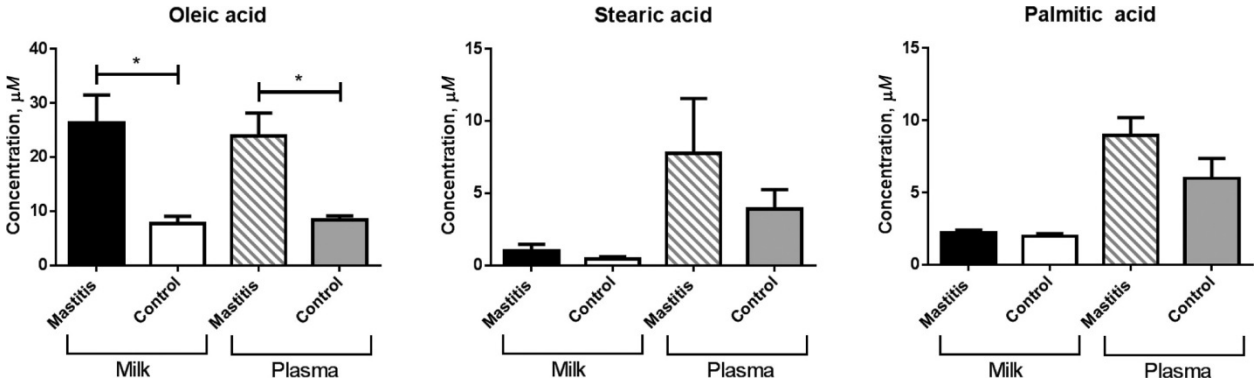

Figure 3. Milk and plasma concentrations (mean ± SEM; µ*M*) of oleic acid were greater in coliform mastitis (n = 11) than control (n = 13) cows but no differences were detected for stearic and palmitic acids. Solid and open black bars represent milk samples; diagonally striped and gray bars represent plasma samples. **P* < 0.05.

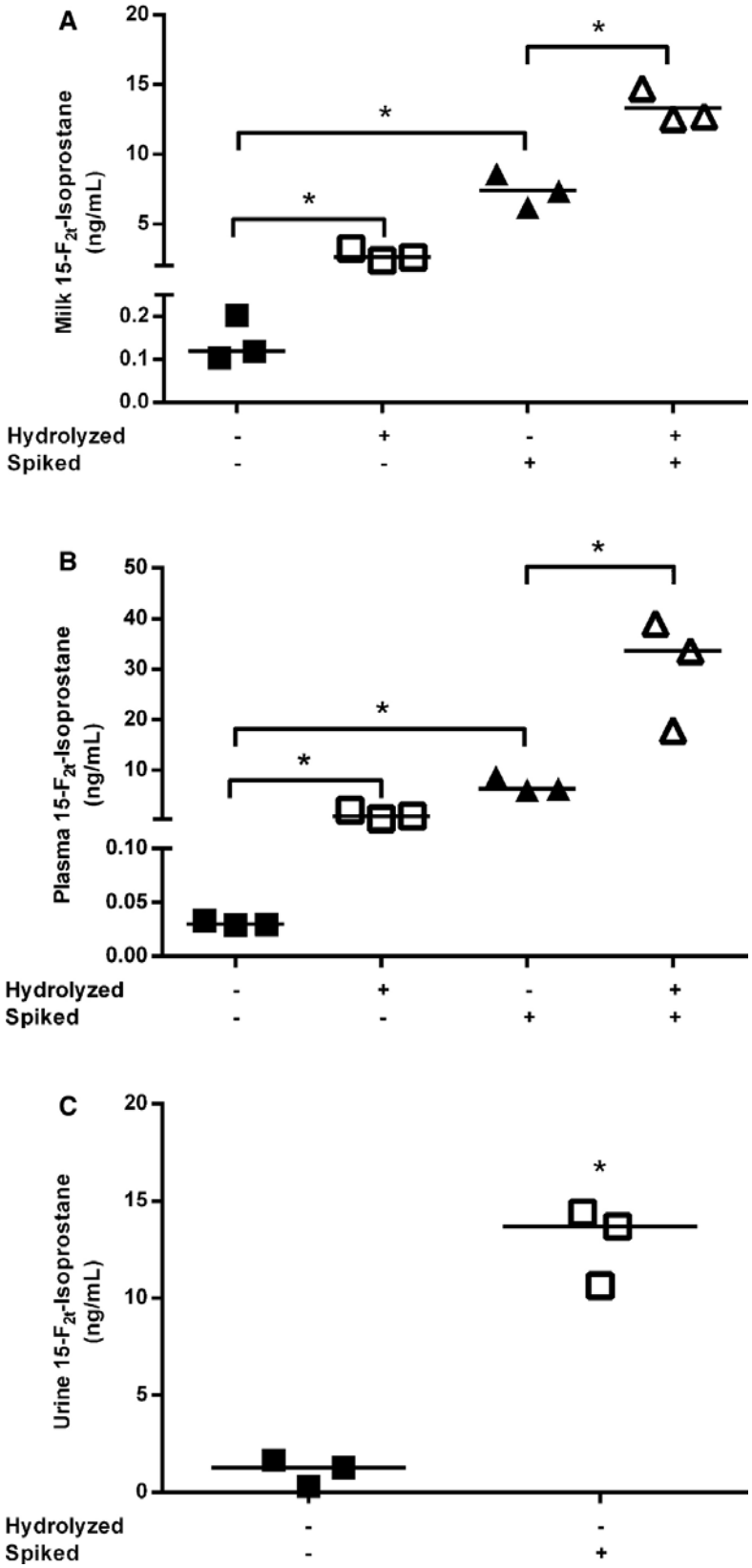
A
Milk 15-F2t-Isoprostane (ng/mL)
20
15
10
5
0.2
0.1
0.0
*
*
*
Hydrolyzed - + - +
Spiked - - + +
B
Plasma 15-F2t-Isoprostane (ng/mL)
50
40
30
20
10
0.10
0.05
0.00
*
*
*
Hydrolyzed - + - +
Spiked - - + +
C
Urine 15-F2t-Isoprostane (ng/mL)
20
15
10
5
0
*
Hydrolyzed - -
Spiked - +

Figure 4.

Figure 4. (cont'd)
Concentrations (+Median) of 15-F_{2t}-isoprostane in pooled samples from healthy cows (n = 3) quantified by cbELISA (Cell Biolabs, San Diego, CA). Milk (A), plasma (B) and urine (C) samples from cows (n = 3) less than 30 days in milk were pooled by sample type and divided into 3 replicates. Replicates were either treated by alkaline hydrolysis (10 N sodium hydroxide) or not, and spiked with 10 ng/mL 15-F_{2t}-isoprostane (standard) or not as indicated below each graph. The limit of detection (LOD) was 10 pg/μL of sample and limits for accuracy were recovery of standard 15-F_{2t}-Isop was ±20%. Data linked by a horizontal line indicate comparisons of interest and the asterisks label indicates significant difference (Wilcoxon rank sum, $\alpha = 0.05$).

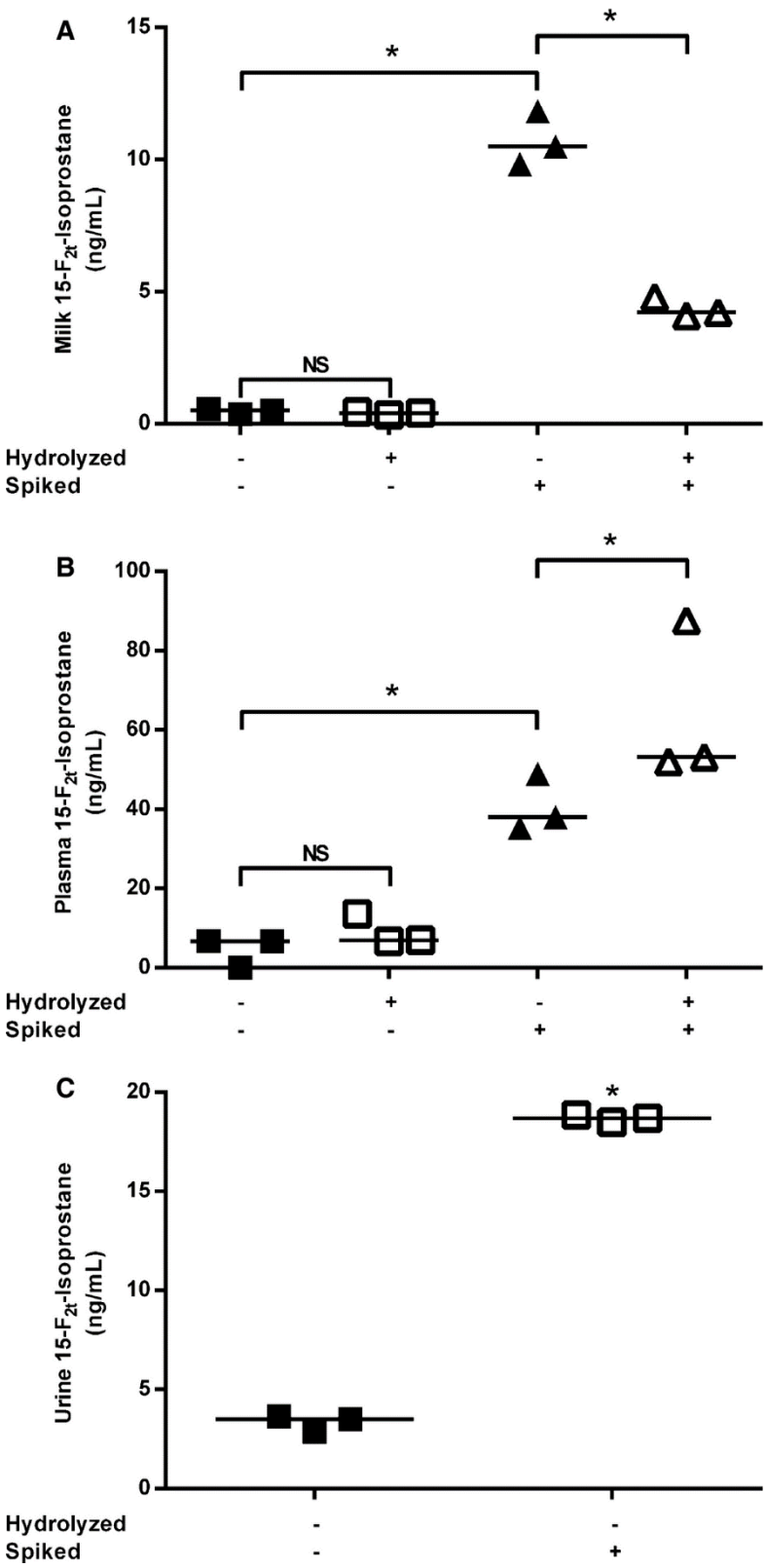
A
Milk 15-F2t-Isoprostane (ng/mL)
15
10
5
0
*
*
NS
Hydrolyzed - + - +
Spiked - - + +
B
Plasma 15-F2t-Isoprostane (ng/mL)
100
80
60
40
20
0
*
*
NS
Hydrolyzed - + - +
Spiked - - + +
C
Urine 15-F2t-Isoprostane (ng/mL)
20
15
10
5
0
*
Hydrolyzed - -
Spiked - +

Figure 5.

Figure 5. (cont'd)
Concentrations (+Median) of 15-F_{2t}-isoprostane in pooled samples from healthy cows (n = 3) quantified by ccELISA (Cayman Chemicals, Ann Arbor, MI). Milk (A), plasma (B) and urine (C) samples from cows (n = 3) less than 30 days in milk were pooled by sample type and divided into 3 replicates. Replicates were either treated by alkaline hydrolysis (10 N Sodium hydroxide) or not, and/or spiked with 10 ng/mL 15-F_{2t}-isoprostane (standard). The limit of detection (LOD) was 2.7 pg/μL of sample and limits for accuracy were recovery of standard 15-F_{2t}-Isop was ±20%. Data linked by a horizontal line indicate comparisons of interest and the asterisks label indicates significant difference (Wilcoxon rank sum, $\alpha = 0.05$); NS, not significant

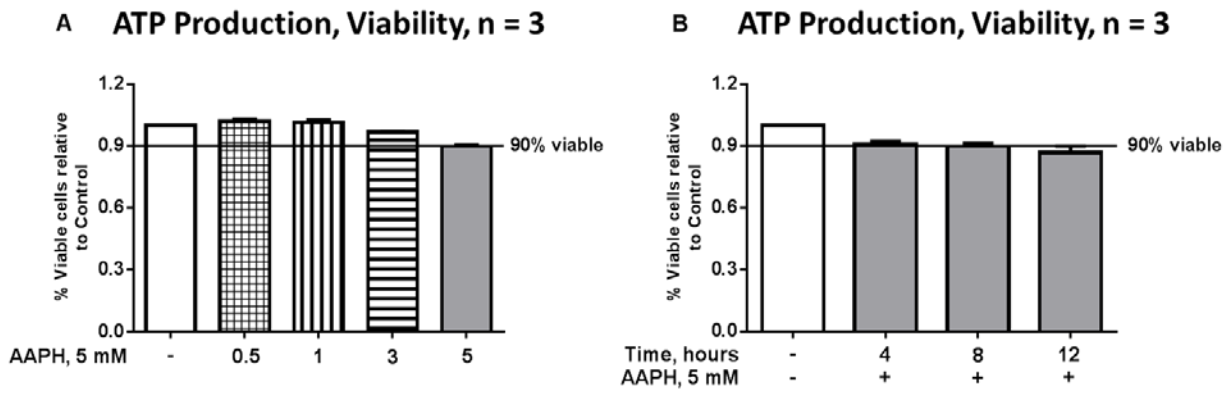

Figure 6. Effect of AAPH on cell viability in BAEC. Data are expressed as % viable cells relative to untreated controls (open bars). Cell viability of ≥ 90% (black line) was considered adequate for evaluating cellular responses. Data are an average of at least 3 independent experiments.

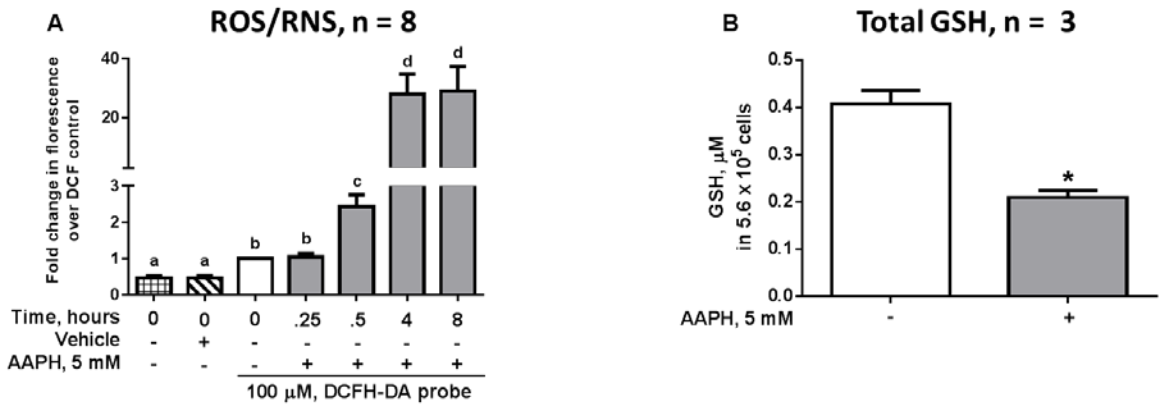

Figure 7. Reactive metabolite (ROS/RNS) production (A) and changes in total glutathione (B) in BAEC treated with AAPH (gray bars). Fluorescence (ROS/RNS) are expressed as fold changes over untreated controls (open bars). Different letters on graphs denote significant differences among treatments based on a one-way ANOVA and Tukey adjustment for multiple comparisons ($\alpha = 0.05$). Total glutathione concentrations are mean (±SEM) µM concentrations in 5.6 x 10^5 cells/sample. The asterisk (*) indicates significant difference ($P < 0.05$) between untreated control and AAPH treated BAECs compared by an unpaired t-test.

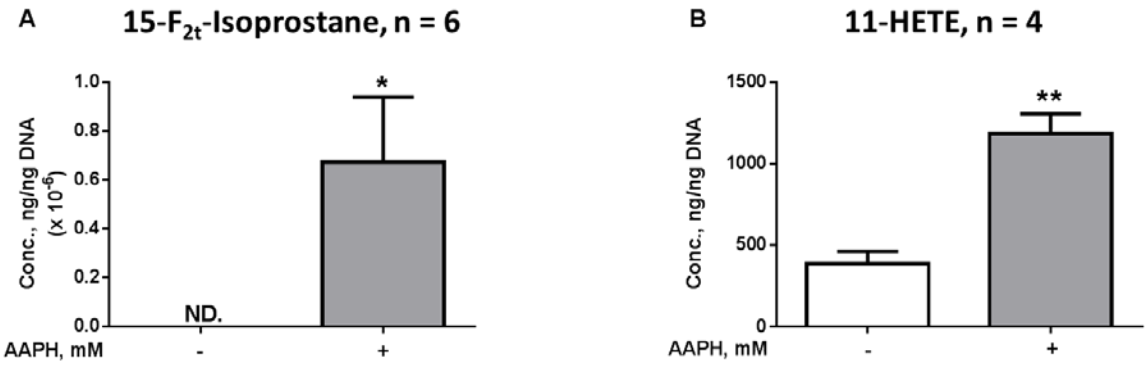

Figure 8. Lipid oxygenation in BAEC under oxidative stress. 15-F_{2t}-isoprostane (A) and 11-HETE (B) were quantified in cells by LC-MS/MS. *P < 0.05, **P < 0.01, - significant difference between untreated control (open bars) and AAPH-treated (gray bars) BAECs compared by unpaired t-tests. In untreated controls, 15-F_{2t}-isoprostane was not detected (ND.).

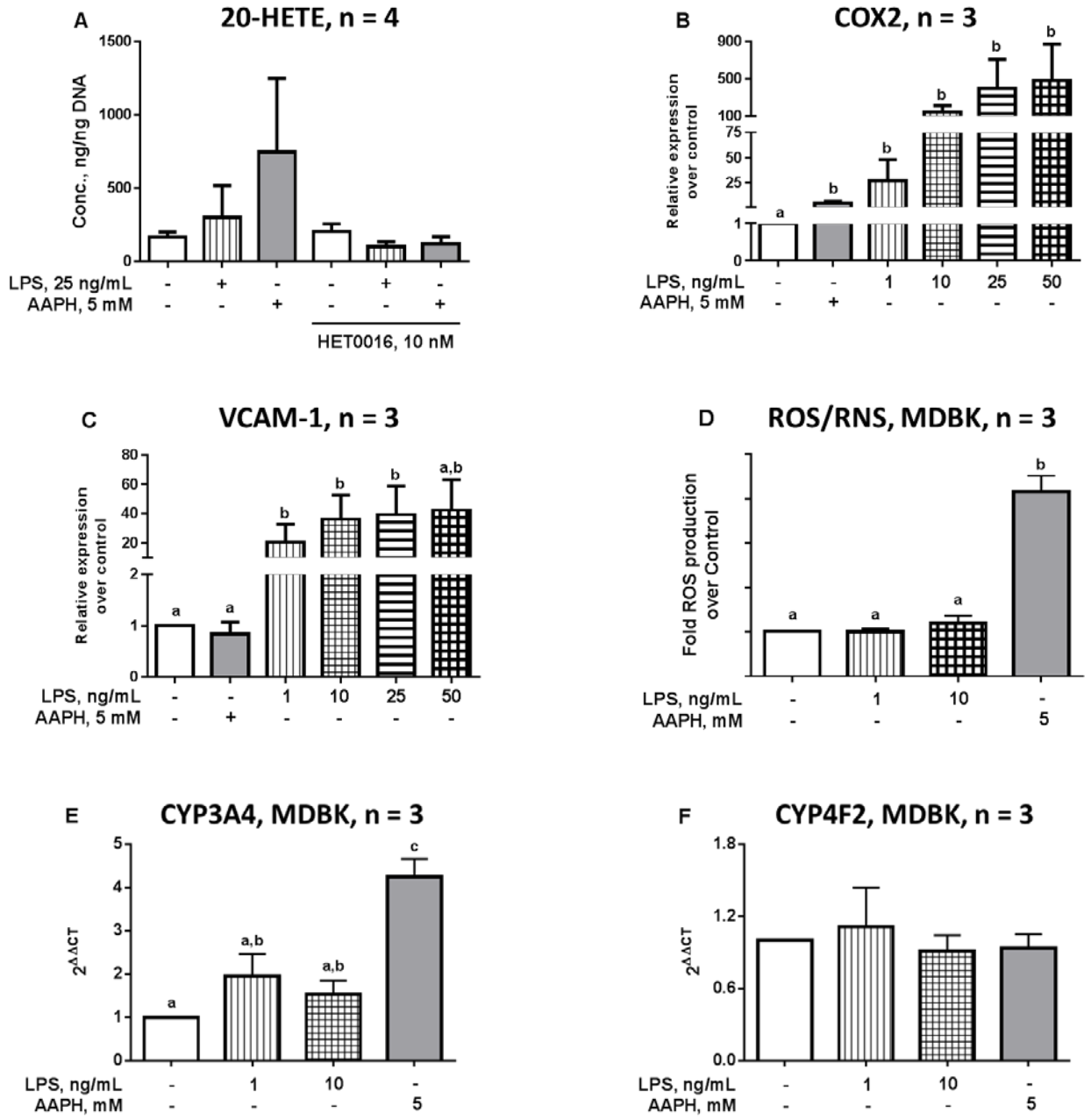

Figure 9. Production of 20-HETE, inflammatory gene expression, and cytochrome P450 (CYP) gene expression during oxidative stress. 20-HETE was quantified by LC-MS/MS in cells treated with AAPH or LPS in the presence or absence of the CYP hydroxylase inhibitor (HET0016). Cells were pre-incubated for 1-hour with HET0016 before treatments were added (A). Gene expression was quantified by qRT-PCR for COX2 (B) and VCAM-1 (C) in BAEC treated with AAPH or LPS for 8 hours. CYP gene expression, CYP3A4 (E) and CYP4F2 (F), was determined in a bovine kidney cell line (MDBK) using the same treatments for AAPH and lower doses (1- and 10 ng/mL) of LPS for a 24-hour duration. Production of reactive metabolites

Figure 9. (cont'd)
was also determined in MDBK cells (D). All data are presented as fold change relative to untreated controls (open bars). Different letters on graphs denote significant differences among treatments based on a one-way ANOVA and Tukey adjustment for multiple comparisons ($\alpha = 0.05$).

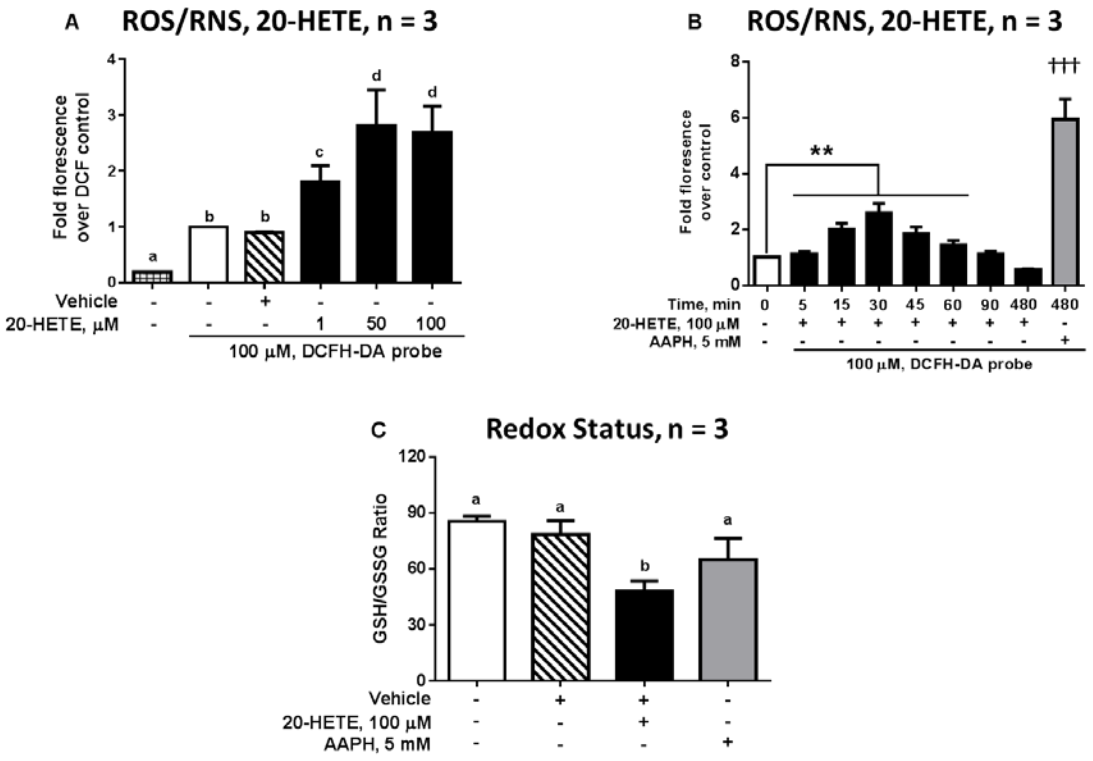

Figure 10. Effects of 20-HETE on reactive metabolite production and reduced (GSH) and oxidized (GSSG) glutathione. Production of reactive metabolites was quantified in BAEC to determine the effect of dose (A) and time (B) when treated with 20-HETE. The ratio of GSH/GSSG was determined as a proxy for redox status (C) after treatment with 20-HETE for 90 minutes. Reactive metabolites data are presented as fold change relative to untreated control (open bars) and AAPH (gray bars) was used as a positive control. Different letters on graphs denote significant differences among treatments based on a one-way ANOVA and Tukey adjustment for multiple comparisons ($\alpha = 0.05$). **$P < 0.01$ for 20-HETE treatments relative to untreated control at the beginning of experiment (time = 0). $^{\dagger\dagger\dagger}P < 0.001$ for positive control (AAPH) compared to 20-HETE treatments at the beginning (t = 0) and peak ROS/RNS production (t = 30 minutes).

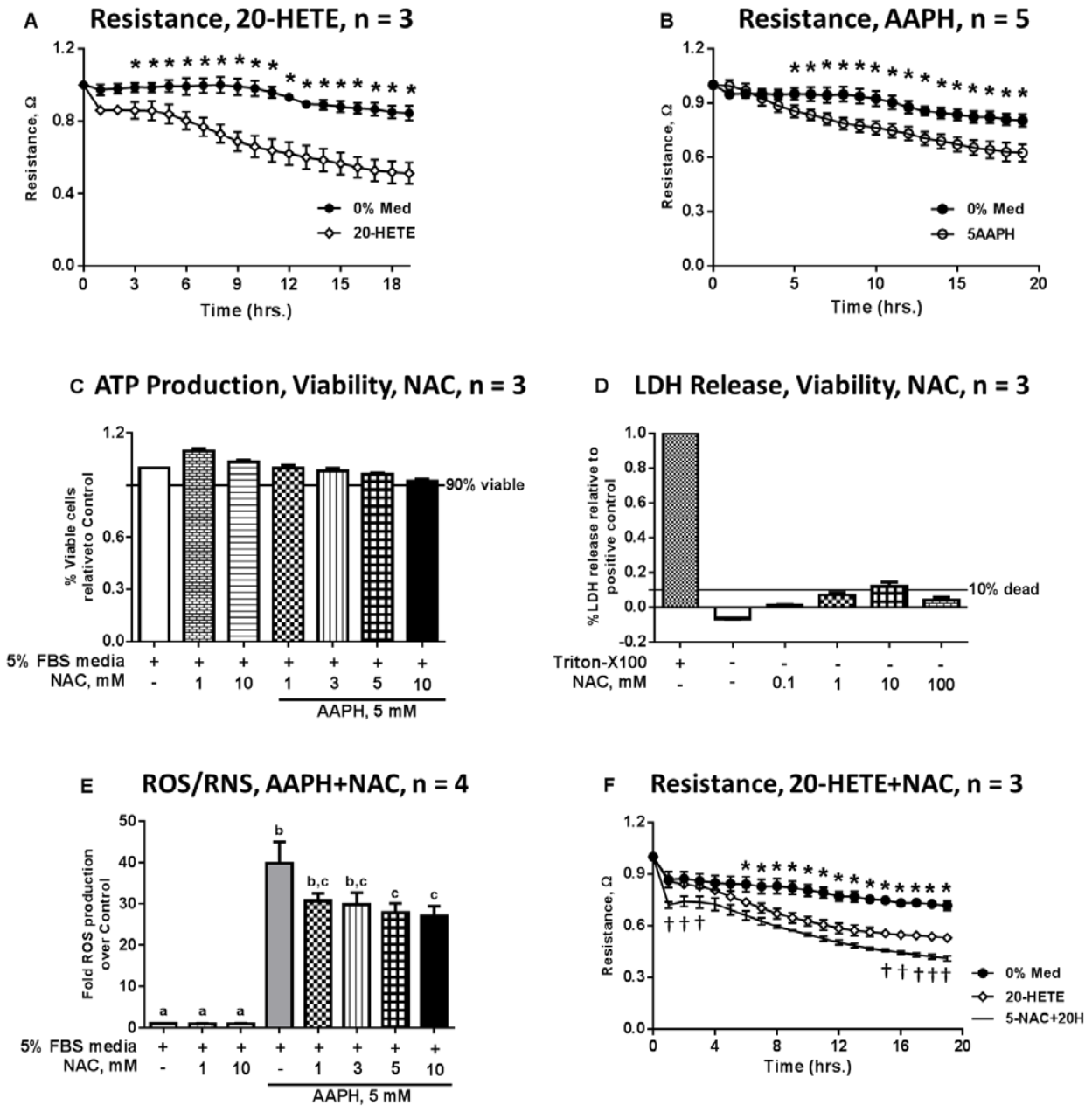

Figure 11. Effect of N-acetylcysteine (NAC) on barrier integrity of BAEC exposed to 20-HETE. Mean (± SEM) normalized endothelial resistance after 20-HETE (A) and AAPH (B) treatments. Effect of NAC alone on cell viability was determined based on ATP production (C) and lactate dehydrogenase (LDH) enzyme release (D). The dose of 5 mM NAC was selected based on significantly decreasing AAPH-induced ROS/RNS production (E). NAC failed to rescue 20-HETE-induced decrease in endothelial resistance (F). Different letters on graphs denote significant differences among treatments based on a one-way ANOVA and Tukey adjustment for multiple comparisons ($\alpha = 0.05$). Endothelial resistance was analyzed by 2-way ANOVA with repeated measures and Tukey adjustment for multiple comparisons ($\alpha = 0.05$). *P < 0.05 for comparisons

Figure 11. (cont'd)
between treatment with 20-HETE (open diamonds) or AAPH (open circles) and untreated control (0% serum media, bold black circles) within a time period. †$P < 0.05$ for comparisons between 20-HETE alone and 20-HETE+5 mM NAC based on a 2-way ANOVA with repeated measures and Tukey adjustment for multiple comparisons (F).

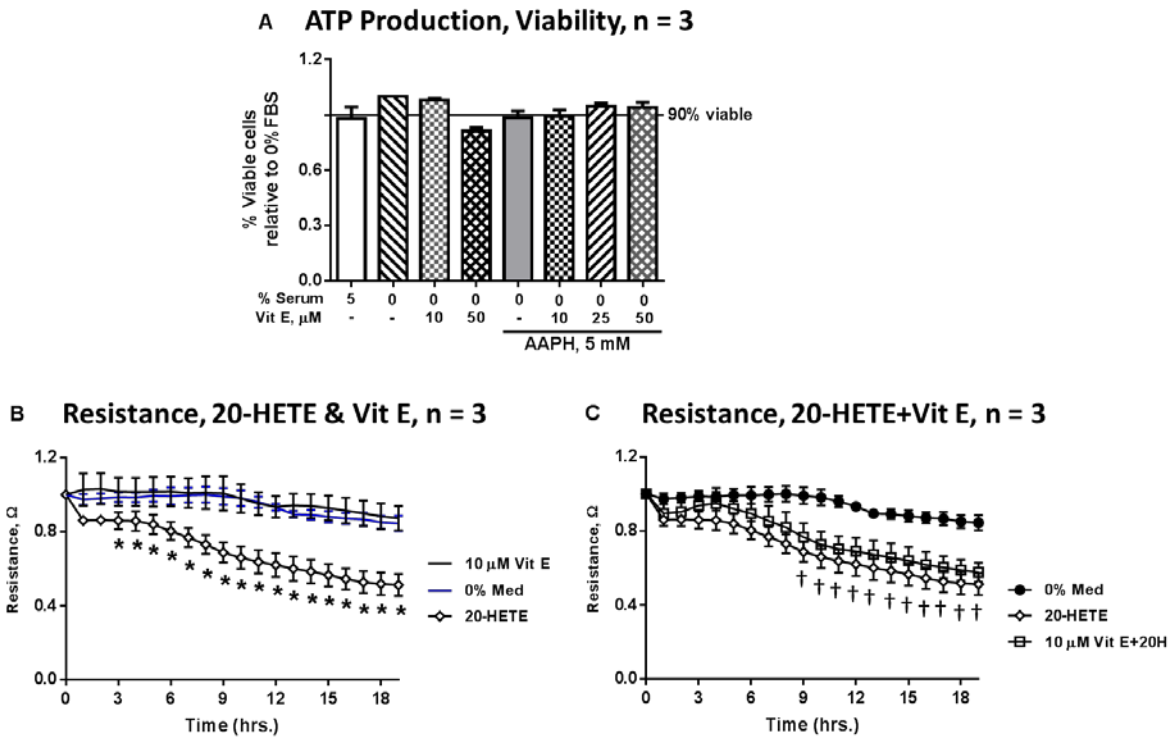

Figure 12. Effect of vitamin E on barrier integrity of BAEC exposed to 20-HETE. Vitamin E at 10 µM was selected on the basis of maintaining at least 90% cell viability based on ATP production (A). The effect of vitamin E alone (black line) on endothelial resistance compared to untreated media control (blue line) is displayed in (B). Co-exposure of BAEC to 20-HETE and vitamin E (open squares) delayed the decrease in endothelial resistance (C). Endothelial resistance data were analyzed by 2-way ANOVA with repeated measures and Tukey adjustment for multiple comparisons (F). *$P < 0.05$ for 20-HETE alone compared to untreated (0% serum media) control. †$P < 0.05$ for 20-HETE+vitamin E compared to untreated 0% media control.

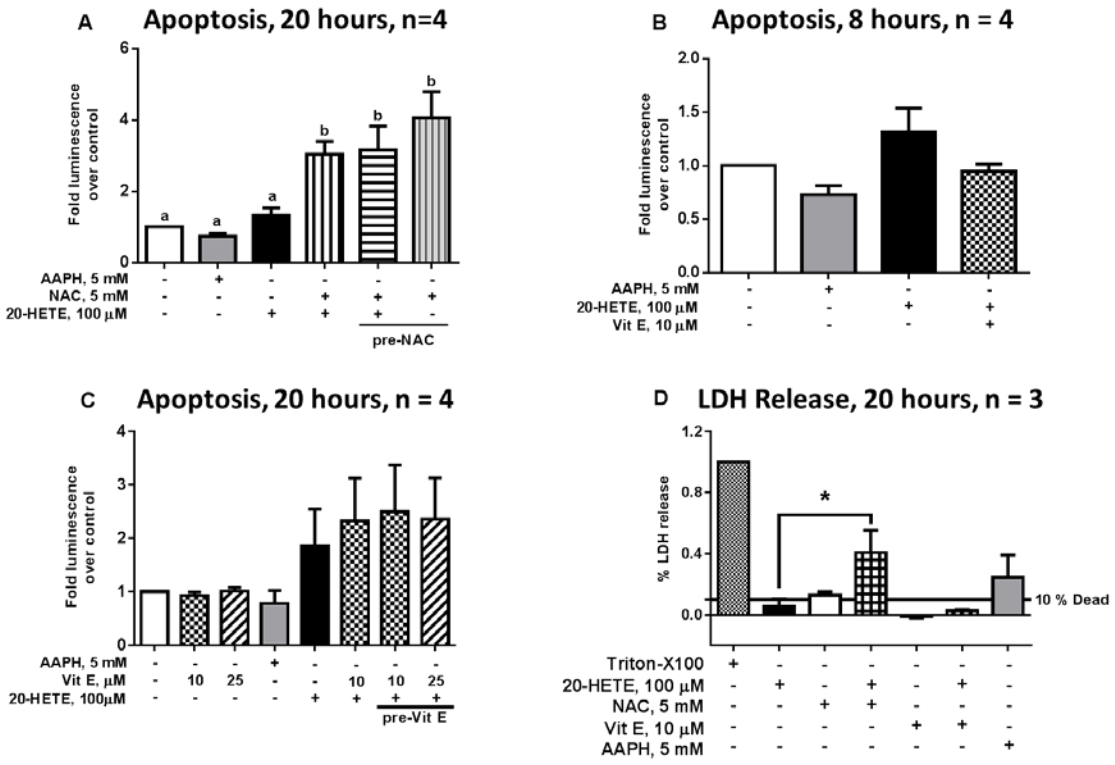

Figure 13. Apoptosis of BAEC exposed to 20-HETE with or without antioxidants, N-acetyl cysteine (NAC) and DL-α-tocopherol (Vitamin E). Relative to untreated controls, exposure of BAEC to AAPH or 20-HETE alone did not change the activity of caspase 3/7 enzymes (A – C). Apoptosis of BAEC occurred on exposure to co-exposure to NAC and 20-HETE or when exposed to NAEC alone (A). Exposure to vitamin E alone or together with 20-HETE did not induce significant apoptosis for 8- (B) or 20- hour (C) incubations. Cell death induced by BAEC exposure to NAC and 20-HETE together (D), also occurred by necrosis as shown by significantly greater LDH release than cells exposed to 20-HETE alone. All data are from at least 3 independent experiments and were analyzed by one-way ANOVA with Tukey adjustment for multiple comparisons. *$P < 0.05$, $\alpha = 0.05$. pre-Vit E and pre-NAC represent pre-incubation of BAEC with antioxidant for 12 hours before treatments were added.

Appendix D. Supplemental figures

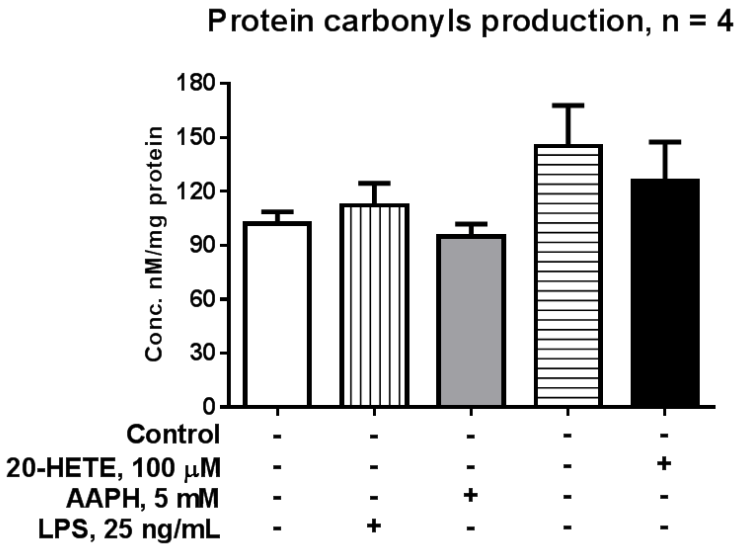

Figure 14. Protein oxidation in BAEC under oxidative stress. Protein carbonyls were quantified in cells using an OxiSelect ELISA assay. No significant differences were detected among treatments and their controls; untreated control for AAPH and LPS (open bar) and untreated control for 20-HETE (horizontal gray lines). Data for protein carbonyls induced by LPS (vertical gray lines) and AAPH (gray bar) were analyzed by one-way ANOVA with Tukey adjustment for multiple comparisons. Data for protein carbonyls induced by 20-HETE (black bar) were analyzed by unpaired t – test. Significance was set at $\alpha \leq 0.05$.

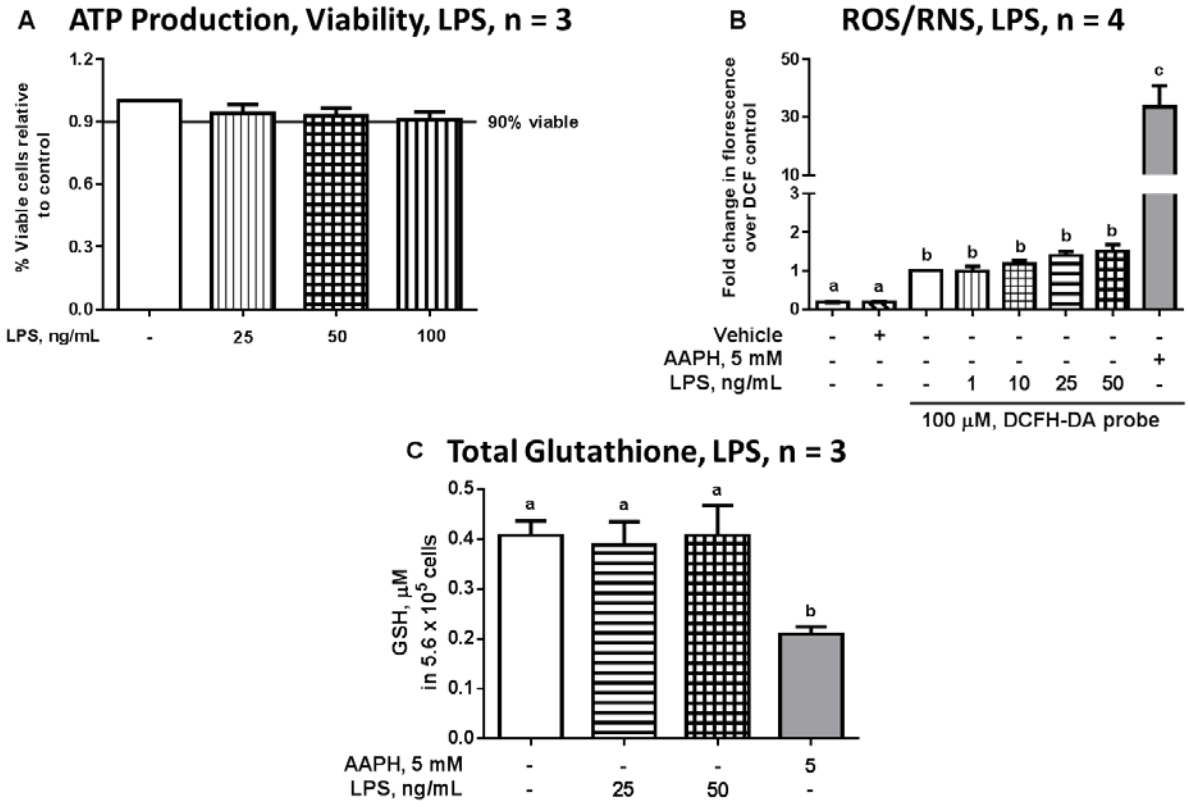

Figure 15. Effect of LPS on cell viability in BAEC. Cell viability data (A) are expressed as % viable cells relative to untreated controls (open bars). Reactive metabolite (ROS/RNS) production (B) and changes in total glutathione (C) in BAEC treated with LPS relative to untreated controls (open bars). AAPH (gray bars) was used as a positive control. Different letters on graphs denote significant differences among treatments based on a one-way ANOVA and Tukey adjustment for multiple comparisons ($\alpha = 0.05$).

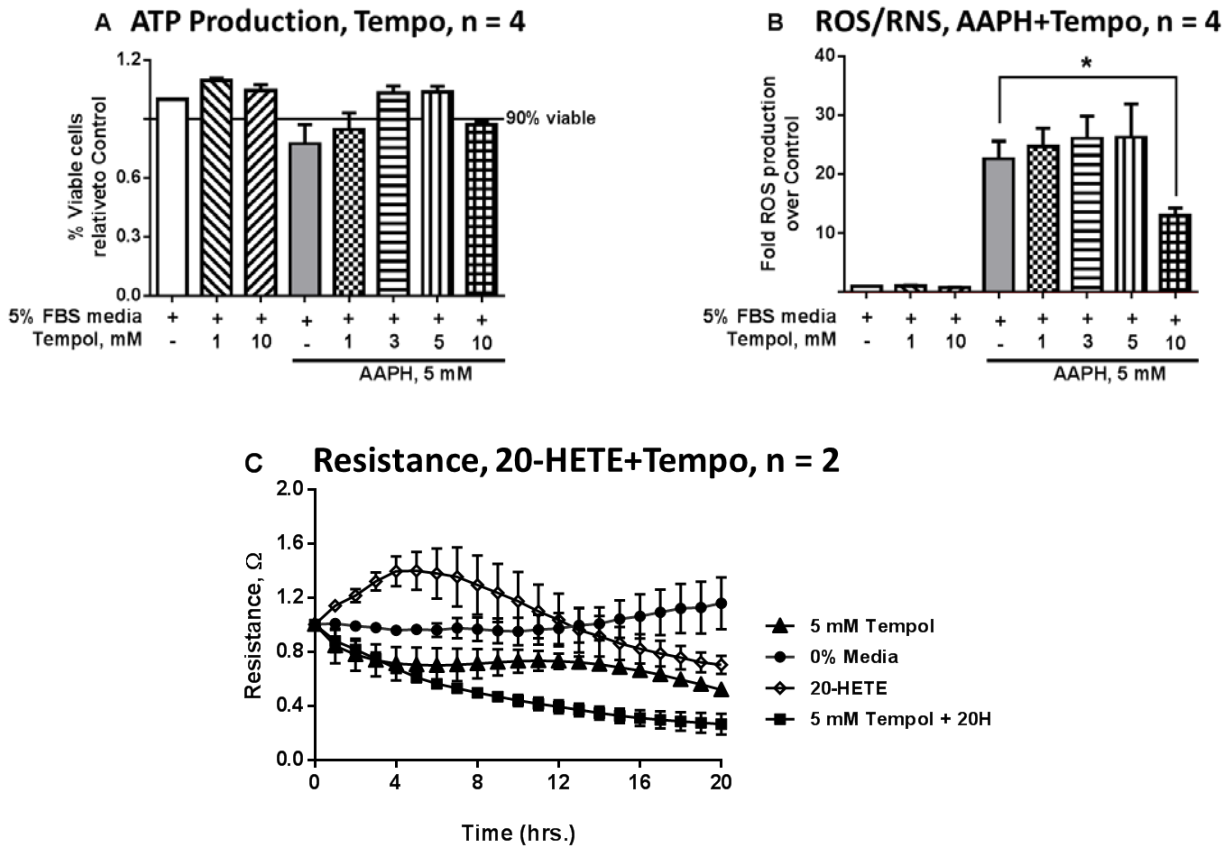

Figure 16. Effect of Tempo on endothelial barrier integrity of BAEC exposed to 20-HETE. Tempo at 5 mM was selected on the basis of viability (A). The effect of Tempo alone and on AAPH induced reactive metabolite production is displayed in (B). The effect of Tempo alone (black triangles), 20-HETE alone (open diamonds), 20-HETE+Tempo (black squares) and untreated controls (black circles) on endothelial resistance are displayed in (C). Reactive metabolite production data were analyzed by a one-way ANOVA with Tukey adjustment for multiple comparisons, $\alpha = 0.05$. No statistical comparisons were performed for endothelial barrier resistance data because of an n = 2.

REFERENCES

REFERENCES

Aitken, S. L., C. M. Corl, and L. M. Sordillo. 2011a. Immunopathology of mastitis: insights into disease recognition and resolution. J Mammary Gland Biol Neoplasia 16(4):291-304.

Aitken, S. L., C. M. Corl, and L. M. Sordillo. 2011b. Pro-inflammatory and pro-apoptotic responses of TNF-α stimulated bovine mammary endothelial cells. Vet Immunol Immunopathol 140(3):282-290.

Aitken, S. L., E. L. Karcher, P. Rezamand, J. C. Gandy, M. J. VandeHaar, A. V. Capuco, and L. M. Sordillo. 2009. Evaluation of antioxidant and proinflammatory gene expression in bovine mammary tissue during the periparturient period. J Dairy Sci 92(2):589-598.

Al-Gubory, K. H., P. A. Fowler, and C. Garrel. 2010. The roles of cellular reactive oxygen species, oxidative stress and antioxidants in pregnancy outcomes. Int J Biochem Cell Biol 42(10):1634-1650.

Aliche-Djoudi, F., N. Podechard, A. Collin, M. Chevanne, E. Provost, M. Poul, L. Le Hegarat, D. Catheline, P. Legrand, M. T. Dimanche-Boitrel, D. Lagadic-Gossmann, and O. Sergent. 2013. A role for lipid rafts in the protection afforded by docosahexaenoic acid against ethanol toxicity in primary rat hepatocytes. Food Chem Toxicol 60:286-296.

Altmann, R., M. Hausmann, T. Spottl, M. Gruber, A. W. Bull, K. Menzel, D. Vogl, H. Herfarth, J. Scholmerich, W. Falk, and G. Rogler. 2007. 13-Oxo-ODE is an endogenous ligand for PPARgamma in human colonic epithelial cells. Biochem Pharmacol 74(4):612-622.

Anderson, D. E. and W. W. Muir. 2005. Pain management in ruminants. Vet Clin North Am Food Anim Pract 21(1):19-31.

Anderson, K. L., H. Kindahl, A. R. Smith, L. E. Davis, and B. K. Gustafsson. 1986. Endotoxin-induced bovine mastitis: arachidonic acid metabolites in milk and plasma and effect of flunixin meglumine. Am J Vet Res 47(6):1373-1377.

Anwar-mohamed, A., B. N. Zordoky, M. E. Aboutabl, and A. O. El-Kadi. 2010. Alteration of cardiac cytochrome P450-mediated arachidonic acid metabolism in response to lipopolysaccharide-induced acute systemic inflammation. Pharmacol Res 61(5):410-418.

Arnold, C., A. Konkel, R. Fischer, and W. H. Schunck. 2010a. Cytochrome P450-dependent metabolism of omega-6 and omega-3 long-chain polyunsaturated fatty acids. Pharmacol Rep 62(3):536-547.

Arnold, C., M. Markovic, K. Blossey, G. Wallukat, R. Fischer, R. Dechend, A. Konkel, C. von Schacky, F. C. Luft, D. N. Muller, M. Rothe, and W. H. Schunck. 2010b. Arachidonic acid-metabolizing cytochrome P450 enzymes are targets of {omega}-3 fatty acids. J Biol Chem 285(43):32720-32733.

Askari, A. A., S. Thomson, M. L. Edin, F. B. Lih, D. C. Zeldin, and D. Bishop-Bailey. 2014. Basal and inducible anti-inflammatory epoxygenase activity in endothelial cells. Biochem Biophys Res Commun 446(2):633-637.

Atroshi, F., A. Rizzo, R. Kangasniemi, S. Sankari, T. Tyopponen, T. Osterman, and J. Parantainen. 1989a. Role of plasma fatty acids, prostaglandins and antioxidant balance in bovine mastitis. Zentralbl Veterinarmed 36(9):702-711.

Atroshi, F., A. Rizzo, T. Osterman, and J. Parantainen. 1989b. Free fatty acids and lipid peroxidation in normal and mastitic bovine milk. Zentralbl Veterinarmed 36(5):321-330.

Avila, J. G., I. Echeverri, C. A. de Plata, and A. Castillo. 2015. Impact of oxidative stress during pregnancy on fetal epigenetic patterns and early origin of vascular diseases. Nutr Rev 73(1):12-21.

Balvers, M. G., K. C. Verhoeckx, J. Meijerink, S. Bijlsma, C. M. Rubingh, H. M. Wortelboer, and R. F. Witkamp. 2012. Time-dependent effect of in vivo inflammation on eicosanoid and endocannabinoid levels in plasma, liver, ileum and adipose tissue in C57BL/6 mice fed a fish-oil diet. Int Immunopharmacol 13(2):204-214.

Bao, Y., X. Wang, W. Li, D. Huo, X. Shen, Y. Han, J. Tan, Q. Zeng, and C. Sun. 2011a,b. 20-hete induces apoptosis in neonatal rat cardiomyocytes through mitochondrial-dependent pathways. J Cardiovasc Pharmacol 57(3):294-301.

Basu, S. 1998. Radioimmunoassay of 8-iso-prostaglandin F2alpha: an index for oxidative injury via free radical catalyzed lipid peroxidation. Prostaglandins Leukot Essent Fatty Acids 58(4):319-325.

Bauer, J., A. Ripperger, S. Frantz, S. Ergün, E. Schwedhelm, and R. A. Benndorf. 2014. Pathophysiology of isoprostanes in the cardiovascular system: implications of isoprostane-mediated thromboxane A2 receptor activation. Br J Pharmacol 171(13):3115-3131.

Bernabucci, U., B. Ronchi, N. Lacetera, and A. Nardone. 2005. Influence of body condition score on relationships between metabolic status and oxidative stress in periparturient dairy cows. J Dairy Sci 88(6):2017-2026.

Bhattacharyya, A., R. Chattopadhyay, S. Mitra, and S. E. Crowe. 2014. Oxidative stress: an essential factor in the pathogenesis of gastrointestinal mucosal diseases. Physiol Rev 94(2):329-354.

Biswas, S. K. 2016. Does the interdependence between oxidative stress and inflammation explain the antioxidant paradox? Oxid Med Cell Longev 2016:5698931.

Bondy, S. C. and S. Naderi. 1994. Contribution of hepatic cytochrome P450 systems to the generation of reactive oxygen species. Biochem Pharmacol 48(1):155-159.

Boulis, T. S., B. Rochelson, O. Novick, X. Xue, P. K. Chatterjee, M. Gupta, M. H. Solanki, M. Akerman, and C. N. Metz. 2014. Omega-3 polyunsaturated fatty acids enhance cytokine production and oxidative stress in a mouse model of preterm labor. J Perinat Med 42(6):693-698.

Brooks, J. D., E. S. Musiek, T. R. Koestner, J. N. Stankowski, J. R. Howard, E. M. Brunoldi, A. Porta, G. Zanoni, G. Vidari, J. D. Morrow, G. L. Milne, and B. McLaughlin. 2011. The fatty acid oxidation product 15-A3t-isoprostane is a potent inhibitor of NFkappaB transcription and macrophage transformation. J Neurochem 119(3):604-616.

Bruins, M. J., A. D. Dane, K. Strassburg, R. J. Vreeken, J. W. Newman, N. Salem, Jr., C. Tyburczy, and J. T. Brenna. 2013. Plasma oxylipin profiling identifies polyunsaturated vicinal diols as responsive to arachidonic acid and docosahexaenoic acid intake in growing piglets. J Lipid Res 54(6):1598-1607.

Buczynski, M. W., D. S. Dumlao, and E. A. Dennis. 2009. Thematic review series: proteomics. An integrated omics analysis of eicosanoid biology. J Lipid Res 50(6):1015-1038.

Bulger, E. M. and R. V. Maier. 2000. Lipid mediators in the pathophysiology of critical illness. Crit Care Med 28(4 Suppl):N27-36.

Burvenich, C., E. Monfardini, J. Mehrzad, A. V. Capuco, and M. J. Paape. 2004. Role of neutrophil polymorphonuclear leukocytes during bovine coliform mastitis: physiology or pathology? Verh K Acad Geneeskd Belg 66(2):97-150; discussion 150-153.

Burvenich, C., V. V. Merris, J. Mehrzad, A. Diez-Fraile, and L. Duchateau. 2003. Severity of E. coli mastitis is mainly determined by cow factors. Vet Res 34(5):521-564.

Cabreiro, F., D. Ackerman, R. Doonan, C. Araiz, P. Back, D. Papp, B. P. Braeckman, and D. Gems. 2011. Increased life span from overexpression of superoxide dismutase in Caenorhabditis elegans is not caused by decreased oxidative damage. Free Radic Biol Med 51(8):1575-1582.

Cachia, O., J. E. Benna, E. Pedruzzi, B. Descomps, M. A. Gougerot-Pocidalo, and C. L. Leger. 1998. alpha-tocopherol inhibits the respiratory burst in human monocytes. Attenuation of p47 (phox) membrane translocation and phosphorylation. J Biol Chem 273(49):32801-32805.

Calder, P. C. 2008. The relationship between the fatty acid composition of immune cells and their function. Prostaglandins Leukot Essent Fatty Acids 79(3):101-108.

Cao, Y.-Z., C. C. Reddy, and L. M. Sordillo. 2000a. Altered eicosanoid biosynthesis in selenium-deficient endothelial cells. Free Radic Biol Med 28(3):381-389.

Carpenter, C. T., P. V. Price, and B. W. Christman. 1998. Exhaled breath condensate isoprostanes are elevated in patients with acute lung injury or ARDS. Chest 114(6):1653-1659.

Celi, P. 2011. Biomarkers of oxidative stress in ruminant medicine. Immunopharmacol Immunotoxicol 33(2):233-240.

Chan, E. D. and D. W. H. Riches. 2001. IFN-γ + LPS induction of iNOS is modulated by ERK, JNK/SAPK, and p38 MAPK in a mouse macrophage cell line. Am J Physiol Cell Physiol 280(3):C441-C450.

Chen, J.-K., J. Capdevila, and R. C. Harris. 2001. Cytochrome p450 epoxygenase metabolism of arachidonic acid inhibits apoptosis. Mol Cell Biol 21(18):6322-6331.

Chen, Q., M. Galleano, and A. I. Cederbaum. 1997. Cytotoxicity and apoptosis produced by arachidonic acid in Hep G2 cells overexpressing human cytochrome P4502E1. J Biol Chem 272(23):14532-14541.

Chen, X., B. T. Andresen, M. Hill, J. Zhang, F. Booth, and C. Zhang. 2008. Role of reactive oxygen species in tumor necrosis factor-alpha induced endothelial dysfunction. Curr Hypertens Rev 4(4):245-255.

Cheng, J., C. C. Wu, K. H. Gotlinger, F. Zhang, J. R. Falck, D. Narsimhaswamy, and M. L. Schwartzman. 2010. 20-hydroxy-5,8,11,14-eicosatetraenoic acid mediates endothelial dysfunction via IkappaB kinase-dependent endothelial nitric-oxide synthase uncoupling. J Pharmacol Exp Ther 332(1):57-65.

Cheng, J., J. S. Ou, H. Singh, J. R. Falck, D. Narsimhaswamy, K. A. Pritchard, Jr., and M. L. Schwartzman. 2008. 20-hydroxyeicosatetraenoic acid causes endothelial dysfunction via eNOS uncoupling. Am J Physiol Heart Circ Physiol 294(2):H1018-1026.

Cheng, Z. and Y. Li. 2007. What is responsible for the initiating chemistry of iron-mediated lipid peroxidation: an update. Chem Rev 107(3):748-766.

Childs, S., A. A. Hennessy, J. M. Sreenan, D. C. Wathes, Z. Cheng, C. Stanton, M. G. Diskin, and D. A. Kenny. 2008. Effect of level of dietary n-3 polyunsaturated fatty acid supplementation on systemic and tissue fatty acid concentrations and on selected reproductive variables in cattle. Theriogenology 70(4):595-611.

Cho, K.-J., J.-M. Seo, and J.-H. Kim. 2011. Bioactive lipoxygenase metabolites stimulation of NADPH oxidases and reactive oxygen species. Mol Cells 32(1):1-5.

Cohen, G. and P. Hochstein. 1963. Glutathione peroxidase: The primary agent for the elimination of hydrogen peroxide in erythrocytes. Biochemistry 2(6):1420-1428.

Collins, X. H., S. D. Harmon, T. L. Kaduce, K. B. Berst, X. Fang, S. A. Moore, T. V. Raju, J. R. Falck, N. L. Weintraub, and G. Duester. 2005. ω-Oxidation of 20-hydroxyeicosatetraenoic acid (20-HETE) in cerebral microvascular smooth muscle and endothelium by alcohol dehydrogenase 4. J Biol Chem 280(39):33157-33164.

Comporti, M., C. Signorini, B. Arezzini, D. Vecchio, B. Monaco, and C. Gardi. 2008. F 2-isoprostanes are not just markers of oxidative stress. Free Radic Biol Med 44(3):247-256.

Contreras, G. A. and L. M. Sordillo. 2011. Lipid mobilization and inflammatory responses during the transition period of dairy cows. Comp Immunol Microbiol Infect Dis 34(3):281-289.

Contreras, G. A., W. Raphael, S. A. Mattmiller, J. Gandy, and L. M. Sordillo. 2012a. Nonesterified fatty acids modify inflammatory response and eicosanoid biosynthesis in bovine endothelial cells. J Dairy Sci 95(9):5011-5023.

Contreras, G. A., W. Raphael, S. A. Mattmiller, J. Gandy, and L. M. Sordillo. 2012b. Nonesterified fatty acids modify inflammatory response and eicosanoid biosynthesis in bovine endothelial cells. J Dairy Sci 95(9):5011-5023.

Corl, C., J. Gandy, and L. Sordillo. 2008. Platelet activating factor production and proinflammatory gene expression in endotoxin-challenged bovine mammary endothelial cells. J Dairy Sci 91(8):3067-3078.

Cosentino, F., M. Eto, P. De Paolis, B. van der Loo, M. Bachschmid, V. Ullrich, A. Kouroedov, C. Delli Gatti, H. Joch, M. Volpe, and T. F. Luscher. 2003. High glucose causes upregulation of cyclooxygenase-2 and alters prostanoid profile in human endothelial cells: role of protein kinase C and reactive oxygen species. Circulation 107(7):1017-1023.

Dalle-Donne, I., A. Scaloni, D. Giustarini, E. Cavarra, G. Tell, G. Lungarella, R. Colombo, R. Rossi, and A. Milzani. 2005. Proteins as biomarkers of oxidative/nitrosative stress in diseases: the contribution of redox proteomics. Mass Spectrom Rev 24(1):55-99.

Dalle-Donne, I., R. Rossi, R. Colombo, D. Giustarini, and A. Milzani. 2006. Biomarkers of oxidative damage in human disease. Clin Chem 52(4):601-623.

Darley-usmar, V. M., N. Hogg, V. J. O'Leary, M. T. Wilson, and S. Moncada. 1992. The simultaneous generation of superoxide and nitric oxide can initiate lipid peroxidation in human low density lipoprotein. Free Radic Res Commun 17(1):9-20.

Davies, S. S. and L. Guo. 2013. Lipid Peroxidation and Nitration. Pages 49-70 in Molecular Basis of Oxidative Stress. John Wiley & Sons, Inc., Hoboken, NJ.

Dhanasekaran, A., R. Al-Saghir, B. Lopez, D. Zhu, D. D. Gutterman, E. R. Jacobs, and M. Medhora. 2006. Protective effects of epoxyeicosatrienoic acids on human endothelial cells from the pulmonary and coronary vasculature. Am J Physiol Heart Circ Physiol 291(2):H517-531.

Dhanasekaran, A., S. Bodiga, S. Gruenloh, Y. Gao, L. Dunn, J. R. Falck, J. N. Buonaccorsi, M. Medhora, and E. R. Jacobs. 2009. 20-HETE increases survival and decreases apoptosis in pulmonary arteries and pulmonary artery endothelial cells. Am J Physiol Heart Circ Physiol 296(3):H777-H786.

Dhanasekaran, A., S. Kotamraju, C. Karunakaran, S. V. Kalivendi, S. Thomas, J. Joseph, and B. Kalyanaraman. 2005. Mitochondria superoxide dismutase mimetic inhibits peroxide-induced oxidative damage and apoptosis: role of mitochondrial superoxide. Free Radic Biol Med 39(5):567-583.

Dhanasekaran, A., S. Kotamraju, S. V. Kalivendi, T. Matsunaga, T. Shang, A. Keszler, J. Joseph, and B. Kalyanaraman. 2004. Supplementation of endothelial cells with mitochondria-targeted antioxidants inhibit peroxide-induced mitochondrial iron uptake, oxidative damage, and apoptosis. J Biol Chem 279(36):37575-37587.

Dixon, S. J. and B. R. Stockwell. 2014. The role of iron and reactive oxygen species in cell death. Nat Chem Biol 10(1):9-17.

Dorris, S. L. and R. S. Peebles. 2012. PGI(2) as a regulator of inflammatory diseases. Mediators Inflamm 2012:926968.

Doughan, A. K., D. G. Harrison, and S. I. Dikalov. 2008. Molecular mechanisms of angiotensin ii–mediated mitochondrial dysfunction: linking mitochondrial oxidative damage and vascular endothelial dysfunction. Circ Res 102(4):488-496.

Dunn, K. M., M. Renic, A. K. Flasch, D. R. Harder, J. Falck, and R. J. Roman. 2008. Elevated production of 20-HETE in the cerebral vasculature contributes to severity of ischemic stroke and oxidative stress in spontaneously hypertensive rats. Am J Physiol Heart Circ Physiol 295(6):H2455-H2465.

Erlemann, K. R., C. Cossette, S. Gravel, A. Lesimple, G. J. Lee, G. Saha, J. Rokach, and W. S. Powell. 2007b. Airway epithelial cells synthesize the lipid mediator 5-oxo-ETE in response to oxidative stress. Free Radic Biol Med 42(5):654-664.

Erlemann, K. R., C. Cossette, S. Gravel, P. B. Stamatiou, G. J. Lee, J. Rokach, and W. S. Powell. 2006. Metabolism of 5-hydroxy-6,8,11,14-eicosatetraenoic acid by human endothelial cells. Biochem Biophys Res Commun 350(1):151-156.

Erlemann, K.-R., C. Cossette, Gail E. Grant, G.-J. Lee, P. Patel, J. Rokach, and William S. Powell. 2007a. Regulation of 5-hydroxyeicosanoid dehydrogenase activity in monocytic cells. Biochem J 403(Pt 1):157-165.

Erskine, R., R. Eberhart, L. Hutchinson, S. Spencer, and M. Campbell. 1988. Incidence and types of clinical mastitis in dairy herds with high and low somatic cell counts. J Am Vet Med Assoc 192(6):761-765.

Fang, X., F. M. Faraci, T. L. Kaduce, S. Harmon, M. L. Modrick, S. Hu, S. A. Moore, J. R. Falck, N. L. Weintraub, and A. A. Spector. 2006. 20-Hydroxyeicosatetraenoic acid is a potent dilator of mouse basilar artery: role of cyclooxygenase. Am J Physiol Heart Circ Physiol 291(5):H2301-H2307.

Fleming, I., U. R. Michaelis, D. Bredenkotter, B. Fisslthaler, F. Dehghani, R. P. Brandes, and R. Busse. 2001. Endothelium-derived hyperpolarizing factor synthase (Cytochrome P450 2C9) is a functionally significant source of reactive oxygen species in coronary arteries. Circ Res 88(1):44-51.

Frost, A. J. and B. E. Brooker. 1986. Hyperacute Escherichia coli mastitis of cattle in the immediate post-partum period. Aust Vet J 63(10):327-331.

Gao, L., W. E. Zackert, J. J. Hasford, M. E. Danekis, G. L. Milne, C. Remmert, J. Reese, H. Yin, H. H. Tai, S. K. Dey, N. A. Porter, and J. D. Morrow. 2003. Formation of prostaglandins E2 and D2 via the isoprostane pathway: a mechanism for the generation of bioactive prostaglandins independent of cyclooxygenase. J Biol Chem 278(31):28479-28489.

George, L. W., T. J. Divers, N. Ducharme, and F. L. Welcome. 2008. Chapter 8 - Diseases of the teats and udder. Pages 327-394 in Rebhun's Diseases of Dairy Cattle (Second Edition). T. J. Divers and F. Peek, ed. W.B. Saunders, Saint Louis, MO.

Gertow, K., E. Nobili, L. Folkersen, J. W. Newman, T. L. Pedersen, J. Ekstrand, J. Swedenborg, H. Kuhn, C. E. Wheelock, G. K. Hansson, U. Hedin, J. Z. Haeggstrom, and A. Gabrielsen. 2011. 12- and 15-lipoxygenases in human carotid atherosclerotic lesions: associations with cerebrovascular symptoms. Atherosclerosis 215(2):411-416.

Ghosh, R., A. Alajbegovic, and A. V. Gomes. 2015. NSAIDs and cardiovascular diseases: role of reactive oxygen species. Oxid Med Cell Longev 2015:536962.

Glasauer, A. and N. S. Chandel. 2013. ROS. Curr Biol 23(3):R100-R102.

Go, Y.-M. and D. P. Jones. 2008. Redox compartmentalization in eukaryotic cells. Biochim Biophys Acta 1780(11):1273-1290.

Gouveia-Figueira, S. and M. L. Nording. 2014. Development and validation of a sensitive UPLC-ESI-MS/MS method for the simultaneous quantification of 15 endocannabinoids and related compounds in milk and other biofluids. Anal Chem 86(2):1186-1195.

Guo, R. F. and P. A. Ward. 2007. Role of oxidants in lung injury during sepsis. Antioxid Redox Signal 9(11):1991-2002.

Gutiérrez-Venegas, G., A. Guadarrama-Solís, C. Muñoz-Seca, and J. A. Arreguín-Cano. 2015. Hydrogen peroxide-induced apoptosis in human gingival fibroblasts. Int J Clin Exp Pathol 8(12):15563-15572.

Halliwell, B. 2007. Biochemistry of oxidative stress. Biochem Soc Trans 35(5):1147-1150.

Halliwell, B. and C. Y. Lee. 2010. Using isoprostanes as biomarkers of oxidative stress: some rarely considered issues. Antioxid Redox Signal 13(2):145-156.

Han, Y., H. Zhao, H. Tang, X. Li, J. Tan, Q. Zeng, and C. Sun. 2013. 20-Hydroxyeicosatetraenoic acid mediates isolated heart ischemia/reperfusion injury by increasing NADPH oxidase-derived reactive oxygen species production. Circ J 77(7):1807-1816.

Haskew-Layton, R. E., J. B. Payappilly, H. Xu, S. A. Bennett, and R. R. Ratan. 2013. 15-Deoxy-Delta12,14-prostaglandin J2 (15d-PGJ2) protects neurons from oxidative death via an Nrf2 astrocyte-specific mechanism independent of PPARgamma. J Neurochem 124(4):536-547.

Hassoun, P. M., F. S. Yu, C. G. Cote, J. J. Zulueta, R. Sawhney, K. A. Skinner, H. B. Skinner, D. A. Parks, and J. J. Lanzillo. 1998. Upregulation of xanthine oxidase by lipopolysaccharide, interleukin-1, and hypoxia. Role in acute lung injury. Am J Respir Crit Care Med 158(1):299-305.

Ho, C. T. and A. C. Chan. 1992. Regeneration of vitamin E in rat polymorphonuclear leucocytes. FEBS Lett 306(2-3):269-272.

Hoeben, D., C. Burvenich, E. Trevisi, G. Bertoni, J. Hamann, Ouml, Rn, R. M. Bruckmaier, J. Blum, Uuml, and R. W. 2000. Role of endotoxin and TNF-α in the pathogenesis of experimentally induced coliform mastitis in periparturient cows. J Dairy Res 67(04):503-514.

Hogan, J. and K. L. Smith. 2003. Coliform mastitis. Vet Res 34(5):507-519.

Hogan, J. S., R. N. Gonzales, R. J. Harmon, S. C. Nickerson, S. P. Oliver, J. W. Pankey, and K. L. Smith. 1999. Laboratory hand-book on bovine mastitis. Rev. ed. National Mastitis Council Inc., Madison, WI.

Holmstrom, K. and T. Finkel. 2014. Cellular mechanisms and physiological consequences of redox-dependent signaling. Nat Rev Mol Cell Biol 15(6):411-421.

Huet, O., A. Harrois, and J. Duranteau. 2009. Oxidative stress and endothelial dysfunction during sepsis. Pages 59-64 in Intensive Care Medicine. Springer, New York.

Huet, O., C. Cherreau, C. Nicco, L. Dupic, M. Conti, D. Borderie, F. Pene, E. Vicaut, D. Benhamou, and J.-P. Mira. 2008. Pivotal role of glutathione depletion in plasma-induced endothelial oxidative stress during sepsis. Crit Care Med 36(8):2328-2334.

Hunt, K. M., J. E. Williams, B. Shafii, M. K. Hunt, R. Behre, R. Ting, M. K. McGuire, and M. A. McGuire. 2013. Mastitis is associated with increased free fatty acids, somatic cell count, and interleukin-8 concentrations in human milk. Breastfeed Med 8(1):105-110.

Hye Khan, M. A., S. H. Hwang, A. Sharma, J. A. Corbett, B. D. Hammock, and J. D. Imig. 2016. A dual COX-2/sEH inhibitor improves the metabolic profile and reduces kidney injury in Zucker diabetic fatty rat. Prostaglandins Other Lipid Mediat 125:40-47.

Ishizuka, T., J. Cheng, H. Singh, M. D. Vitto, V. L. Manthati, J. R. Falck, and M. Laniado-Schwartzman. 2008. 20-Hydroxyeicosatetraenoic acid stimulates nuclear factor-κB activation and the production of inflammatory cytokines in human endothelial cells. J Pharmacol Exp Ther 324(1):103-110.

Ivanov, I., D. Heydeck, K. Hofheinz, J. Roffeis, V. B. O'Donnell, H. Kuhn, and M. Walther. 2010. Molecular enzymology of lipoxygenases. Arch Biochem Biophys 503(2):161-174.

Jain, M. and N. S. Chandel. 2013. Rethinking antioxidants in the intensive care unit. Am J Respir Crit Care Med 188(11):1283-1285.

Janero, D. R. 1990. Malondialdehyde and thiobarbituric acid-reactivity as diagnostic indices of lipid peroxidation and peroxidative tissue injury. Free Radic Biol Med 9(6):515-540.

Janicka, M., A. Kot-Wasik, J. Paradziej-Lukowicz, G. Sularz-Peszynska, A. Bartoszek, and J. Namiesnik. 2013. LC-MS/MS determination of isoprostanes in plasma samples collected from mice exposed to doxorubicin or tert-butyl hydroperoxide. Int J Mol Sci 14(3):6157-6169.

Jira, W., G. Spiteller, W. Carson, and A. Schramm. 1998. Strong increase in hydroxy fatty acids derived from linoleic acid in human low density lipoproteins of atherosclerotic patients. Chem Phys Lipids 91(1):1-11.

Kansanen, E., A. M. Kivelä, and A.-L. Levonen. 2009. Regulation of Nrf2-dependent gene expression by 15-deoxy-Δ 12, 14-prostaglandin J 2. Free Radic Biol Med 47(9):1310-1317.

Kasuga, K., R. Yang, T. F. Porter, N. Agrawal, N. A. Petasis, D. Irimia, M. Toner, and C. N. Serhan. 2008. Rapid appearance of resolvin precursors in inflammatory exudates: novel mechanisms in resolution. J Immunol 181(12):8677-8687.

Kehrer, J. P. 2000. The Haber–Weiss reaction and mechanisms of toxicity. Toxicology 149(1):43-50.

Klawitter, J., M. Haschke, T. Shokati, J. Klawitter, and U. Christians. 2011. Quantification of 15-F2t-isoprostane in human plasma and urine: results from enzyme-linked immunoassay and liquid chromatography/tandem mass spectrometry cannot be compared. Rapid Commun Mass Spectrom 25(4):463-468.

Klumpp, G., S. Schildknecht, W. Nastainczyk, V. Ullrich, and M. Bachschmid. 2005. Prostacyclin in the cardiovascular system: new aspects and open questions. Pharmacol Rep 57 Suppl:120-126.

Konkel, A. and W.-H. Schunck. 2011. Role of cytochrome P450 enzymes in the bioactivation of polyunsaturated fatty acids. Biochim Biophys Acta 1814(1):210-222.

Kuhn, H., D. Heydeck, I. Hugou, and C. Gniwotta. 1997. In vivo action of 15-lipoxygenase in early stages of human atherogenesis. J Clin Invest 99(5):888-893.

Kuhn, H., S. Banthiya, and K. van Leyen. 2015. Mammalian lipoxygenases and their biological relevance. Biochim Biophys Acta 1851(4):308-330.

Kulmacz, R. J., W. A. van der Donk, and A. L. Tsai. 2003. Comparison of the properties of prostaglandin H synthase-1 and -2. Prog Lipid Res 42(5):377-404.

Kumar, A., S. Sharma, A. Prashar, and R. Deshmukh. 2015. Effect of licofelone--a dual COX/5-LOX inhibitor in intracerebroventricular streptozotocin-induced behavioral and biochemical abnormalities in rats. J Mol Neurosci 55(3):749-759.

Kushibiki, S., K. Hodate, H. Shingu, Y. Obara, E. Touno, M. Shinoda, and Y. Yokomizo. 2003. Metabolic and lactational responses during recombinant bovine tumor necrosis factor-alpha treatment in lactating cows. J Dairy Sci 86(3):819-827.

Labuschagne, C. F., N. J. van den Broek, P. Postma, R. Berger, and A. B. Brenkman. 2013. A protocol for quantifying lipid peroxidation in cellular systems by F2-isoprostane analysis. PLoS One 8(11):e80935.

Lakhkar, A., V. Dhagia, S. R. Joshi, K. Gotlinger, D. Patel, D. Sun, M. S. Wolin, M. L. Schwartzman, and S. A. Gupte. 2016. 20-HETE-induced mitochondrial superoxide production and inflammatory phenotype in vascular smooth muscle is prevented by glucose-6-phosphate dehydrogenase inhibition. Am J Physiol Heart Circ Physiol 310(9):H1107-H1117.

Leclercq, I. A., G. C. Farrell, J. Field, D. R. Bell, F. J. Gonzalez, and G. R. Robertson. 2000. CYP2E1 and CYP4A as microsomal catalysts of lipid peroxides in murine nonalcoholic steatohepatitis. J Clin Invest 105(8):1067-1075.

Lee, A. C. and M. Murray. 2010. Up-regulation of human CYP2J2 in HepG2 cells by butylated hydroxyanisole is mediated by c-Jun and Nrf2. Mol Pharmacol 77(6):987-994.

Lee, S. F. and S. Pervaiz. 2011. Assessment of oxidative stress-induced DNA damage by immunoflourescent analysis of 8-oxodG. Methods Cell Biol 103:99-113.

Li, Q., M. Mao, Y. Qiu, G. Liu, T. Sheng, X. Yu, S. Wang, and D. Zhu. 2016. Key role of ROS in the process of 15-lipoxygenase/15-hydroxyeicosatetraenoiccid-induced pulmonary vascular remodeling in hypoxia pulmonary hypertension. PLoS One 11(2):e0149164.

Liu, J.-Y., N. Li, J. Yang, N. Li, H. Qiu, D. Ai, N. Chiamvimonvat, Y. Zhu, and B. D. Hammock. 2010. Metabolic profiling of murine plasma reveals an unexpected biomarker in rofecoxib-mediated cardiovascular events. Proc Natl Acad Sci 107(39):17017-17022.

Liu, M., T. Boussetta, K. Makni-Maalej, M. Fay, F. Driss, J. El-Benna, M. Lagarde, and M. Guichardant. 2014a. Protectin DX, a double lipoxygenase product of DHA, inhibits both ROS production in human neutrophils and cyclooxygenase activities. Lipids 49(1):49-57.

Liu, W. J., T. Wang, B. Wang, X. T. Liu, X. W. He, Y. J. Liu, Z. X. Li, R. Tan, and H. S. Zeng. 2015. CYP2C8-derived epoxyeicosatrienoic acids decrease oxidative stress-induced endothelial apoptosis in development of atherosclerosis: role of Nrf2 activation. J Huazhong Univ Sci Technolog Med Sci 35(5):640-645.

Liu, W., B. Wang, H. Ding, D. W. Wang, and H. Zeng. 2014b. A potential therapeutic effect of CYP2C8 overexpression on anti-TNF-alpha activity. Int J Mol Med 34(3):725-732.

Liu, Y. and J. P. Roth. 2016. A revised mechanism for human cyclooxygenase-2. J Biol Chem 291(2):948-958.

Liu, Y., Y. Zhang, K. Schmelzer, T. S. Lee, X. Fang, Y. Zhu, A. A. Spector, S. Gill, C. Morisseau, B. D. Hammock, and J. Y. Shyy. 2005. The antiinflammatory effect of laminar flow: the role of PPARgamma, epoxyeicosatrienoic acids, and soluble epoxide hydrolase. Proc Natl Acad Sci 102(46):16747-16752.

Lonkar, P. and P. C. Dedon. 2011. Reactive species and DNA damage in chronic inflammation: reconciling chemical mechanisms and biological fates. Int J Cancer 128(9):1999-2009.

Lu, Y. and A. I. Cederbaum. 2008. CYP2E1 and oxidative liver injury by alcohol. Free Radic Biol Med 44(5):723-738.

Lukaszewicz, K. M. and J. H. Lombard. 2013. Role of the CYP4A/20-HETE pathway in vascular dysfunction of the Dahl salt-sensitive rat. Clin Sci 124(12):695-700.

Lv, X., J. Wan, J. Yang, H. Cheng, Y. Li, Y. Ao, and R. Peng. 2008. Cytochrome P450 ω-hydroxylase inhibition reduces cardiomyocyte apoptosis via activation of ERK1/2 signaling in rat myocardial ischemia-reperfusion. Eur J Pharmacol 596(1–3):118-126.

Lykkesfeldt, J. and O. Svendsen. 2007. Oxidants and antioxidants in disease: oxidative stress in farm animals. Vet J 173(3):502-511.

Maddox, J. F., R. J. Eberhart, C. C. Reddy, and R. W. Scholz. 1990. The effect of dietary selenium on eicosanoid concentration in blood and milk during coliform mastitis. J Dairy Sci 73(Supplement 1):151.

Maddox, J. F., C. C. Reddy, R. J. Eberhart, and R. W. Scholz. 1991. Dietary selenium effects on milk eicosanoid concentration in dairy cows during coliform mastitis. Prostaglandins 42(4):369-378.

Maier, N. K., S. H. Leppla, and M. Moayeri. 2015. The cyclopentenone prostaglandin 15d-PGJ2 inhibits the NLRP1 and NLRP3 inflammasomes. J Immunol 194(6):2776-2785.

Mallat, Z., T. Nakamura, J. Ohan, G. Leseche, A. Tedgui, J. Maclouf, and R. C. Murphy. 1999. The relationship of hydroxyeicosatetraenoic acids and F2-isoprostanes to plaque instability in human carotid atherosclerosis. J Clin Invest 103(3):421-427.

Marji, J. S., M.-H. Wang, and M. Laniado-Schwartzman. 2002. Cytochrome P-450 4A isoform expression and 20-HETE synthesis in renal preglomerular arteries. Am J Physiol Renal Physiol 283(1):F60-F67.

Mas, E., R. J. Woodman, V. Burke, I. B. Puddey, L. J. Beilin, T. Durand, and T. A. Mori. 2010. The omega-3 fatty acids EPA and DHA decrease plasma F(2)-isoprostanes: Results from two placebo-controlled interventions. Free Radic Res 44(9):983-990.

Mattmiller, S. A., B. A. Carlson, and L. M. Sordillo. 2013. Regulation of inflammation by selenium and selenoproteins: impact on eicosanoid biosynthesis. J Nutr Sci 2:e28.

Mattmiller, S. A., B. A. Carlson, J. C. Gandy, and L. M. Sordillo. 2014a. Reduced macrophage selenoprotein expression alters oxidized lipid metabolite biosynthesis from arachidonic and linoleic acid. J Nutr Biochem 25(6):647-654.

Mavangira, V., J. C. Gandy, C. Zhang, V. E. Ryman, A. Daniel Jones, and L. M. Sordillo. 2015. Polyunsaturated fatty acids influence differential biosynthesis of oxylipids and other lipid mediators during bovine coliform mastitis. J Dairy Sci 98(9):6202-6215.

Mavangira, V., M. J. Mangual, J. C. Gandy, and L. M. Sordillo. 2016a. 15-F2t-Isoprostane concentrations and oxidant status in lactating dairy cattle with acute coliform mastitis. J Vet Int Med 30(1):339-347.

Mccord, J. M. And I. Fridovich. 1969. Superoxide dismutase: an enzymic function for erythrocuprein (hemocuprein). J Biol Chem 244(22):6049-6055.

McCullough, L., L. Wu, N. Haughey, X. Liang, T. Hand, Q. Wang, R. M. Breyer, and K. Andreasson. 2004. Neuroprotective function of the PGE2 EP2 receptor in cerebral ischemia. J Neurosci 24(1):257-268.

Medeiros-Lima, D. J., A. C. Mendes-Ribeiro, T. M. Brunini, M. A. Martins, W. V. Mury, R. A. Freire, W. D. Monteiro, P. T. Farinatti, and C. Matsuura. 2016. Erythrocyte nitric oxide availability and oxidative stress following exercise. Clin Hemorheol Microcirc (Oct 3, Epub).

Medhora, M., Y. Chen, S. Gruenloh, D. Harland, S. Bodiga, J. Zielonka, D. Gebremedhin, Y. Gao, J. R. Falck, S. Anjaiah, and E. R. Jacobs. 2008. 20-HETE increases superoxide production and activates NAPDH oxidase in pulmonary artery endothelial cells. Am J Physiol Lung Cell Mol Physiol 294(5):L902-911.

Meirer, K., D. Steinhilber, and E. Proschak. 2014. Inhibitors of the arachidonic acid cascade: interfering with multiple pathways. Basic Clin Pharmacol Toxicol 114(1):83-91.

Milatovic, D., M. VanRollins, K. Li, K. S. Montine, and T. J. Montine. 2005. Suppression of murine cerebral F2-isoprostanes and F4-neuroprostanes from excitotoxicity and innate immune response in vivo by alpha- or gamma-tocopherol. J Chromatogr B Analyt Technol Biomed Life Sci 827(1):88-93.

Milne, G. L., H. Yin, K. D. Hardy, S. S. Davies, and L. J. Roberts. 2011. Isoprostane generation and function. Chem Rev 111(10):5973-5996.

Milne, G. L., Q. Dai, and L. J. Roberts, 2nd. 2015. The isoprostanes-25 years later. Biochim Biophys Acta 1851(4):433-445.

Montine, T. J., D. Milatovic, R. C. Gupta, T. Valyi-Nagy, J. D. Morrow, and R. M. Breyer. 2002. Neuronal oxidative damage from activated innate immunity is EP2 receptor-dependent. J Neurochem 83(2):463-470.

Mori, T. A., R. J. Woodman, V. Burke, I. B. Puddey, K. D. Croft, and L. J. Beilin. 2003. Effect of eicosapentaenoic acid and docosahexaenoic acid on oxidative stress and inflammatory markers in treated-hypertensive type 2 diabetic subjects. Free Radic Biol Med 35(7):772-781.

Morisseau, C. and B. D. Hammock. 2013. Impact of soluble epoxide hydrolase and epoxyeicosanoids on human health. Ann Rev Pharmacol Toxicol 53:37-58.

Morrow, J. D., J. A. Awad, H. J. Boss, I. A. Blair, and L. J. Roberts. 1992a. Non-cyclooxygenase-derived prostanoids (F2-isoprostanes) are formed in situ on phospholipids. Proc Nat Acad Sci 89(22):10721-10725.

Morrow, J. D., J. A. Awad, T. Kato, K. Takahashi, K. F. Badr, L. Roberts 2nd, and R. F. Burk. 1992. Formation of novel non-cyclooxygenase-derived prostanoids (F2-isoprostanes) in carbon tetrachloride hepatotoxicity. An animal model of lipid peroxidation. J Clin Invest 90(6):2502.

Munoz, M., A. Sanchez, M. Pilar Martinez, S. Benedito, M. E. Lopez-Oliva, A. Garcia-Sacristan, M. Hernandez, and D. Prieto. 2015. COX-2 is involved in vascular oxidative stress and endothelial dysfunction of renal interlobar arteries from obese Zucker rats. Free Radic Biol Med 84:77-90.

Murakami, M., Y. Taketomi, Y. Miki, H. Sato, T. Hirabayashi, and K. Yamamoto. 2011. Recent progress in phospholipase A(2) research: From cells to animals to humans. Prog Lipid Res 50(2):152-192.

Musiek, E. S., L. Gao, G. L. Milne, W. Han, M. B. Everhart, D. Wang, M. G. Backlund, R. N. DuBois, G. Zanoni, G. Vidari, T. S. Blackwell, and J. D. Morrow. 2005. Cyclopentenone

isoprostanes inhibit the inflammatory response in macrophages. J Biol Chem 280(42):35562-35570.

Nakamura, T., M. Sato, H. Kakinuma, N. Miyata, K. Taniguchi, K. Bando, A. Koda, and K. Kameo. 2003. Pyrazole and isoxazole derivatives as new, potent, and selective 20-hydroxy-5, 8, 11, 14-eicosatetraenoic acid synthase inhibitors. J Med Chem 46(25):5416-5427.

Natarajan, R., M. A. Reddy, K. U. Malik, S. Fatima, and B. V. Khan. 2001. Signaling mechanisms of nuclear factor-kappaB-mediated activation of inflammatory genes by 13-hydroperoxyoctadecadienoic acid in cultured vascular smooth muscle cells. Arterioscler Thromb Vasc Biol 21(9):1408-1413.

Nilakantan, V., C. Maenpaa, G. Jia, R. J. Roman, and F. Park. 2008. 20-HETE-mediated cytotoxicity and apoptosis in ischemic kidney epithelial cells. Am J Physiol Renal Physiol 294(3):F562-F570.

Noguchi, N., H. Yamashita, J. Hamahara, A. Nakamura, H. Kühn, and E. Niki. 2002. The specificity of lipoxygenase-catalyzed lipid peroxidation and the effects of radical-scavenging antioxidants. Biol Chem 383(3-4):619-626.

Nwose, E. U., H. F. Jelinek, R. S. Richards, and P. G. Kerr. 2008. The 'vitamin E regeneration system' (VERS) and an algorithm to justify antioxidant supplementation in diabetes – A hypothesis. Med Hypotheses 70(5):1002-1008.

O'Donnell, V. B., B. Maskrey, and G. W. Taylor. 2009. Eicosanoids: generation and detection in mammalian cells. Pages 1-19 in Lipid Signaling Protocols. Springer, New York, NY.

Oliveira, L., C. Hulland, and P. Ruegg. 2013. Characterization of clinical mastitis occurring in cows on 50 large dairy herds in Wisconsin. J Dairy Sci 96(12):7538-7549.

Ono, E., S. Dutile, S. Kazani, M. E. Wechsler, J. Yang, B. D. Hammock, D. N. Douda, Y. Tabet, R. Khaddaj-Mallat, M. Sirois, C. Sirois, E. Rizcallah, E. Rousseau, R. Martin, E. R. Sutherland, M. Castro, N. N. Jarjour, E. Israel, and B. D. Levy. 2014. Lipoxin generation is related to soluble epoxide hydrolase activity in severe asthma. Am J Respir Crit Care Med 190(8):886-897.

Ortiz de Montellano, P. R. 2010. Hydrocarbon Hydroxylation by Cytochrome P450 Enzymes. Chem Rev 110(2):932.

Othman, A., S. Ahmad, S. Megyerdi, R. Mussell, K. Choksi, K. R. Maddipati, A. Elmarakby, N. Rizk, and M. Al-Shabrawey. 2013. 12/15-Lipoxygenase-derived lipid metabolites induce retinal endothelial cell barrier dysfunction: contribution of NADPH oxidase. PLoS One 8(2):e57254.

Pan, Y., L. Yu, W. Lei, Y. Guo, J. Wang, H. Yu, Y. Tang, and J. Yang. 2015. Beraprost sodium protects against chronic brain injury in aluminum-overload rats. Behav Brain Funct 11:6.

Park, C. M., Y. S. Cha, H. J. Youn, C. W. Cho, and Y. S. Song. 2010. Amelioration of oxidative stress by dandelion extract through CYP2E1 suppression against acute liver injury induced by carbon tetrachloride in Sprague-Dawley rats. Phytother Res 24(9):1347-1353.

Picklo, M. J., Sr. and J. W. Newman. 2015. Antioxidant supplementation and obesity have independent effects on hepatic oxylipin profiles in insulin-resistant, obesity-prone rats. Free Radic Biol Med 89:182-191.

Plumb, G. W., M. S. Dupont, and G. Williamson. 1997. Modulation of AAPH-induced oxidative stress in cell culture by flavonoids. Biochem Soc Trans 25(4):S560.

Pober, J. S. and W. C. Sessa. 2007. Evolving functions of endothelial cells in inflammation. Nat Rev Immunol 7(10):803-815.

Powell, W. S., F. Gravelle, and S. Gravel. 1994. Phorbol myristate acetate stimulates the formation of 5-oxo-6,8,11,14-eicosatetraenoic acid by human neutrophils by activating NADPH oxidase. J Biol Chem 269(41):25373-25380.

Puntarulo, S. and A. I. Cederbaum. 1998. Production of reactive oxygen species by microsomes enriched in specific human cytochrome P450 enzymes. Free Radic Biol Med 24(7-8):1324-1330.

Qanungo, S., M. Wang, and A.-L. Nieminen. 2004. N-Acetyl-L-cysteine enhances apoptosis through inhibition of nuclear factor-κB in hypoxic murine embryonic fibroblasts. J Biol Chem 279(48):50455-50464.

Quoilin, C., A. Mouithys-Mickalad, S. Lecart, M. P. Fontaine-Aupart, and M. Hoebeke. 2014. Evidence of oxidative stress and mitochondrial respiratory chain dysfunction in an in vitro model of sepsis-induced kidney injury. Biochim Biophys Acta 1837(10):1790-1800.

Randriamboavonjy, V., R. Busse, and I. Fleming. 2003. 20-HETE–induced contraction of small coronary arteries depends on the activation of Rho-kinase. Hypertension 41(3):801-806.

Ranjan, R., D. Swarup, R. Naresh, and R. C. Patra. 2005. Enhanced erythrocytic lipid peroxides and reduced plasma ascorbic acid, and alteration in blood trace elements level in dairy cows with mastitis. Vet Res Commun 29(1):27-34.

Rao, G. N., W. C. Glasgow, T. E. Eling, and M. S. Runge. 1996. Role of hydroperoxyeicosatetraenoic acids in oxidative stress-induced activating protein 1 (AP-1) activity. J Biol Chem 271(44):27760-27764.

Re, R., N. Pellegrini, A. Proteggente, A. Pannala, M. Yang, and C. Rice-Evans. 1999. Antioxidant activity applying an improved ABTS radical cation decolorization assay. Free Radic Biol Med 26(9-10):1231-1237.

Renic, M., S. N. Kumar, D. Gebremedhin, M. A. Florence, N. Z. Gerges, J. R. Falck, D. R. Harder, and R. J. Roman. 2012. Protective effect of 20-HETE inhibition in a model of oxygen-glucose deprivation in hippocampal slice cultures. Am J Physiol Heart Circ Physiol 302(6):H1285-H1293.

Rifkind, A. B., C. Lee, T. K. Chang, and D. J. Waxman. 1995. Arachidonic acid metabolism by human cytochrome P450s 2C8, 2C9, 2E1, and 1A2: regioselective oxygenation and evidence for a role for CYP2C enzymes in arachidonic acid epoxygenation in human liver microsomes. Arch Biochem Biophys 320(2):380-389.

Roche, M., E. Tarnus, P. Rondeau, and E. Bourdon. 2009. Effects of nutritional antioxidants on AAPH- or AGEs-induced oxidative stress in human SW872 liposarcoma cells. Cell Biol Toxicol 25(6):635-644.

Rose, D. M., S. N. Giri, J. S. Cullor, and R. B. Bushnell. 1991. The combined use of lipoxygenase and cyclooxygenase inhibitors in Klebsiella pneumoniae-induced bovine mastitis. J Vet Med 38(2):99-106.

Rosenthal, M. D., B. A. Rzigalinski, P. F. Blackmore, and R. C. Franson. 1995. Cellular regulation of arachidonate mobilization and metabolism. Prostaglandins Leukot Essent Fatty Acids 52(2-3):93-98.

Roshanravan, H., E. Y. Kim, and S. E. Dryer. 2016. 20-Hydroxyeicosatetraenoic Acid (20-HETE) Modulates Canonical Transient Receptor Potential-6 (TRPC6) Channels in Podocytes. Front Physiol 7:351.

Ruiz, S., P. E. Pergola, R. A. Zager, and N. D. Vaziri. 2013. Targeting the transcription factor Nrf2 to ameliorate oxidative stress and inflammation in chronic kidney disease. Kidney Int 83(6):1029-1041.

Ruiz, S., P. E. Pergola, R. A. Zager, and N. D. Vaziri. 2013. Targeting the transcription factor Nrf2 to ameliorate oxidative stress and inflammation in chronic kidney disease. Kidney Int 83(6):1029-1041.

Ryman, V. E., N. Packiriswamy, and L. M. Sordillo. 2016. Apoptosis of endothelial cells by 13-HPODE contributes to impairment of endothelial barrier integrity. Mediators Inflamm 2016:13.

Sancho, P., P. Martín-Sanz, and I. Fabregat. 2011. Reciprocal regulation of NADPH oxidases and the cyclooxygenase-2 pathway. Free Radic Biol Med 51(9):1789-1798.

Scarpato, R., C. Gambacciani, B. Svezia, D. Chimenti, and G. Turchi. 2011. Cytotoxicity and genotoxicity studies of two free-radical generators (AAPH and SIN-1) in human microvascular endothelial cells (HMEC-1) and human peripheral lymphocytes. Mutat Res 722(1):69-77.

Schildknecht, S. and V. Ullrich. 2009. Peroxynitrite as regulator of vascular prostanoid synthesis. Arch Biochem Biophys 484(2):183-189.

Schmelzer, K. R., L. Kubala, J. W. Newman, I.-H. Kim, J. P. Eiserich, and B. D. Hammock. 2005. Soluble epoxide hydrolase is a therapeutic target for acute inflammation. Proc Natl Acad Sci 102(28):9772-9777.

Schneider, C. A., W. S. Rasband, and K. W. Eliceiri. 2012. NIH image to ImageJ: 25 years of image analysis. Nat Meth 9(7):671-675.

Schneider, C., D. A. Pratt, N. A. Porter, and A. R. Brash. 2007. Control of oxygenation in lipoxygenase and cyclooxygenase catalysis. Chem Biol 14(5):473-488.

Senol, S. P., M. Temiz, D. S. Guden, P. Cecen, A. N. Sari, S. Sahan-Firat, J. R. Falck, R. Dakarapu, K. U. Malik, and B. Tunctan. 2016. Contribution of PPARα/β/γ, AP-1, importin-α3,

and RXRα to the protective effect of 5,14-HEDGE, a 20-HETE mimetic, against hypotension, tachycardia, and inflammation in a rat model of septic shock. Inflamm. Res. 65(5):367-387.

Sergent, O., M. Pereira, C. Belhomme, M. Chevanne, L. Huc, and D. Lagadic-Gossmann. 2005. Role for membrane fluidity in ethanol-induced oxidative stress of primary rat hepatocytes. J Pharmacol Exp Ther 313(1):104-111.

Serhan, C. N. 1997. Lipoxins and novel aspirin-triggered 15-epi-lipoxins (ATL): A jungle of cell-cell interactions or a therapeutic opportunity? Prostaglandins 53(2):107-137.

Serhan, C. N., N. Chiang, and T. E. Van Dyke. 2008. Resolving inflammation: dual anti-inflammatory and pro-resolution lipid mediators. Nat Rev Immunol 8(5):349-361.

Shi, J., Q. Wang, J. U. Johansson, X. Liang, N. S. Woodling, P. Priyam, T. M. Loui, M. Merchant, R. M. Breyer, T. J. Montine, and K. Andreasson. 2012. Inflammatory prostaglandin E2 signaling in a mouse model of Alzheimer disease. Ann Neurol 72(5):788-798.

Shibata, T. 2015. 15-Deoxy-Δ12,14-prostaglandin J2 as an electrophilic mediator. Biosci Biotechnol Biochem 79(7):1044-1049.

Shibata, T., M. Kondo, T. Osawa, N. Shibata, M. Kobayashi, and K. Uchida. 2002. 15-Deoxy-Δ12,14-prostaglandin J2 : a prostaglandin d2 metabolite generated during inflammatory processes. J Biol Chem 277(12):10459-10466.

Shuster, D. E., R. J. Harmon, J. A. Jackson, and R. W. Hemken. 1991. Suppression of milk production during endotoxin-induced mastitis. J Dairy Sci 74(11):3763-3774.

Slim, R., B. D. Hammock, M. Toborek, L. W. Robertson, J. W. Newman, C. H. Morisseau, B. A. Watkins, V. Saraswathi, and B. Hennig. 2001. The role of methyl-linoleic acid epoxide and diol metabolites in the amplified toxicity of linoleic acid and polychlorinated biphenyls to vascular endothelial cells. Toxicol Appl Pharmacol 171(3):184-193.

Smith, K. A., J. Shepherd, A. Wakil, and E. S. Kilpatrick. 2011. A comparison of methods for the measurement of 8-isoPGF(2alpha): a marker of oxidative stress. Ann Clin Biochem 48(Pt 2):147-154.

Smith, K. L., J. H. Harrison, D. D. Hancock, D. A. Todhunter, and H. R. Conrad. Effect of Vitamin E and Selenium Supplementation on Incidence of Clinical Mastitis and Duration of Clinical Symptoms. J Dairy Sci 67(6):1293-1300.

Soffler, C., V. L. Campbell, and D. M. Hassel. 2010. Measurement of urinary F2-isoprostanes as markers of in vivo lipid peroxidation: a comparison of enzyme immunoassays with gas chromatography–mass spectrometry in domestic animal species. J Vet Diagn Invest 22(2):200-209.

Sordillo, L. and J. Peel. 1992. Effect of interferon-γ on the production of tumor necrosis factor during acute Escherichia coli mastitis. J Dairy Sci 75(8):2119-2125.

Sordillo, L. and V. Mavangira. 2014. The nexus between nutrient metabolism, oxidative stress and inflammation in transition cows. Anim Prod Sci 54(9):1204-1214.

Sordillo, L. M. and S. L. Aitken. 2009. Impact of oxidative stress on the health and immune function of dairy cattle. Vet Immunol Immunopathol 128(1-3):104-109.

Sordillo, L. M., G. A. Contreras, and S. L. Aitken. 2009. Metabolic factors affecting the inflammatory response of periparturient dairy cows. Anim Health Res Rev 10(1):53-63.

Sordillo, L. M., J. A. Weaver, Y. Z. Cao, C. Corl, M. J. Sylte, and I. K. Mullarky. 2005. Enhanced 15-HPETE production during oxidant stress induces apoptosis of endothelial cells. Prostaglandins Other Lipid Mediat 76(1-4):19-34.

Sordillo, L. M., K. L. Streicher, I. K. Mullarky, J. C. Gandy, W. Trigona, and C. M. Corl. 2008. Selenium inhibits 15-hydroperoxyoctadecadienoic acid-induced intracellular adhesion molecule expression in aortic endothelial cells. Free Radic Biol Med 44(1):34-43.

Sordillo, L., N. O'Boyle, J. Gandy, C. Corl, and E. Hamilton. 2007. Shifts in thioredoxin reductase activity and oxidant status in mononuclear cells obtained from transition dairy cattle. J Dairy Sci 90(3):1186-1192.

Sorokin, A. 2016. Nitric oxide synthase and cyclooxygenase pathways: a complex interplay in cellular signaling. Curr Med Chem 23(24):2559-2578.

Soumya, S. J., S. Binu, A. Helen, P. Reddanna, and P. R. Sudhakaran. 2014. 15-LOX metabolites and angiogenesis: angiostatic effect of 15(S)-HPETE involves induction of apoptosis in adipose endothelial cells. PeerJ 2:e635.

Spector, A. A., X. Fang, G. D. Snyder, and N. L. Weintraub. 2004. Epoxyeicosatrienoic acids (EETs): metabolism and biochemical function. Prog Lipid Res 43(1):55-90.

Stafforini, D. M., J. R. Sheller, T. S. Blackwell, A. Sapirstein, F. E. Yull, T. M. McIntyre, J. V. Bonventre, S. M. Prescott, and L. J. Roberts, 2nd. 2006. Release of free F2-isoprostanes from esterified phospholipids is catalyzed by intracellular and plasma platelet-activating factor acetylhydrolases. J Biol Chem 281(8):4616-4623.

Takahashi, K., T. M. Nammour, M. Fukunaga, J. Ebert, J. D. Morrow, L. J. Roberts, 2nd, R. L. Hoover, and K. F. Badr. 1992. Glomerular actions of a free radical-generated novel prostaglandin, 8-epi-prostaglandin F2 alpha, in the rat. Evidence for interaction with thromboxane A2 receptors. J Clin Invest 90(1):136-141.

Tam, V. C. 2013. Lipidomic profiling of bioactive lipids by mass spectrometry during microbial infections. Semin Immunol 25(3):240-248.

Theken, K. N., Y. Deng, M. A. Kannon, T. M. Miller, S. M. Poloyac, and C. R. Lee. 2011. Activation of the acute inflammatory response alters cytochrome P450 expression and eicosanoid metabolism. Drug Metab Dispos 39(1):22-29.

Tian, X. Y., W. T. Wong, F. P. Leung, Y. Zhang, Y.-X. Wang, H. K. Lee, C. F. Ng, Z. Y. Chen, X. Yao, C. L. Au, C. W. Lau, P. M. Vanhoutte, J. P. Cooke, and Y. Huang. 2011. Oxidative stress-dependent cyclooxygenase-2-derived prostaglandin F2α impairs endothelial function in renovascular hypertensive rats. Antioxid Redox Signal 16(4):363-373.

Tirmenstein, M. A., F. A. Nicholls-Grzemski, J. G. Zhang, and M. W. Fariss. 2000. Glutathione depletion and the production of reactive oxygen species in isolated hepatocyte suspensions. Chem Biol Interact 127(3):201-217.

Toguri, J. T., C. Lehmann, R. B. Laprairie, A. M. Szczesniak, J. Zhou, E. M. Denovan-Wright, and M. E. Kelly. 2014. Anti-inflammatory effects of cannabinoid CB(2) receptor activation in endotoxin-induced uveitis. Br J Pharmacol 171(6):1448-1461.

Toth, P., A. Csiszar, D. Sosnowska, Z. Tucsek, P. Cseplo, Z. Springo, S. Tarantini, W. E. Sonntag, Z. Ungvari, and A. Koller. 2013. Treatment with the cytochrome P450 ω-hydroxylase inhibitor HET0016 attenuates cerebrovascular inflammation, oxidative stress and improves vasomotor function in spontaneously hypertensive rats. Br J Pharmacol 168(8):1878-1888.

Trachootham, D., W. Lu, M. A. Ogasawara, R. D. Nilsa, and P. Huang. 2008. Redox regulation of cell survival. Antioxid Redox Signal 10(8):1343-1374.

Tunctan, B., A. N. Sari, M. Kacan, D. Unsal, C. K. Buharalioglu, S. Sahan-Firat, B. Korkmaz, J. R. Falck, and K. U. Malik. 2013b. NS-398 reverses hypotension in endotoxemic rats: Contribution of eicosanoids, NO, and peroxynitrite. Prostaglandins Other Lipid Mediat 104–105:93-108.

Tunctan, B., B. Korkmaz, A. N. Sari, M. Kacan, D. Unsal, M. S. Serin, C. K. Buharalioglu, S. Sahan-Firat, T. Cuez, W. H. Schunck, J. R. Falck, and K. U. Malik. 2013a. 5,14-HEDGE, a 20-HETE mimetic, reverses hypotension and improves survival in a rodent model of septic shock: contribution of soluble epoxide hydrolase, CYP2C23, MEK1/ERK1/2/IKKbeta/IkappaB-alpha/NF-kappaB pathway, and proinflammatory cytokine formation. Prostaglandins Other Lipid Mediat 102-103:31-41.

Tunctan, B., B. Korkmaz, A. N. Sari, M. Kacan, D. Unsal, M. S. Serin, C. K. Buharalioglu, S. Sahan-Firat, T. Cuez, W. H. Schunck, V. L. Manthati, J. R. Falck, and K. U. Malik. 2013a. Contribution of iNOS/sGC/PKG pathway, COX-2, CYP4A1, and gp91(phox) to the protective effect of 5,14-HEDGE, a 20-HETE mimetic, against vasodilation, hypotension, tachycardia, and inflammation in a rat model of septic shock. Nitric Oxide 33:18-41.

Tunctan, B., B. Korkmaz, A. Nihal Sari, M. Kacan, D. Unsal, M. Sami Serin, C. Kemal Buharalioglu, S. Sahan-Firat, W.-H. Schunck, and J. R Falck. 2012. A novel treatment strategy for sepsis and septic shock based on the interactions between prostanoids, nitric oxide, and 20-hydroxyeicosatetraenoic acid. Antiinflamm Antiallergy Agents Med Chem 11(2):121-150.

Valko, M., D. Leibfritz, J. Moncol, M. T. Cronin, M. Mazur, and J. Telser. 2007. Free radicals and antioxidants in normal physiological functions and human disease. Int J Biochem Cell Biol 39(1):44-84.

Vangroenweghe, F., I. Lamote, and C. Burvenich. 2005. Physiology of the periparturient period and its relation to severity of clinical mastitis. Domest Anim Endocrinol 29(2):283-293.

Van't Erve, T. J., F. B. Lih, C. Jelsema, L. J. Deterding, T. E. Eling, R. P. Mason, and M. B. Kadiiska. 2016. Reinterpreting the best biomarker of oxidative stress: the 8-iso-prostaglandin F2α/prostaglandin F2α ratio shows complex origins of lipid peroxidation biomarkers in animal models. Free Radic Biol Med 95:65-73.

Vernunft, A., T. Viergutz, C. Plinski, and J. M. Weitzel. 2014. Postpartum levels of 8-iso-prostaglandin F2alpha in plasma and milk phospholipid fractions as biomarker of oxidative stress in first-lactating dairy cows. Prostaglandins Other Lipid Mediat 112:34-38.

Villamena, F. A. 2013. Chemistry of reactive species. Pages 1-48 in Molecular Basis of Oxidative Stress: Chemistry, Mechanisms, and Disease Pathogenesis. Wiley & Sons, Inc., Hoboken, NJ

Viswanathan, S., B. D. Hammock, J. W. Newman, P. Meerarani, M. Toborek, and B. Hennig. 2003. Involvement of CYP 2C9 in mediating the proinflammatory effects of linoleic acid in vascular endothelial cells. J Am Coll Nutr 22(6):502-510.

Waldman, M., S. J. Peterson, M. Arad, and E. Hochhauser. The role of 20-HETE in cardiovascular diseases and its risk factors. Prostaglandins Other Lipid Mediat 125:108-117.

Wang, J., H. Li, J. He, B. Li, Q. Bao, X. Zhang, Z. Lv, Y. Zhang, J. Han, D. Ai, and Y. Zhu. 2015. 20-Hydroxyeicosatetraenoic acid involved in endothelial activation and thrombosis. Am J Physiol Heart Circ Physiol 308(11):H1359-1367.

Wang, L., R. Yuan, C. Yao, Q. Wu, M. Christelle, W. Xie, X. Zhang, W. Sun, H. Wang, and S. Yao. 2014a. Effects of resolvin D1 on inflammatory responses and oxidative stress of lipopolysaccharide-induced acute lung injury in mice. Chin Med J 127(5):803-809.

Wang, Y., A. M. Armando, O. Quehenberger, C. Yan, and E. A. Dennis. 2014b. Comprehensive ultra-performance liquid chromatographic separation and mass spectrometric analysis of eicosanoid metabolites in human samples. J Chromatogr 1359:60-69.

Ware, L. B., J. P. Fessel, A. K. May, and L. J. Roberts, 2nd. 2011. Plasma biomarkers of oxidant stress and development of organ failure in severe sepsis. Shock 36(1):12-17.

Weaver, J. A., J. F. Maddox, Y. Z. Cao, I. K. Mullarky, and L. M. Sordillo. 2001. Increased 15-HPETE production decreases prostacyclin synthase activity during oxidant stress in aortic endothelial cells. Free Radic Biol Med 30(3):299-308.

Weiss, W. P., J. S. Hogan, and K. L. Smith. Changes in vitamin c concentrations in plasma and milk from dairy cows after an intramammary infusion of Escherichia coli. J Dairy Sci 87(1):32-37.

Weiss, W. P., J. S. Hogan, D. A. Todhunter, and K. L. Smith. 1997. Effect of Vitamin E Supplementation in Diets with a Low Concentration of Selenium on Mammary Gland Health of Dairy Cows. J Dairy Sci 80(8):1728-1737.

Wenz, J. R., G. M. Barrington, F. B. Garry, K. D. McSweeney, R. P. Dinsmore, G. Goodell, and R. J. Callan. 2001. Bacteremia associated with naturally occuring acute coliform mastitis in dairy cows. J Am Vet Med Assoc 219(7):976-981.

Werz, O., D. Szellas, and D. Steinhilber. 2000. Reactive oxygen species released from granulocytes stimulate 5-lipoxygenase activity in a B-lymphocytic cell line. Eur J Biochem 267(5):1263-1269.

Westphal, C., A. Konkel, and W.-H. Schunck. 2015. Cytochrome P450 Enzymes in the Bioactivation of Polyunsaturated Fatty Acids and Their Role in Cardiovascular Disease. Pages 151-187 in Monooxygenase, Peroxidase and Peroxygenase Properties and Mechanisms of Cytochrome P450. Springer, Switzerland.

Willenberg, I., K. Rund, S. Rong, N. Shushakova, F. Gueler, and N. H. Schebb. 2015. Characterization of changes in plasma and tissue oxylipin levels in LPS and CLP induced murine sepsis. Inflamm Res 65(2):133-142.

Wu, G., J. M. Lu, W. A. van der Donk, R. J. Kulmacz, and A. L. Tsai. 2011. Cyclooxygenase reaction mechanism of prostaglandin H synthase from deuterium kinetic isotope effects. J Inorg Biochem 105(3):382-390.

Wu, H., T. Wu, X. Han, J. Wan, C. Jiang, W. Chen, H. Lu, Q. Yang, and J. Wang. 2016. Cerebroprotection by the neuronal PGE2 receptor EP2 after intracerebral hemorrhage in middle-aged mice. J Cereb Blood Flow Metab. Jan 8 (Epub).

Wu, L., H. H. Li, Q. Wu, S. Miao, Z. J. Liu, P. Wu, and D. Y. Ye. 2015. Lipoxin A4 Activates Nrf2 Pathway and Ameliorates Cell Damage in Cultured Cortical Astrocytes Exposed to Oxygen-Glucose Deprivation/Reperfusion Insults. J Mol Neurosci 56(4):848-857.

Wu, M. S., G. S. Lien, S. C. Shen, L. Y. Yang, and Y. C. Chen. 2014. N-acetyl-L-cysteine enhances fisetin-induced cytotoxicity via induction of ROS-independent apoptosis in human colonic cancer cells. Mol Carcinog 53(S1):E119-29.

Yamauchi, R. 1997. Vitamin E: Mechanism of Its Antioxidant Activity. Food Sci Technol Int 3(4):301-309.

Yoshida, Y., M. Hayakawa, O. Cynshi, K. Jishage, and E. Niki. 2008. Acceleration of lipid peroxidation in alpha-tocopherol transfer protein-knockout mice following the consumption of drinking water containing a radical initiator. J Oleo Sci 57(10):577-583.

Yu, G., X. Zeng, H. Wang, Q. Hou, C. Tan, and Q. Xu. 2015. 14, 15-Epoxyeicosatrienoic acid suppresses cigarette smoke extract-induced apoptosis in lung epithelial cells by inhibiting endoplasmic reticulum stress. Cell Physiol Biochem 36(2):474-486.

Zarbock, A., M. R. Distasi, E. Smith, J. M. Sanders, G. Kronke, B. L. Harry, S. von Vietinghoff, K. Buscher, J. L. Nadler, and K. Ley. 2009. Improved survival and reduced vascular permeability by eliminating or blocking 12/15-lipoxygenase in mouse models of acute lung injury (ALI). J Immunol 183(7):4715-4722.

Zeng, Q., Y. Han, Y. Bao, W. Li, X. Li, X. Shen, X. Wang, F. Yao, S. T. O'Rourke, and C. Sun. 2010. 20-HETE increases NADPH oxidase-derived ROS production and stimulates the L-type Ca2+ channel via a PKC-dependent mechanism in cardiomyocytes. Am J Physiol Heart Circ Physiol 299(4):H1109-1117.

Zhang, D., X. Xie, Y. Chen, B. D. Hammock, W. Kong, and Y. Zhu. 2012. Homocysteine upregulates soluble epoxide hydrolase in vascular endothelium in vitro and in vivo. Circ Res 110(6):808-817.

Zhang, H., P. Limphong, J. Pieper, Q. Liu, C. K. Rodesch, E. Christians, and I. J. Benjamin. 2012. Glutathione-dependent reductive stress triggers mitochondrial oxidation and cytotoxicity. FASEB J 26(4):1442-1451.

Zhou, W., D. R. Dowell, M. W. Geraci, T. S. Blackwell, R. D. Collins, V. V. Polosukhin, W. E. Lawson, P. Wu, T. Sussan, S. Biswal, K. Goleniewska, J. O'Neal, D. C. Newcomb, S. Toki, J. D. Morrow, and R. S. Peebles. 2011. PGI synthase overexpression protects against bleomycin-induced mortality and is associated with increased Nqo 1 expression. Am J Physiol Lung Cell Mol Physiol 301(4):L615-L622.

Zou, M. H. and V. Ullrich. 1996. Peroxynitrite formed by simultaneous generation of nitric oxide and superoxide selectively inhibits bovine aortic prostacyclin synthase. FEBS Lett 382(1–2):101-104.

Zubrzycki, M., A. Liebold, A. Janecka, and M. Zubrzycka. 2014a. A new face of endocannabinoids in pharmacotherapy. Part I: protective role of endocannabinoids in hypertension and myocardial infarction. J Physiol Pharmacol 65(2):171-181.

Zubrzycki, M., A. Liebold, A. Janecka, and M. Zubrzycka. 2014b. A new face of endocannabinoids in pharmacotherapy. Part II: role of endocannabinoids in inflammation-derived cardiovascular diseases. J Physiol Pharmacol 65(2):183-191.